CONGENITAL MYASTHENIC SYNDROMES:

CURRENT DIAGNOSTIC AND THERAPEUTIC ASPECTS

SARAH FINLAYSON

ST. ANNE'S COLLEGE

A thesis submitted for the degree of

Doctor of Philosophy in Clinical Neurosciences

at the

University of Oxford

Trinity Term 2014

DECLARATION

This thesis is the result of my own work unless otherwise stated. Parts of this thesis have been published in the following refereed journals and textbook:

Chapter 1:

Finlayson, Sarah, David Beeson, and Jacqueline Palace. 2013. "Congenital Myasthenic Syndromes: An Update." *Practical Neurology* 13 (2): 80–91. doi:10.1136/practneurol-2012-000404.

Finlayson, Sarah, and Jacqueline Palace. 2014. "Inherited myasthenic syndromes." Chap. 19 in *The Oxford Textbook of Neuromuscular Disorders*, edited by David Hilton-Jones and Martin R. Turner. Oxford: Oxford University Press.

Chapter 3:

Cossins, Judith, Katsiaryna Belaya, Debbie Hicks, Mustafa A Salih, Sarah Finlayson, Nicola Carboni, Wei Wei Liu, et al. 2013. "Congenital Myasthenic Syndromes due to Mutations in ALG2 and ALG14." *Brain: A Journal of Neurology*, February. doi:10.1093/brain/awt010.

Finlayson, Sarah, Jacqueline Palace, Katsiaryna Belaya, Timothy J Walls, Fiona Norwood, Georgina Burke, Janice L Holton, Samuel I Pascual-Pascual, Judith Cossins, and David Beeson. 2013. "Clinical Features of Congenital Myasthenic Syndrome due to Mutations in DPAGT1." *Journal of Neurology, Neurosurgery, and Psychiatry*, February. doi:10.1136/jnnp-2012-304716.

Co-authored content from these sources is indicated by footnotes within the text.

CONGENITAL MYASTHENIC SYNDROMES:
CURRENT DIAGNOSTIC AND THERAPEUTIC ASPECTS

Sarah Finlayson

St. Anne's College

Submitted for the degree of Doctor of Philosophy in Clinical Neurosciences

Trinity Term 2014

Abstract

This DPhil thesis presents four separate studies on diagnostic and therapeutic aspects of the congenital myasthenic syndromes (CMS). The first is a clinical characterization of syndromes associated with four novel CMS disease genes; *DPAGT1, ALG2, ALG14* and *GFPT1,* which encode proteins involved in glycosylation pathways. These conditions are likely under-diagnosed and this characterization should help facilitate recognition of these disorders. Typically patients have prominent limb-girdle weakness and are pyridostigmine responsive. Minimal craniobulbar symptoms and the finding of tubular aggregates on muscle biopsy help to distinguish these disorders from the majority of other forms of CMS. The second is a prospective imaging study which investigates lower limb muscle MRI findings in patients with congenital myasthenia. Twenty one patients with eight CMS subtypes and ten healthy controls were imaged using T1 and short-tau-inversion-recovery (STIR) sequences. Overall a wide range of MRI appearance from normal imaging to marked abnormality was seen depending upon CMS subtype. T1 images seem to be especially abnormal in glycosylation pathway forms of CMS. No selective pattern of muscle involvement was identified. Muscle MRI could have a role in differentiating CMS subtypes, preclude the use of muscle biopsy, and may have a role in monitoring treatment effects in the future. In the final two studies separate drugs; lamotrigine and metoclopramide, are assessed as possible symptomatic treatments in transgenic mouse models of CMS. Electrophysiological measurement of neurotransmission and tests of sustained muscle effort were performed. A reduction in endplate potential decay time that could support an open-channel blocking effect of lamotrigine was observed in a model of slow channel congenital myasthenia. However, no benefit was observed during *in vivo* treatment trials with lamotrigine or in experiments with metoclopramide in a model of acetylcholine receptor deficiency syndrome. Overall there was no convincing evidence to clearly support therapeutic use of either agent.

ACKNOWLEDGEMENTS

I thank the Myasthenia Gravis Association who, in providing funding, made the muscle MRI project in Chapter 4 possible. I am extremely grateful to both supervisors, Dr Jackie Palace and Professor David Beeson, for all their help and support, and from whom I have learnt so much over the last few years. All other members, past and present, of the CMS team have also been very helpful and a pleasure to work with. I am indebted to the many that helped get the muscle imaging project up and running, but especially to Dr Jasper Morrow and Professor Tarek Yousry, for their guidance and expertise. Special thanks also to Dr Richard Webster for his unofficial supervision in the lab, to Mrs Susan Maxwell for genotyping, and to all my other lab co-workers and the countless others who have helped along the way. This thesis is dedicated to my partner Roddy, without whose flexibility and support I couldn't have taken this on. Many thanks also to both my parents for lending an ear.

CONTENTS

LIST OF TABLES

LIST OF FIGURES

ABBREVIATIONS

3,4-DAP	3,4-diaminopyridine
ACh	acetylcholine
AChE	acetylcholinesterase
AChR	acetylcholine receptor
AIMG	autoimmune myasthenia gravis
AMC	arthrogryposis multiplex congenita
AP	action potential
ChAT	choline acetyltransferase
CDG	congenital disorder of glycosylation
CDT	carbohydrate deficient transferrin
CK	creatine kinase
CMAP	compound muscle action potential
CMS	congenital myasthenic syndrome
DOK7	downstream of kinase 7
DPAGT1	dolichyl-phosphate (UDP-N-acetylglucosamine) N acetylglucosaminephosphotransferase 1
DOLK	dolichol kinase
DNA	deoxyribonucleic acid
ECG	electrocardiogram
EM	electron microscopy
EOM	extraocular muscles
EPP	endplate potential
GFPT1	glutamine-fructose-6-phosphate transaminase 1

HEK	human embryonic kidney
HBP	hexosamine biosynthetic pathway
IEF	isoelectric focussing
IU	international units
LAMB2	laminin beta 2
LRP4	low density lipoprotein receptor-related protein 4
MEPP	miniature endplate potential
MRC	Medical Research Council
MuSK	muscle specific kinase
NMJ	neuromuscular junction
RNA	ribonucleic acid
RNS	repetitive nerve stimulation
ROI	Republic of Ireland
SCS	slow channel syndrome
SFEMG	single fibre electromyography
SR	sarcoplasmic reticulum
STIM1	stromal interaction molecule 1
STIR	short-tau-inversion-recovery
T1w	T1 weighted
TAM	tubular aggregate myopathy
Tf	transferrin
TNM	transient neonatal myasthenia
UK	United Kingdom
$VGNa^{+}C$	voltage-gated sodium channel

Chapter 1

Introduction

In recent decades significant advances in diagnostics and therapeutics have no doubt improved the lives of people affected by congenital myasthenic syndromes (CMS). Specifically, the characterization of these distinct clinical syndromes, galvanized by the ability to establish definitive genetic diagnoses, has led to the evolution of subtype specific treatment regimens. So while congenital myasthenic syndromes are incurable and lifelong disorders the story certainly doesn't end there.

Congenital myasthenic syndromes are a group of inherited disorders of signal transmission at the neuromuscular synapse. They result from mutations in genes that encode synaptic components and, unlike autoimmune myasthenia gravis (AIMG), have no immunological basis. The syndromes typically manifest with fatigable muscle weakness which is usually of early onset. Typically there is evidence of a neuro-transmission defect on electrophysiological testing with single-fibre electromyography (SFEMG) or repetitive nerve stimulation (RNS). With the exception of slow channel syndrome they are of autosomal recessive inheritance. The severity of weakness varies between individuals, but as respiratory muscles can be affected some patients are at risk of death.

Without doubt the provision of a specialist national CMS service has helped enormously in the expansion of our knowledge of these neuromuscular disorders. Increased sophistication in both clinical practice and healthcare delivery now allows patients to access a broad range of essential services regardless of where in the UK they live. In addition to effective drug treatments, this includes genetic counselling and physiotherapy, as well as effective respiratory management. Indeed, for some patients it has likely meant avoiding the iatrogenic weakness caused by pyridostigmine that is seen in some CMS subtypes.

The research topics presented within this thesis have been identified as currently relevant areas in which there is potential to lead to further improvements in care. The choices were influenced by insight gained by working within the national CMS service and include a combination of clinical and laboratory work relating to the diagnosis and treatment of these disorders. First a clinical characterization of four novel CMS subtypes in which aberrant glycosylation is thought to underlie the defect in neurotransmission is presented. Next is a prospective imaging study investigating whether muscle MRI is of diagnostic utility in CMS. The last two results chapters detail laboratory studies in which the potential benefit of two novel drug treatments was investigated in transgenic mouse models of CMS.

A general review of current knowledge and understanding of congenital myasthenic syndromes follows in this introductory chapter, along with a brief introduction to each research topic and the general aims of the work undertaken. Detailed methods relating to laboratory work are provided in Chapter 2 and a more detailed review of current literature relating to each topic is presented in the relevant chapters.

1.1 Epidemiology [1]

To date at least 18 genes associated with CMS have been identified (Table 1.1). The syndromes are collectively and individually rare, though mutations in three genes; that encoding the acetylcholine receptor (AChR) ε-subunit (*CHRNE*), *RAPSN* and *DOK7* account for approximately 75% of UK CMS. An analysis of all genetically confirmed cases known to the CMS service found an overall UK prevalence of 3.8 per million. However, a recent study of paediatric genetically confirmed cases found the UK prevalence of CMS in children under 18 years to be 9.2 per million (Parr et al. 2014). Prevalence varied considerably between regions, most widely in the paediatric study, ranging from 2.8 - 15.5 per million in different UK strategic health authorities or devolved nations. Although this variability may be partially explained by differences in the racial composition of populations and familial clustering it is likely that many patients are undiagnosed.

1.2 Normal neuromuscular junction transmission [1]

Pathological mechanisms differ between CMS subtypes and are governed by the normal function of the affected protein at the synapse. Thus an understanding of normal neuromuscular junction (NMJ) assembly and function is necessary.

The nicotinic AChR of the NMJ has been comprehensively studied since its isolation in 1971(Miledi, Molinoff, and Potter 1971). Considered the archetypal ligand gated ion channel; its functional properties were the first to be described with single-channel patch clamp recordings (Neher and Sakmann 1976; Unwin 2013). More

[1] Adapted with permission from Finlayson and Palace 2014, 175-183, © Oxford University Press.

recently, through electron microscopy and crystallography techniques, structural properties and complexities of its gating mechanism have been described in detail (Unwin 2013). Discovery of other synaptic components and signalling pathways integral to NMJ transmission as well as to the development of the synapse have occurred in parallel. A great deal of effort has been concentrated on unravelling the mechanisms of AChR clustering, and much of this knowledge has been gained through molecular biological techniques, such as experiments with cultured muscle cells. Relatively less is known about how retrograde signals direct presynaptic differentiation, but this area will likely continue to become increasingly complex (Wu, Xiong, and Mei 2010). A fully comprehensive review is beyond the scope of this thesis and the following brief discussion outlines the key concepts.

Normal neuromuscular transmission is a robust process that elicits muscle contraction in response to a nerve terminal action potential. The electrical nerve impulse is transduced into chemical energy in the form of synaptic neurotransmitter acetylcholine (ACh) and then back to electrical energy, generating an action potential (AP) within the muscle.

The synapse acts as a switch with rapid and precise control over movement. Although each nerve action potential yields a muscle contraction in a 1:1 ratio the amount of neurotransmitter released by the nerve is estimated to be three to five times over the threshold for generating a muscle action potential (Wood and Slater 2001). This overcompensation is termed the ‘safety factor’ and means that transmission does not fail under normal conditions.

SYNDROME	GENE	PROTEIN
	Presynaptic	
ChAT	• *CHAT*	Choline acetyltransferase
	Synaptic	
Acetylcholinesterase deficiency (COLQ)	• *COLQ*	Collagen- like subunit tail of acetylcholinesterase
LAMB2	• *LAMB2*	Laminin beta2 subunit
	Postsynaptic	
Acetylcholine receptor (AChR) deficiency	• ***CHRNE**** • *CHRNA* • *CHRNB* • *CHRND*	AChR epsilon subunit AChR alpha subunit AChR beta subunit AChR delta subunit
Kinetic abnormalities (fast and slow channel syndrome)	• *CHRNE* • *CHRNA* • *CHRNB* • *CHRND*	
Rapsyn	• *RAPSN*	Receptor associated protein of the synapse
DOK7	• *DOK7*	Downstream of kinase 7
MuSK	• *MUSK*	Muscle specific tyrosine kinase
GFPT1	• *GFPT1*	Glutamine-fructose-6-phosphate transaminase 1
DPAGT1	• *DPAGT1*	Dolichyl-phosphate (UDP-N-acetylglucosamine) N-acetylglucosaminephosphotransferase 1
ALG2	• *ALG2*	An alpha-1, 3-mannosyltransferase
ALG14	• *ALG14*	Interacts with other proteins to form a multiglycosyltransferase complex
Agrin	• *AGRN*	Agrin
Sodium channel	• *SCN4A*	Skeletal muscle sodium channel ($Na_v1.4$)
LRP4	• *LRP4*	Low density lipoprotein receptor-related protein 4
Escobar syndrome**	• *CHRNG*	AChR gamma subunit

Table 1.1: Congenital myasthenic syndromes: *Predominantly *CHRNE* affected.
**Consequences of muscle weakness during early gestation causes phenotype. Neuromuscular transmission is thought to be normal post-natally. Adapted from Finlayson and Palace 2014, 175-183, by permission of Oxford University Press. © Oxford University Press.

A number of features contribute to the efficiency of this process. The safety factor is reliant on both structural and functional integrity at the synapse. While presynaptic neurotransmitter release can be modulated in response to shifting requirements almost immediately, the structure of the postsynaptic region cannot. However, the architecture of the postsynaptic region exhibits specific features that allow an economical and effective response to neurotransmitter release, thereby conserving the safety factor.

The neurotransmitter ACh is packaged in synaptic vesicles within the nerve terminal (Figure 1.1). Each vesicle is thought to contain between 5000 – 10000 molecules of ACh (Kuffler and Yoshikami 1975) and the contents of an individual vesicle are commonly referred to as a quantum. The vesicles cluster in areas termed 'active zones'. Vesicle exocytosis is stimulated by calcium influx triggered by the nerve action potential, releasing ACh into the synaptic cleft where by diffusion it reaches the AChR. The postsynaptic membrane has deep folds, the openings of which are situated opposite the active zones. Acetylcholine receptors are concentrated at high density on the crests of these folds.

Adult AChR are pentameric structures comprising alpha (α), beta (β), delta (δ), and epsilon (ε) subunits in a ratio of 2:1:1:1 (Figure 1.2). A separate gene encodes each subunit. The fetal form of AChR contains a gamma (γ) subunit in place of the ε-subunit, and is thought to play a role in organogenesis of the nerve–muscle junction (Hoffmann et al. 2006). AChR channel opening is triggered by ACh binding which allows a flow of cations through the central pore, thereby depolarizing the postsynaptic muscle membrane and generating an endplate potential (EPP). If the EPP reaches a critical threshold, voltage-gated sodium channels ($VGNa^{+}C$) at the folds open generating an action potential leading to actin-myosin coupling and muscle contraction.

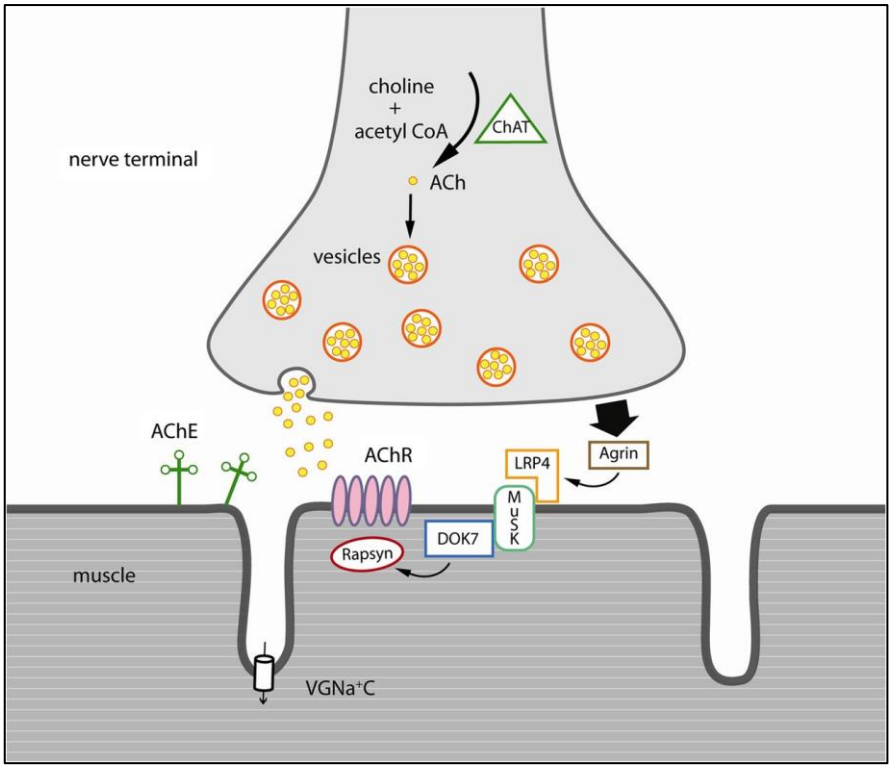

Figure 1.1: The neuromuscular junction with proteins involved in neuromuscular transmission: ACh, acetylcholine; AChE, acetylcholinesterase; AChR, acetylcholine receptor; ChAT, choline acetyltransferase; DOK7, downstream of kinase 7; LRP4, low density lipoprotein receptor-related protein 4; MuSK, muscle specific kinase; VGNa^{+}C, voltage-gated sodium channel. Reproduced from Finlayson, Beeson, and Palace 2013 (URL: http://www.pn.bmj.com/content/13/2/80).

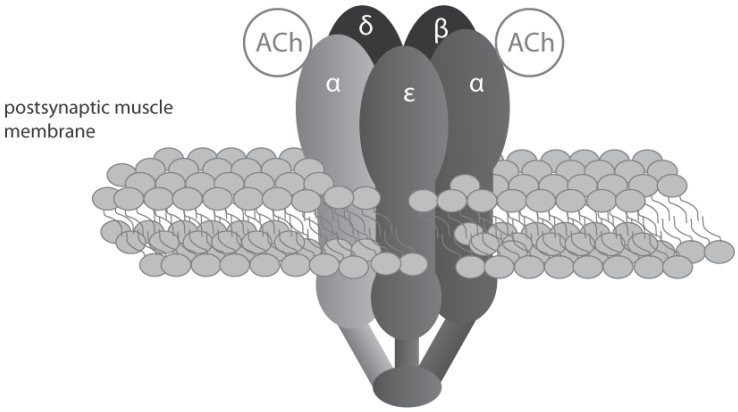

Figure 1.2: The adult acetylcholine (ACh) receptor: Di-liganded binding of ACh to the α-subunits triggers opening of the central ion channel. Reproduced from Finlayson and Palace 2014, 175-183, by permission of Oxford University Press. © Oxford University Press.

In addition to EPPs generated by nerve terminal AP, individual quanta are spontaneously released into the cleft with a frequency of at least several per minute. These quanta cause small depolarizations of the muscle membrane, miniature endplate potentials (MEPPs), which are not sufficient to generate muscle contraction.

The narrow morphology of the interfold spaces and clusters of voltage-gated sodium channels at the depths of the folds both serve to amplify the neurotransmitter effect, thereby making efficient use of the available ACh. The basal lamina within the cleft is a single-layer extracellular matrix rich in proteins and glycoproteins not found at non-synaptic regions. These include laminin, agrin, and acetylcholinesterase (AChE) which terminates NMJ transmission by enzymatically cleaving ACh into acetate and choline. The resulting choline is transported back to the nerve terminal, where it is recycled by choline acetyltransferase (ChAT).

Localization and clustering of AChRs on the crests of folds is critical for maintaining safety factor and is triggered by a number of proteins. A signalling cascade involving the CMS associated proteins agrin, LRP4, MuSK and DOK7 promotes rapsyn mediated AChR clustering. Additionally, there is emerging evidence that Wnt signalling plays a role in NMJ synaptogenesis. Wnts are a family of glycoproteins with diverse regulatory roles, and while they have been speculated to interact with MuSK, their effect at the NMJ remains to be clearly defined (Wu, Xiong, and Mei 2010).

Several genes involved in different aspects of the formation and maintenance of this specialized synapse have now been identified. Mutations in these genes can disrupt structure and/or function by various methods, but ultimately result in loss of the safety factor and failure of NMJ transmission. While some genes, such as *RAPSN* or *DOK7*, are associated with individual syndromes, the genes encoding AChR subunits are

associated with more than one subtype of CMS and may be implicated in fast or slow channel syndrome or AChR deficiency syndrome. Figure 1.3 shows the percentage distribution of CMS subtypes occurring in the UK and Republic of Ireland.

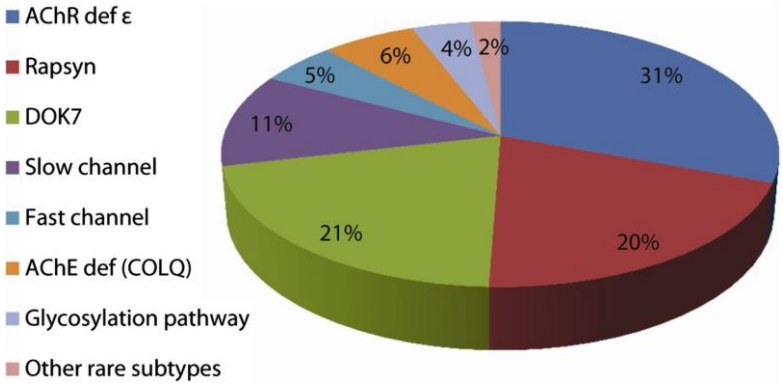

Figure 1.3: Proportions of genetically defined congenital myasthenic syndrome (CMS) subtypes in the British Isles: total n=255, AChR def ε: acetylcholine receptor deficiency due to ε-subunit mutations; DOK7, downstream of kinase-7; AChE def (COLQ), acetylcholinesterase deficiency. Reproduced from Finlayson, Beeson, and Palace 2013 (URL: http://www.pn.bmj.com/content/13/2/80).

1.2.1 Electrophysiological measurement of neurotransmission

Microelectrode studies of endplate regions in isolated nerve-muscle preparations can allow recording of electrophysiological parameters of neurotransmission. Both spontaneous MEPPs and nerve-evoked EPPs can be recorded. In patients with congenital myasthenic syndromes biopsied intercostal muscles have been studied using this technique, whereas in rodents phrenic-nerve hemidiaphragm preparations are typically used. This kind of approach has allowed normative data in different species (Boyd and Martin 1956; Fatt and Katz 1951) to be measured and also lends itself to the

pathophysiological study of CMS in transgenic mouse models. This experimental method was used in both of the laboratory studies presented in this thesis and a more detailed description of this technique is given in Chapter 2.

The concept of the safety factor and its estimation is of interest in that it can provide information about the normal function and development of the NMJ, as well as shedding light upon the pathophysiological mechanisms of NMJ disorders. The definitions and measurement techniques of the safety factor have previously been described in detail (Wood and Slater 2001). Estimation of the safety factor usually involves a comparison of the amount of neurotransmitter released per nerve impulse with that required to generate an action potential. However, it is not possible to determine both of these parameters in the same experiment. Because of this, and other technical factors, much experimental work focuses on electrophysiological recordings of the postsynaptic effects of the neurotransmitter, the results of which can be used as a proxy of sorts for the safety factor. Typically the safety factor is expressed in terms of quantal content (i.e. the number of quanta typically released per nerve impulse) which can vary significantly even during normal activity. Various methods of calculating the quantal content exist, but the most accurate method, according to Wood and Slater 2001, is the ‘direct method’ whereby quantal content is ascertained by dividing the amplitude of stimulated endplate currents by the amplitude of spontaneous miniature endplate currents. To calculate quantal content from measurements of endplate potentials, rather than current, requires additional mathematical correction for variations of resting membrane potential and for the effect of non-linear summation of EPP amplitude with each additional quantum. Further detail of these corrections is given in Chapter 2.

1.3 Subtypes of congenital myasthenia [2]

Much of the current understanding of different CMS subtypes has come from published single case reports or small case series, sometimes with electrophysiological studies on muscle tissue, which have helped to unravel the underlying mechanisms of NMJ transmission failure. The accumulation of this knowledge over time has resulted in a number of reviews of the clinical features of this group of disorders (Abicht et al. 2012; Engel 2011; Chaouch et al. 2012; Lorenzoni et al. 2012; Finlayson, Beeson, and Palace 2013). Traditionally the subtypes have been classified as presynaptic, synaptic or postsynaptic disorders, according to the main site of the underlying defect. A description of each of the known CMS subtypes follows.

1.3.1 Presynaptic

Choline acetyltransferase (ChAT) deficiency

The enzyme ChAT is active in the presynaptic nerve terminal where it functions in the resynthesis of ACh molecules. This condition is typically associated with sudden episodes of respiratory distress with apnoea and bulbar weakness and patients may be relatively strong in between such crises. Symptoms may be apparent from birth and continue episodically following initial improvement. However, affected children may be normal at birth and develop episodic apnoeas later during infancy or in childhood. The respiratory weakness may be prolonged, requiring days to weeks of artificial ventilation (Beeson et al. 2005) and infection is a common precipitant of these crises, which tend to reduce with age. There may be a background of other myasthenic

[2] 1.3.1, 1.3.2 and 1.3.3 adapted from Finlayson and Palace 2014, 175-183, by permission of Oxford University Press. © Oxford University Press.

symptoms. The condition is rare, but the published literature would suggest that while ptosis is a feature the extraocular muscles are spared (Kraner et al. 2003). Decrement on RNS and increased jitter on SFEMG may not be apparent in affected patients, particularly if they are tested between episodes. To demonstrate abnormal NMJ transmission it has been recommended that the tested muscle should be fatigued, either with exercise or with 10 Hz stimulation for up to 5 minutes (Beeson 2008, 239-254). This is challenging in the young. AChE inhibitors are helpful in providing symptomatic relief, as may be 3,4-diaminopyridine (3,4-DAP), which stimulates presynaptic ACh release. There is a theoretical concern that 3,4-DAP might further diminish the limited presynaptic ACh stores, but this does not appear to be a problem in practice. Prophylactic AChE treatment is advocated by some sources (Parr and Jayawant 2007; Beeson 2008, 239-254) as a means to reduce life-threatening apnoeas. The older classifications of ‘familial myasthenic syndrome’ and ‘CMS with episodic apnoea’ were attributed to a presynaptic abnormality. It is now appreciated that episodic apnoeas are also typical features in rapsyn and fast channel CMS.

1.3.2 Synaptic

Acetylcholinesterase deficiency (COLQ CMS)

Mutations in the AChE collagen-like tail subunit gene (*COLQ*) account for approximately 6% of genetically diagnosed CMS. At the normal NMJ this subunit tail anchors the enzyme to the basal lamina where it terminates neuromuscular transmission by hydrolyzing ACh. *COLQ* mutations cause loss of this enzyme, resulting in prolonged ACh lifetime in the synapse with consequent prolonged EPPs. This leads to a desensitization of the AChR and depolarization blockade. In addition the prolonged

endplate currents mean the muscle endplate is bombarded with cations, leading to a secondary excitotoxic myopathy. As a result the postsynaptic architecture is disrupted with loss of junctional folding. Typically the condition causes severe and progressive weakness from birth or early infancy. However, later onset and milder phenotypes are also recognized. Weakness often affects the respiratory muscles, with both respiratory crises and chronic hypoventilation occurring.

Prevalence of eye signs is variable in COLQ CMS. While ptosis and ophthalmoplegia are common they were both absent in just over 18% of patients in the largest published case series (Mihaylova et al. 2008). A slow pupillary response to light has classically been described, but was only demonstrated in 25% of patients within the same case series. Neurophysiological tests may show a repetitive compound muscle action potential (CMAP) response to single stimuli. This can also be seen in conditions other than COLQ CMS, including slow channel syndrome, or in cholinergic toxicity secondary to excess pyridostigmine or 3,4-DAP, or organophosphate poisoning. Patients may improve with ephedrine (Bestue-Cardiel et al. 2005; Mihaylova et al. 2008) or oral salbutamol (Liewluck, Selcen, and Engel 2011), both of which are adrenergic agonists. Their mechanism of action is incompletely understood, but both drugs are thought to improve the secondary myopathy by stabilizing the postsynaptic muscle membrane. Importantly, patients with COLQ CMS and some other subtypes can experience significant clinical deterioration with AChE inhibitor (Table 1.2). Paradoxically there may be initial short-term improvement, which can mislead. Although 3,4-DAP would theoretically be expected to worsen the underlying AChR desensitization and depolarization blockade characteristic of COLQ CMS, reports of it being useful in some patients exist (Wargon et al. 2011; Mihaylova et al. 2008).

Subtype	Typically worsen with	
	AChE inhibitors	3,4-DAP
Slow channel syndrome	+	+
Acetylcholinesterase deficiency (COLQ)	+	+*
DOK7	+	+/-

Table 1.2: Patient subtypes and clinical deterioration with acetylcholinesterase (AChE) inhibitor or 3,4-diaminopyridine (3,4-DAP) medication: +; associated with, +*; theoretical (see text above),+/- may worsen or improve symptoms. Adapted from Finlayson and Palace 2014, 175-183, by permission of Oxford University Press.

1.3.3 Postsynaptic

Acetylcholine receptor deficiency

This is the most common of the CMS subtypes with genetic screening most often revealing two different mutations in the ε-subunit (i.e. compound heterozygotes). A common mutation, 1267delG, has been reported to be present on at least one allele in 20% of a large cohort of patients (Palace and Beeson 2008). This arises from an ancient founder mutation in the Indian subcontinent, which was brought to Europe with the Roma migration, and is usually associated with a relatively mild phenotype (Morar et al. 2004). However, the majority of kinships have private mutations. Although normal maturational change in receptor conformation causes fetal γ-subunits to be replaced by ε-subunits during late gestation, low levels of fetal AChR expression continue into adulthood and can be increased when muscle is denervated. Thus the survival of patients with ε-subunit mutations is probably due to utilization of background fetal AChR which may function more effectively than the mutated adult form. The degree of this compensatory change may vary between patients, with some retaining a greater proportion of fetal AChR than others (Palace and Beeson 2008). There are few cases of

mutations in non ε-subunits. In these cases the phenotype tends to be severe and this is probably because the fetal form of AChR also contains the mutated subunit and so cannot compensate.

Symptom onset is usually at birth or in infancy. Feeding difficulties in early life and ptosis are common presenting features. Motor milestones are typically delayed. Unlike in rapsyn CMS, which also results in a functional deficiency of AChR, arthrogryposis is not a typical feature. While early 'worsenings' do occur in AChR deficiency they are not as dramatic as the crises seen in rapsyn or ChAT CMS. Ophthalmoplegia is striking in this type of CMS, where it is invariably a feature and virtually complete. Generalized weakness is typically present. Mild bulbar weakness is not uncommon, and respiratory weakness may be a feature though is less frequent than in many other CMS subtypes. The severity of this condition is highly variable, but most patients have a stable lifetime course. However, as with other types of CMS, exacerbation can occur with infection. Patients tend to have a good sustained response to cholinesterase inhibitors. 3,4-DAP is often used as a second-line agent in combination with cholinesterase inhibitors. Anecdotally, 3,4-DAP appears to have a better effect at reducing ptosis than pyridostigmine. Despite the other beneficial effects of these medications they tend to have no or little effect on the ophthalmoplegia seen in AChR deficiency and other subtypes.

Kinetic abnormalities

Some mutations in either α, β, δ or ε-subunits lead to a change in the kinetic properties of the channel. Those that cause abnormally brief channel openings result in fast channel syndrome (Ohno et al. 1996; Wang et al. 1999) and conversely slow channel

syndrome results from abnormally prolonged AChR channel opening (Engel et al. 1982). Despite the contrasting pathophysiology both ultimately lead to loss of safety factor and failure of neuromuscular transmission.

Fast channel syndrome

Here channel openings are brief as a result of either abnormally rapid closure of the channel or reduced probability of channel opening, or a combination of both mechanisms (Engel and Sine 2005). Typically, genetic analysis reveals one fast channel mutation combined with a low expresser or null mutation on the second allele. Thus far mutations in the α, δ, and ε-subunits have been reported. A common fast channel mutation, εP121L, was identifiable in at least one allele in 90% of a UK series (Palace et al. 2012).

Patients with fast channel syndrome tend to be symptomatic from birth or early infancy. In the same UK case series, where early history was available, all patients presented at birth with bulbar symptoms (Palace et al. 2012). Other symptoms at onset included ptosis, hypotonia, weak cry, and respiratory symptoms, which were common—with some infants requiring respiratory support at birth. Congenital stridor was reported in two patients, one of whom had bilateral vocal cord paralysis documented following microlaryngobronchoscopy. Arthrogryposis was reported in three. Notably this has not been reported thus far in AChR deficiency syndrome. The major concern in fast channel syndrome is of sudden life-threatening apnoeas often leading to repeated admissions to intensive care. These deteriorations may occur outwith episodes of infection and can be dramatic. In contrast to rapsyn and ChAT CMS, patients commonly remain weak in between crises. Involvement of a respiratory

specialist is usually necessary and parents and carers should be trained in cardiopulmonary resuscitation. Respiratory function may be normal between crises. In the UK series apnoeic attacks ceased in those who had survived childhood. Ophthalmoplegia is generally complete, although often not initially recognized, and is typically accompanied by ptosis. Patients usually respond to pyridostigmine, although the effect may diminish over time and the addition of 3,4-DAP may be needed.

Slow channel syndrome

This is the only dominantly inherited CMS. Here the mutation results in abnormally prolonged AChR channel opening with consequent prolonged EPPs. Like AChE deficiency it is associated with a depolarization blockade and nerve conduction studies can show repetitive CMAP to single stimuli. This overstimulation of muscle and the prolonged endplate currents lead to a secondary excitotoxic myopathy. Mutations occur in any of the adult receptor subunits, although about 70% of UK cases are affected by the α-subunit point mutation G153S (Finlayson, Beeson, and Palace 2013). Different mechanisms underlie the altered channel kinetics and depend upon the site of the mutation. Mutations in the extracellular amino-terminal domain tend to cause increased affinity of the receptor for ACh molecules, whereas mutations in the pore-lining M2 domain usually result in stabilization and hence prolongation of the open state. The age of onset of symptoms is widely variable but may be later than in many of the other CMS subtypes. Most patients present in childhood with neck flexion weakness or difficulty running. Some patients are affected from birth, but the typical early problems of feeding difficulties and apnoea seen frequently in other subtypes are not common. Onset has been recognized in the third and even fourth decade. Overall this condition

tends to be milder than the other subtypes and asymptomatic relatives are occasionally identified. A pattern of selective weakness of cervical and upper limb muscles, particularly affecting the distal arm and hand, has been identified (Engel et al. 1982; Oosterhuis et al. 1987). Within the hand, thumb abduction weakness is striking (Finlayson, Beeson, and Palace 2013). While ophthalmoplegia is common it does not tend to be as severe as in AChR deficiency or fast channel syndrome, and down gaze and adduction are relatively spared. Treatment for slow channel syndrome (SCS) relies on medications which block the AChR when in its open state. Thus the channel opening times and resulting cationic overload of the muscle endplate are reduced. Further discussion of these treatments follows below (Section 1.5.3). Patients may show a lack of response or even worsening of weakness with AChE inhibitors and 3,4-DAP and thus both drugs should be avoided.

Rapsyn

Rapsyn (receptor associated protein of the synapse) is a key protein in the initiation and maintenance of synaptic structures and specifically in clustering of AChR at the muscle endplate. Endplate studies in affected individuals and clustering assays in human embryonic kidney (HEK) cells (Ohno et al. 2002) and muscle cells expressing rapsyn mutations (Burke et al. 2003) show a reduced number of ACh receptors. However, rapsyn CMS presents a distinctly different phenotype compared with AChR deficiency syndromes due to AChR subunit mutations.

The N88K missense mutation is a common cause of rapsyn CMS in Europeans (Müller et al. 2003). Genotypic analysis has shown that this mutation arises from a common ancient Indo-European ancestor. Over 90% of rapsyn CMS patients harbour

the N88K mutation on at least one allele, making genetic screening for the majority of *RAPSN* cases relatively straightforward (Palace and Beeson 2008).

Two phenotypes of this recessive CMS have been described, early and late onset (Burke et al. 2004). The typical early onset pattern is of presentation at birth or early infancy with respiratory failure, feeding difficulties, or generalized hypotonia. Fetal akinesia *in utero* gives rise to characteristic dysmorphic facies and usually mild arthrogryposis which tends to resolve with physiotherapy. Patients commonly have a high arched palate, a feature that is not usually seen in other forms of CMS. Weakness is typically generalized and includes facial muscles. Ophthalmoplegia is not a feature, but ptosis may be present. Strabismus, usually divergent, is very common in rapsyn CMS and is a useful distinguishing feature. However, the main caveat to this is the high frequency of strabismus, convergent more than divergent, in the general population.

Exacerbations are frequent in the first few years of life and usually, but not always, occur in the context of intercurrent infection. Similar to ChAT CMS these episodic exacerbations can be associated with respiratory failure and apnoea and little weakness in between attacks. Although the frequency and severity of these life-threatening crises diminish during childhood and usually resolve around 6 years of age (Burke et al. 2004), the good response to AChE inhibitors, with or without 3,4-DAP, justifies early treatment to reduce early morbidity and mortality.

Less frequently patients present later in life, in adolescence or adulthood. Presentation in the fifth decade has been described (Burke et al. 2004). Their symptoms are milder than those with a typical early onset pattern and it is possible that early involvement has been overlooked. Homozygous N88K mutations are detected in both early and late onset phenotypes. Late onset rapsyn CMS may mimic autoimmune

myasthenia gravis. However, a useful differentiating sign when present is ankle dorsiflexion weakness which is unusual in acquired myasthenia gravis but not uncommon in CMS. Rapsyn CMS has a good long-term prognosis; it often improves during childhood and many adults are able to substantially reduce or even stop treatment.

DOK7

DOK7 (downstream of kinase 7) is a cytoplasmic protein that is essential for normal NMJ synaptogenesis (Okada et al. 2006). It interacts with MuSK (muscle-specific kinase) signalling pathways responsible for postsynaptic differentiation including AChR clustering. Mutations in *DOK7* result in a synaptopathy with abnormally simplified NMJs bearing postsynaptic endplate regions with reduced junctional folding. It is postulated that such postsynaptic changes alter retrograde signalling giving rise to the small presynaptic regions that have also been described (Beeson et al. 2006). Individual receptor subunits and AChE are normal in structure and function. Most patients harbour at least one truncating frameshift mutation in exon 7 (Palace and Beeson 2008).

Infants are often asymptomatic with normal early motor milestones and onset is usually in early childhood, presenting with difficulties in walking. However, some patients have earlier symptoms such as ptosis, and more severe cases may present with neonatal stridor or feeding difficulties from birth (Jephson et al. 2010). Weakness in DOK7 CMS is usually generalized and most often proximal predominant in the limbs giving rise to a limb-girdle phenotype. Features that help to distinguish this from other subtypes are tongue wasting and sparing of the extraocular muscles. Ptosis is often

moderate to severe and there may be a pronounced snarling smile. Bulbar and respiratory weakness are common and can present later in the course of the disease. In addition to fatigable weakness, worse towards the end of the day, DOK7 patients can report variation in their symptoms over longer time periods, i.e. weeks to months. Sudden dramatic fluctuations are not typical of DOK7 CMS. The protein encoded by *DOK7* is expressed in cardiac muscle (Okada et al. 2006), but the condition does not appear to be associated with cardiomyopathy and electrocardiograms are typically normal. Patients often have a slowly progressive clinical course. Muscle biopsy tends to show mild myopathic change and the associated myopathic features may be the cause of the progressive weakness and the worsening commonly seen with AChE inhibitors (although a temporary initial response may be noted). 3,4-DAP may also worsen symptoms but can sometimes reduce DOK7 CMS weakness. Ephedrine (Lashley et al. 2010) or oral salbutamol (Liewluck, Selcen, and Engel 2011; Lorenzoni et al. 2013) are the mainstay of treatment; improvement tends to develop slowly, over many months, but may be dramatic.

CMS due to defects in glycosylation pathways

Within the last 5 years four novel CMS disease genes that encode proteins involved in glycosylation pathways have been identified. As glycosylation is a ubiquitous post-translational modification the discovery of these conditions with symptoms limited to mainly an NMJ transmission defect is surprising. Following the discovery of DOK7 CMS in 2006 it was appreciated that there remained a group of patients with limb-girdle weakness in which the gene defect remained unknown. The first of the group to be identified was *GFPT1* (glutamine-fructose-6-phosphate transaminase 1), a rate-limiting cytoplasmic enzyme at the beginning of the hexosamine biosynthesis pathway, the obligatory source of essential amino sugars involved in protein and lipid glycosylation

(Senderek et al. 2011). The condition differs from DOK7 in that the facial muscles are spared and tubular aggregates are seen on muscle biopsy. Additionally there is a good response to AChE inhibitors. Following this discovery mutations in three genes which encode early components of the N-linked glycosylation pathway; *DPAGT1* (Belaya et al. 2012b), *ALG2* and *ALG14* (Cossins et al. 2013), have been associated with congenital myasthenic syndromes similar in phenotype to GFPT1 CMS. A full discussion of the clinical and investigative features of these novel CMS subtypes is presented in Chapter 3.

1.3.4 Other rare subtypes

To date at least five further genes encoding a protein present at the NMJ have been associated with a congenital myasthenic syndrome. All are extremely rare.

CMS caused by mutation in *SCN4A*, the gene encoding the $Na_V1.4$ sodium channel of skeletal muscle, has been reported in one patient. This patient had generalized fatigable weakness and recurrent episodes of respiratory and bulbar muscle weakness from birth. The mode of inheritance is unclear (Tsujino et al. 2003).

One case of a synaptic CMS due to mutation in *LAMB2*, the gene encoding the basal lamina glycoprotein subunit laminin beta 2, has been reported (Maselli et al. 2009). The patient had congenital nephrosis and ocular malformations in addition to myasthenia.

Mutations in *AGRN* (Huzé et al. 2009; Eymard et al. 2013) and *MUSK* (Chevessier et al. 2004; Ben Ammar et al. 2013), both of which code for key proteins involved in postsynaptic differentiation, have been shown to cause congenital

myasthenia. Neural agrin, the product of *AGRN*, is released by the nerve terminal and activates MuSK. Muscle biopsy of a patient with mutant *MUSK* demonstrated abnormal postsynaptic AChR clustering and presynaptic nerve terminal sprouting (Chevessier et al. 2004). Most recently a single patient with heteroallelic mutations in *LRP4*, which encodes a receptor for neural agrin, was reported (Ohkawara et al. 2013). This patient had a CMS with respiratory arrest at birth and moderately severe weakness which worsened following a short trial of pyridostigmine.

Escobar syndrome

Mutations in the γ-subunit cause defective fetal AChR, leading to fetal akinesia and subsequent dysmorphism and may be lethal (Morgan et al. 2006). Characteristically severe arthrogryposis multiplex congenita (AMC) and multiple pterygium are seen. Other features can include scoliosis, pulmonary hypoplasia, neonatal respiratory distress, craniofacial dysmorphism, low-set ears, arachnodactyly, and cryptorchism in males. Reduced intrauterine movement is normally reported and there is often a history of recurrent spontaneous abortion (Hoffmann et al. 2006).

The condition is recessive, and mutations lead to an impaired, truncated, or absent γ-subunit. The fetal form of AChR is considered to be important in NMJ organogenesis in addition to NMJ transmission. In humans the transgression from fetal to adult AChR occurs gradually in the late perinatal and early neonatal period. Thus affected children show no signs of myasthenia after birth and EMG did not show evidence of myasthenia in any of the five children tested in a published case series (Hoffmann et al. 2006).

1.4 Diagnosis of congenital myasthenic syndromes

The characteristic phenotypes described above are often helpful in establishing a genetic diagnosis and the key distinguishing features are summarized in Table 1.3. However, despite these often distinctive phenotypes the diagnosis of CMS is not always straightforward. This may be because the CMS causing gene is not yet discovered. The proportion of patients suspected of having CMS but in whom no genetic defect has been identified varies between reports. In the UK this is thought to represent an estimated 10-20% of patients (Finlayson, Beeson, and Palace 2013), however, in a large European cohort just 44% of patients suspected of having CMS had disease causing mutations identified (Abicht et al. 2012). Another possibility, which may also explain some of this variation, is that patients may be incorrectly diagnosed. Common CMS mimics and the main diagnostic techniques and strategies are discussed below.

1.4.1 Neurophysiological testing [3]

Neurophysiological findings in CMS are typically the same as those found in AIMG. There is usually raised jitter on single-fibre EMG although this can be normal if unaffected muscles are tested (Figure 1.4). Depending upon the severity of NMJ transmission failure, there may be blocking of potentials on SFEMG and the RNS equivalent of abnormal CMAP amplitude decrement (Figure1.5). SFEMG is more sensitive, but less specific, than RNS and increased jitter can be seen in myopathic and neurogenic disorders, although typically the degree of abnormality is less severe than in myasthenia. As with AIMG it is not uncommon to see mild myopathic potentials on standard EMG.

[3] Adapted from Finlayson, Beeson, and Palace 2013 (URL: http://www.pn.bmj.com/content/13/2/80).

SYNDROME	TYPICAL AGE OF ONSET	TYPICAL PRESENTING FEATURES	OCULAR		RESPIRATORY CRISES	OTHER
			Ophthalmoplegia	Other		
Choline acetyltransferase deficiency	birth and infancy	episodic apnoeas	absent		+	may be normal between episodes of apnoea
Acetylcholinesterase deficiency	birth>infancy>childhood	ptosis, falls, slower than peers, poor feeding	present>absent	slowed pupillary response following constriction to light	+	chronic hypoventilation
Acetylcholine receptor deficiency	birth and infancy	ptosis, poor feeding	severe			generally stable course
Rapsyn	birth and infancy	crises, ptosis, poor feeding, contractures may require ventilation at birth.	absent	strabismus: may be convergent or divergent and latent or manifest	+ often resolve in late childhood	dysmorphic features
	a milder late onset phenotype with limb weakness +/- ptosis is also recognized					

Table 1.3: Distinguishing features of subtypes: For ophthalmoplegia the typical findings are listed. +, associated with. Reproduced from Finlayson, Beeson, and Palace 2013 (URL: http://www.pn.bmj.com/content/13/2/80).

Table 1.3: (continued)

SYNDROME	TYPICAL AGE OF ONSET	TYPICAL PRESENTING FEATURES	OCULAR		RESPIRATORY CRISES	OTHER
			Ophthalmoplegia	Other		
DOK7	early childhood e.g. 2-4 years	deterioration in walking/ falls in a child who has achieved normal milestones	absent			limb-girdle weakness, tongue wasting, stridor
	onset at birth with stridor and poor feeding also recognized					
Slow channel syndrome	variable birth-adulthood	hypotonia or weak neck muscles at birth/infancy limb weakness – especially distal upper limb, ptosis, slower than peers, difficulty running	mild-moderate or absent			autosomal dominant
Fast channel syndrome	birth	respiratory crises/apnoea, ptosis, weak cry, poor feeding/choking may require ventilation at birth.	severe		+ abrupt	usually profound weakness
GFPT1, DPAGT1	early childhood	deterioration in walking, falls, limb weakness	absent	ptosis mild or absent		little or no facial weakness, tubular aggregates on muscle biopsy

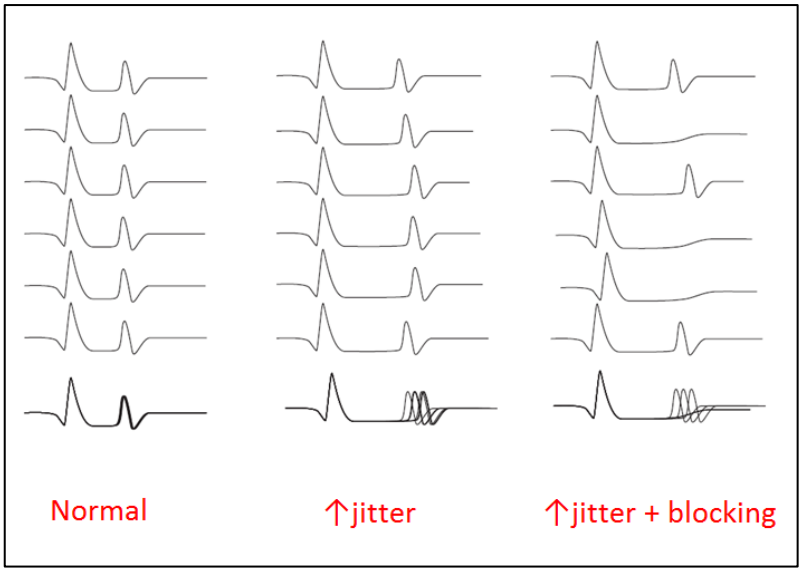

Figure 1.4: Volitional single-fibre EMG: Example recordings of muscle fibre action potential pairs are shown in each column with superimposed traces in the bottom row. Normal recordings (left hand column) superimpose well with little variability in the inter-peak interval. Abnormal jitter measurement occurs when there is excessive variability in inter-peak interval (middle column) and may be associated with the more abnormal finding of blocking (right hand column).

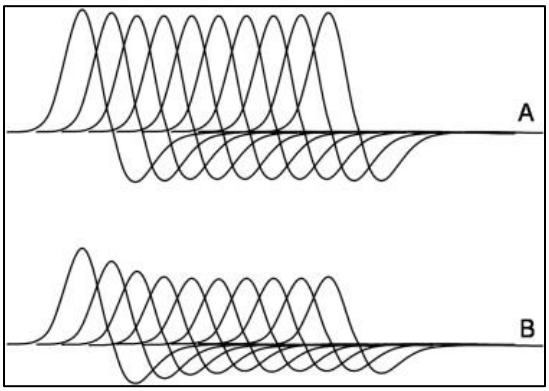

Figure 1.5: Repetitive nerve stimulation: Showing **A.** normal results and **B.** CMAP decrement. [4]

Some syndrome specific features exist which can help to establish the diagnosis. A repetitive CMAP evoked by a single stimulus can sometimes be seen in slow channel syndrome and in COLQ CMS. Usually a double response is seen, but it may be treble or more. This feature was reported in ~67% of patients with COLQ CMS (Mihaylova et al.

[4] Reprinted from Paediatric Neurology, 46 (3), Lorenzoni et al, Congenital Myasthenic Syndrome: A Brief Review, 141-8, Copyright 2012, with permission from Elsevier.

2008) and has been detected in 53% of those tested in the slow channel syndrome cohort seen by the national CMS clinic in Oxford. Like the initial CMAP, the repetitive discharges can exhibit decrement but because they are lower in amplitude may disappear quickly on repetitive stimulation and be overlooked. In SCS and COLQ CMS the degree of CMAP decrement is rate dependent, increasing with higher stimulation frequency.

1.4.2 Differentiating from AIMG

When clinical features or neurophysiology suggest a myasthenic condition but AChR antibodies are negative differentiating congenital from autoimmune myasthenia is critical. By doing so unnecessary thymectomy and immunosuppressive therapy can be avoided. Recently a cell-based assay which uses rapsyn to cluster AChRs to the cell surface has been developed. This assay was able to detect 'low-affinity' AChR antibodies in 66% of a group of 38 patients who were 'seronegative' in the standard radioimmunoprecipitation assay (Leite et al. 2008). However, a proportion of AIMG patients will remain seronegative on both assays.[5] Clinical features that point more towards an autoimmune rather than an inherited process are a) asymmetry of clinical findings (ptosis being an exception in that it may be asymmetrical in CMS also), b) later onset of disease, c) acute onset from normality to ongoing non-resolving weakness (i.e. not typical crisis) and d) spontaneous resolution which appears common in childhood acquired MG. Symptom onset at birth or early infancy is strongly suggestive of congenital myasthenia. [6]

[5] Adapted from Finlayson, Beeson, and Palace 2013 (URL: http://www.pn.bmj.com/content/13/2/80).
[6] Adapted from Finlayson and Palace 2014, 175-183, by permission of Oxford University Press. © Oxford University Press.

1.4.3 Other mimics [7]

Primary muscle disease is another major differential diagnosis and many CMS patients, particularly those with DOK7 CMS, have been initially diagnosed with myopathies such as muscular dystrophies and congenital myopathy. Myopathy can have similar patterns of neuromuscular weakness as CMS, can occasionally show mild symptomatic improvement with AChE inhibitors and can also have raised jitter on SFEMG. Often muscle biopsy is helpful in differentiating.

The role of muscle MRI in the diagnosis of CMS is less clear. In recent years MR imaging, usually of lower limb muscles, has played an increasing role in the diagnosis of muscle disorders (Mercuri et al. 2007; Straub, Carlier, and Mercuri 2012). In the congenital myopathies and dystrophies in particular, muscle MRI can help to direct genetic testing because of the selective pattern of muscle involvement that can sometimes be seen.

Other mimics include fatigue syndromes; distinguished mainly by a lack of objective muscle weakness, and mitochondrial disease which characteristically has multisystem involvement. In addition some congenital cranial dysinnervation disorders (CCDDs) can cause bilateral ptosis and restriction of eye movements and can mimic myasthenia.

In children the finding of hypermobility (joint laxity) with or without dyspraxia can cause significant functional compromise. Mild objective muscle weakness can also

[7] Adapted from Finlayson, Beeson, and Palace 2013 (URL: http://www.pn.bmj.com/content/13/2/80).

be associated making it easy to mistake for CMS, especially as joint laxity is fairly common in CMS, and more so in children.

Another paediatric presentation which may prove challenging to evaluate is a combination of hypotonia, respiratory and bulbar symptoms. These are non-specific features in neonates and infants, of which CMS is only one of many causes. Evaluating these children can be challenging and is further confounded by the difficulty assessing generalized muscle strength at this age.

1.4.4 Next generation DNA sequencing

Next generation DNA sequencing refers to a number of different high-throughput sequencing techniques. These recent technologies allow large regions of DNA or multiple mRNAs to be sequenced much more quickly and cheaply than the previously used Sanger sequencing. While they have revolutionized the study of genomics they do not always cover all genes and require significant post-sequencing data analysis and are not yet universally available for all patients. The genes underlying three of the novel CMS subtypes described in Chapter 3 were identified by such techniques.

1.5 Drug treatments [8]

Choice of treatment in CMS varies by subtype. All treatments in congenital myasthenia are used off-license.

[8] 1.5.1, 1.5.2 and 1.5.3 adapted from Finlayson, Beeson, and Palace 2013 (URL:http://www.pn.bmj.com/content/13/2/80).

1.5.1 Cholinesterase inhibitors and 3,4-diaminopyridine

Both reduce myasthenic weakness by causing an increase in EPP amplitude and therefore an increase in safety factor but achieve this by different mechanisms. Cholinesterase inhibitors prolong the lifetime of ACh at the endplate giving more opportunity for each molecule to bind to a receptor. 3,4-DAP is a potassium channel blocker whose action on the presynaptic nerve terminal results in increased release of ACh into the synaptic cleft. Both drugs are often used together to provide symptomatic relief. As previously mentioned, these treatments will worsen the weakness of some CMS subtypes and they should be avoided in these conditions.

1.5.2 Ephedrine and oral salbutamol

Both agents stimulate muscle β_2-adrenergic receptors and are thought to improve signal transmission by stabilizing the postsynaptic architecture.

Their effect is well established in DOK7 and COLQ CMS where they form the mainstay of treatment. Response can be dramatic, even when therapy is started in adulthood. Small numbers of patients with other subtypes including AChR deficiency, slow channel syndrome (Finlayson et al. 2013b), GFPT1 and DPAGT1 (Finlayson et al. 2013a) have also found some benefit.

Typically improvement begins within a month of starting treatment and continues for a period of approximately 6-9 months before reaching a plateau. It is not clear if either ephedrine or salbutamol is superior although some patients will report a better response to one or other and there is probably a quicker response to salbutamol. The

main side effects to look out for are insomnia, cardiac effects such as tachycardia, palpitations and hypertension and muscle cramps particularly with salbutamol.

1.5.3 Fluoxetine and quinidine in slow channel syndrome

Entirely different treatments are typically used to treat slow channel syndrome compared with other forms of CMS. The primary pathogenic mechanism is of an abnormally prolonged opening of the central ion channel pore of the AChR. Both fluoxetine and quinidine are open channel blockers and bind the channel in its open state preventing cation flow, and thereby reduce channel opening time. It is not known whether either treatment is more effective, however, fluoxetine is the drug of choice. It has a better safety profile than quinidine, which can cause QT interval prolongation and requires ECG and serum level monitoring. A caveat to this is the potential risk of suicidality in children and adolescents treated with fluoxetine. The effective dose of fluoxetine is variable with some patients responding to low doses (20 mg) and others requiring large doses of 120 mg per day, though effective dose titration may be limited by adverse effects in some (Chaouch et al. 2012).

1.6 Aims and objectives

The aims of the work detailed in the following chapters are summarized below.

1.6.1 Chapter 3

The identification of four novel CMS disease genes that are thought to cause aberrant glycosylation widens the pathophysiological spectrum of CMS and is an unexpected cause of isolated neurotransmission defect. While these genes and the associated clinical features have previously been reported, these disorders have not been systematically characterized as a group and are probably underdiagnosed at present. As is evident from the clinical descriptions above, the characterization of syndromes has a pivotal role in best patient management.

The main aims of the work in Chapter 3 are

i. To characterize the CMS syndromes caused by mutations in *DPAGT1*, *ALG2, ALG14* and *GFPT1*.
ii. To compare and contrast the phenotype of these syndromes with other forms of CMS.

1.6.2 Chapter 4

As stated, although muscle MRI is becoming increasingly used in the diagnosis of neuromuscular disorders, and especially in inherited myopathies and dystrophies, its utility in CMS is largely unknown. Since some myopathic and neuropathic disorders may mimic CMS an appreciation of MRI findings is therefore relevant to the investigation of patients with neuromuscular disease. While muscle MRI findings in a small group of children with DOK7 CMS have previously been reported in brief (Klein et al. 2013), no detailed reports comparing MRI appearance between different CMS subtypes have been published. There is some histological evidence to suggest that

muscle imaging may be abnormal in CMS and that some subtypes may demonstrate more abnormality than others. Firstly, muscle biopsies from patients with most CMS subtypes have been shown to exhibit mild myopathic changes (Kinali et al 2008; Klein et al. 2013), though some subtypes have specific pathological features that suggest they are likely to have greater secondary muscle damage than others. Second, the glycosylation pathway subtypes described in Chapter 3 have been associated with the specific finding of inclusions within muscle fibres, known as tubular aggregates, on biopsy. Thus it is possible that patients with CMS could demonstrate abnormal muscle MRI signal and those findings may help to differentiate between the different subtypes. In addition to potential diagnostic utility, the potential role of muscle imaging as a biomarker for CMS, in clinical practice or drug trials, is especially relevant due to the treatable nature of these disorders.

A prospective imaging study using simple 3T-MRI sequences that are ideal for use in routine clinical practice was undertaken. The aims of this study were to:

i. Define the nature and extent of any abnormalities on lower limb muscle MRI in different congenital myasthenic syndromes.
ii. Correlate muscle MRI findings with clinical parameters including CMS subtype.

1.6.3 Chapters 5 & 6

Chapters 5 and 6 describe laboratory work investigating the effect of two potential novel drug treatments in transgenic mouse models of CMS. While treatments are available for CMS some patients have significant and sometimes life-threatening weakness despite receiving all available medication. Each drug tested in either chapter is already licensed for use in another medical condition. In Chapter 5 the effect of the

antiepileptic drug lamotrigine is tested in a transgenic mouse model of slow channel syndrome and in Chapter 6 the antiemetic metoclopramide is tested in a model of AChR deficiency syndrome. Both drugs were chosen as candidate treatments based on patient reports of them leading to an improvement in their myasthenic symptoms. A more detailed discussion of these drugs and speculation as to potential mechanisms by which they could improve neurotransmission is provided in these later chapters. The aim of these studies was to:

i. Evaluate whether lamotrigine could be a potential treatment for slow channel syndrome and whether metoclopramide can augment NMJ transmission in AChR deficiency syndrome.

ii. Evaluation is by a combination of *ex vivo* and *in vivo* electrophysiological techniques, as well as by testing the effect of the drugs on sustained muscle effort. Electrophysiological techniques include microelectrode studies of endplate potentials measured in phrenic-nerve hemidiaphragm preparations and measurements of CMAP decrement obtained by RNS. A description of both techniques follows in Chapter 2.

Chapter 2

Materials and methods

2.1 MRI study

Details of MRI acquisition and analysis technique are given in Chapter 3.

2.2 Transgenic mouse models

Established transgenic mouse models of slow channel syndrome and acetylcholine receptor deficiency syndrome were available in the laboratory. Both models demonstrate fatigable muscle weakness, have muscle wasting and electrophysiological evidence of neuromuscular transmission defect.

2.2.1 Animal work and licences

Same sex groups of mice were housed together in groups of 2-6. Pellet feed and water were continuously available. Their environment was regulated to provide a 12 hour light/12 hour dark cycle. Animal work was performed by myself, and authorized by the Home Office issued project license (PPL 30/2404 and 40/3570) and personal license

(PIL30/9279). Genotyping by polymerase chain reaction of ear clip DNA was performed mainly by Mrs Susan Maxwell.

2.2.2 Slow channel syndrome model

The slow channel syndrome mice were constructed as previously described (Webster et al. 2013). In brief, C57BL6 mice were bred to harbour the point mutation εL221F, tagged with green fluorescent protein, inserted randomly into the genome. εL221F is known to cause slow channel syndrome in humans, however, unlike the human condition, in the presence of one normal ε-subunit allele mice harbouring εL221F are not weak. For the disease to manifest it is necessary to concurrently disrupt the normal mouse ε-subunit by insertion of a neomycin cassette.

2.2.3 Acetylcholine receptor deficiency syndrome model

The acetylcholine receptor deficiency model was constructed as previously described (Cossins et al. 2004). In brief, it was constructed by crossing C57BL6 mice harbouring a knock in human γ-subunit ($h\gamma^{+}$) coding sequence with mice heterozygous for the AChR ε- subunit knockout mutation ($\varepsilon^{+/-}$). Targeted disruption of the mouse ε-subunit was achieved by insertion of a neomycin resistance gene. Progeny with the genotype $h\gamma^{+}\varepsilon^{+/-}$ were crossed with $\varepsilon^{+/-}$ mice to generate offspring with the genotype $h\gamma^{+}\varepsilon^{-/-}$. In contrast to human AChR deficiency syndrome caused by null mutations, where compensatory persistent expression of fetal type receptors typically allows survival to adulthood, mice with ε-subunit null mutations do not compensate and die at 10-14 days. This mouse model is therefore constructed to persistently express human AChR γ-

subunit on an AChR ε -subunit knock-out background meaning that neuromuscular transmission is mediated by fetal type acetylcholine receptors. These model mice can survive for at least 9 months without deterioration. However, they demonstrate the primary pathogenic feature of AChR deficiency syndrome with endplate acetylcholine receptor number significantly reduced to around 20% of wild type mice.

2.3 *Ex vivo* diaphragm electrophysiology

This technique allows the measurement of electrophysiological parameters of NMJ transmission. Both electrically stimulated nerve-evoked endplate potentials (EPPs) and spontaneous miniature endplate potentials (MEPPs) can be recorded by placement of a microelectrode close to muscle endplate. Quantal content can then be calculated by analysis of MEPP and EPP data.

Mice were killed using a rising concentration of CO_2. The thorax was promptly dissected out and immersed in a closed container of Kreb's buffer (Section A.1.1) and transported on ice to the laboratory. The tissue was transferred to a Sylgard coated Petri dish containing Kreb's buffer continuously bubbled with 95% O_2/5% CO_2 for further dissection. Each hemidiaphragm was dissected with the phrenic nerve attached and subsequently pinned out on a smaller Sylgard coated recording bath (Figure 2.1). The phrenic nerve was stimulated via a suction electrode coupled to a pulse generator. To reduce muscle twitch during recording the tissue was bathed in buffer containing μ-Conotoxin GIIIB 2.5 μM (Peptide Institute Inc., Osaka, Japan) which was rinsed off and replaced with buffer after thirty minutes. This toxin originates from the marine snail *Conus geographus* and prevents muscle contraction by blocking muscle sodium channels (Na_v 1.4 subtype).

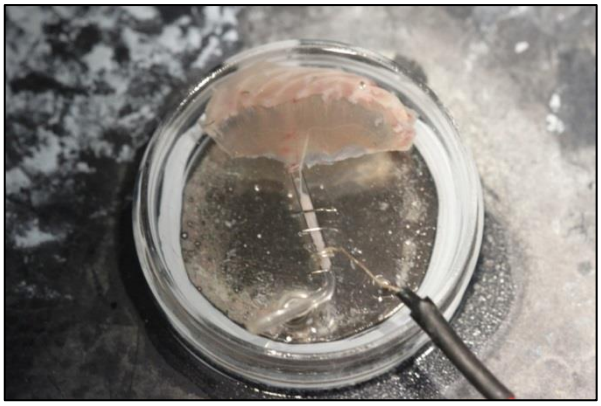

Figure 2.1: A phrenic nerve-hemidiaphragm preparation: the phrenic nerve lies within the glass capillary tube with electrode attached.

Recording electrodes of 10-15 mΩ resistance were pulled from GC150TF-10 borosilicate glass capillary tubes (Harvard Apparatus, Kent, UK) and filled with 3 M KCl solution. Tissue was magnified by upright microscope (Olympus BX51W1) allowing endplate regions to be visualized on a computer screen. Intracellular recordings close to endplates were made using a remote manipulator (Scientifica, East Sussex, UK) to control electrode position. Proximity to endplates was indicated by a fast endplate potential rise time, and MEPPs and EPPs with a rise time of >4 ms for slow channel mice, >3 ms for AChR deficiency and >2 ms for wild type mice were excluded. For each impalement site MEPPs were recorded first, followed by EPPs generated by nerve stimulation with platinum wire electrode (1 Hz, 0.2 ms square wave pulse typically at 5-10 V, [GRASS instruments S48, solid state square wave stimulator, Quincy, USA]). Typically, at least 20 MEPPs and EPPs were recorded at each impalement. Recordings were made via an Axoclamp 2A amplifier and digitized by Digidata 1322A (both Molecular Devices, California, USA). 50 Hz electrical noise was eliminated by a Hum Bug (Quest Scientific Instruments Inc., North Vancouver, Canada). Recordings where the membrane potential was above -50 mV were discarded.

In experiments where a range of drug concentrations were added to the bath five recordings were made per concentration. This was to limit the effect of tissue degradation over time seen with prolonged recordings. When a drug solution was applied the tissue was repeatedly rinsed with and immersed in the solution for 10 minutes before recordings were made. Clampex 9.2 and Clampfit 10.2 software were used during data acquisition and analysis (Molecular Devices, USA).

During analysis all MEPP and EPP recordings were first adjusted to a resting membrane potential of -80 mV to correct for changes in driving force associated with varying postsynaptic membrane potential (Katz and Thesleff 1957; Webster et al 2013). Recordings were performed on mice of 10-14 weeks of age in order to limit variability in endplate parameters, such as endplate potential amplitude, that could result from differences in muscle fibre size. In order to calculate quantal content, the amplitude of adjusted EPPs were first corrected for non-linear summation using the formula (Martin 1976):

$$\text{EPP amplitude} = \text{adj EPP amplitude}/[(1 - 0.8\ \text{adj EPP amplitude})/E]$$

Where adj EPP amplitude is the measured EPP amplitude adjusted to a resting membrane potential of -80 mV, E is the resting membrane potential (-80 mV), and 0.8 is the correction factor for mouse.

This corrected EPP amplitude was then used to estimate quantal content using the direct method as previously described (Wood and Slater 2001):

$$\text{Quantal content} = \text{mean EPP amplitude}/\text{mean MEPP amplitude}$$

2.4 Treatment trials

2.4.1 Drug treatments

In this section the approaches used to calculate a suitable dosage of lamotrigine and metoclopramide and the methods of delivering these drugs are outlined.

2.4.1.1 Drug delivery

Drugs were administered by dissolving them into the drinking water of the mice. Dispersible lamotrigine tablets (Approved Prescription Services, Leeds, UK) were dissolved in water and the excipients removed using a filter system (Corning Inc., NY, USA) powered by a vacuum pump. That the active drug wasn't completely removed by filtration was ascertained by applying the filtrate to a phrenic nerve-hemidiaphragm preparation and confirming it reduced MEPP decay time. Metoclopramide tablets were crushed and dissolved in water without the need for filtration.

Solutions were made to the desired concentration based on the assumption of a daily water intake of 15 ml per 100 g bodyweight per day (Wolfensohn and Lloyd 2003, 233). Fresh solutions were prepared weekly. Treatment was given from 10 weeks of age for a period of 6 weeks in the lamotrigine study and for 4 weeks in the metoclopramide study.

2.4.1.2 Establishing drug dosage for treatment trials

To help establish drug dosages, typical human doses were converted to their mouse equivalent dose per unit of body surface area. The standard calculation was used to calculate body surface area in a typical 20 g mouse:

$$\text{Body surface area } (m^2) = \text{weight } (g)^{2/3} \times K \times 10^{-4}$$

where m = meters, K = Meeh coefficient (mouse = 9.0) (Schmidt-Nielsen 1984).

Average adult human body surface area (Egorin 2003) was divided by calculated mouse body surface area as follows:

$$1.73/0.00663\ m^2 = 260.9$$

The mouse equivalent dose was then calculated by dividing the human dose by a factor of 260.9.

Prior to the treatment trials a range of concentrations of both drugs tested were administered to groups of mice and the serum levels measured. Detection of the drugs in the serum of treated animals confirmed that the method of drug delivery was viable and was used to inform which dosages to use in the treatment trials.

2.4.1.3 Lamotrigine

A target serum concentration range has not been established for lamotrigine and dosage in patients is guided almost entirely by clinical response. However, serum levels were most frequently less than 10 μg/ml in a large study looking at the relationship between dose and toxicity (Hirsch et al. 2004). The same study suggests a ‘therapeutic’ or ‘target’ range to be 1.5-10 μg/ml.

It was intended that the dose used should be equivalent to a relatively high human dose as this is what the index case described in Chapter 5 had received. Using the standard approach of extrapolating from body surface area the equivalent dose was more than double the maximum tolerated dose for mice of 30 mg/kg/day cited by the manufacturer ('Lamotrigine Official FDA Information, Side Effects and Uses.' 2013).

To establish the dose required to produce a serum concentration similar to typical human levels groups of mice were treated with different concentrations of lamotrigine solution (5, 10, 20, 30 and 60 mg/kg/day). Serum was extracted after 2 weeks of treatment and sent for lamotrigine assay at the Therapeutic Drug Monitoring Unit, National Society for Epilepsy, Chalfont St Peter, UK. Results of these assays and the dosages used are given in Chapter 5.

2.4.1.4 Metoclopramide

Serum levels are not used to guide treatment of metoclopramide in patients. Therefore high daily human doses of 30 mg and 60 mg per day were converted to the equivalent daily dose for a mouse by relative body surface area. Metoclopramide was added to drinking water at concentrations of 40 mg/L and 80 mg/L which were calculated to provide the equivalent daily doses within a mouse's normal daily fluid intake. The doses used in the treatment trials are expressed as mg/kg/day based on expected fluid intake by bodyweight. Thus, two doses (6 and 12 mg/kg/day) were administered to separate groups of mice over a 2 week period. Serum was extracted and metoclopramide assay performed by the Cardiff Toxicology Laboratory, Llandough Hospital, Penarth. This assay required a relatively large volume of serum and each assay required pooled serum from between five and seven mice.

2.4.2 Evaluation of myasthenic weakness in transgenic mice

2.4.2.1 The inverted screen test

The inverted screen test involves sustained forced exercise and so is suited to measuring fatigability of muscle weakness. It has been shown to be a sensitive measure of weakness in experimental AIMG (Karachunski et al. 1997) and in the evaluation of transgenic mouse models of CMS (Cossins et al. 2004; Webster et al. 2013).

Mice were placed in the centre of a 43 cm^2 wire grid with 12 mm squares constructed from 1 mm diameter wire (Figure 2.2). A 6.5 cm deep frame contains the test mouse to the underside surface of the grid. The screen was inverted and securely rested over a cushioned surface at a height of 50 cm. The length of time a mouse could hold on for was recorded up to a 600 s limit. If time achieved was less than 600 s, then the best of three attempts was recorded with a 5 minute rest period between each trial.

Figure 2.2: The inverted screen test

2.4.2.2 Repetitive nerve stimulation

Repetitive nerve stimulation is an electromyographic technique that can detect failure of NMJ transmission in myasthenic disorders. When a motor nerve is stimulated a compound muscle action potential (CMAP) can be recorded over a muscle it supplies. The amplitude of the CMAP reflects the number of individual muscle fibres being activated. With repeated stimulation neuromuscular junction transmission may partially fail in myasthenic disorders meaning that fewer fibres are activated and this is reflected by a drop in CMAP amplitude. In humans the degree of transmission failure is usually quantified by comparing the relative amplitude of the 4^{th} or 5^{th} CMAP with that of the initial response elicited by a train of 10 supramaximal stimuli, usually at 3 Hz. Generally CMAP decrement of ≥10% is considered abnormal.

Mice were anaesthetized using a combination of Hypnorm® (Fentanyl [0.8 mg/kg]/fluanisone [25 mg/kg]) induction and 1% isoflurane as maintenance for wild type mice. This protocol had already been established in the laboratory with guidance from veterinary services as least likely to have an effect on neuromuscular transmission. Hypnorm® dosing was modified such that slow channel model animals were given 75% of the dose for a wild type animal of equal weight, and AChR deficiency model animals were given 50% as they are more susceptible to respiratory depression. Depth of anaesthesia, temperature and vital signs were monitored closely throughout the procedure. Core body temperature was maintained between 36-38 °C by heatpad and overhead lamp. Oxygen 2 L/min was administered continuously. Viscotears® was applied to protect the cornea and a subcutaneous injection of replacement fluids and the non-steroidal analgesic Metacam® was administered once all data had been acquired.

The hind limbs of the anaesthetized animal were shaved and cleaned. Using a monopolar electrode (Viasys Healthcare, UK) inserted into the region of the sciatic notch, and a remote reference electrode, the sciatic nerve was stimulated supramaximally (Dual bio amp/stimulator, AD Instruments, UK). CMAP recordings were made via a monopolar electrode inserted into gastrocnemius at a fixed distance of 1 cm above the ankle joint with a distal reference electrode near the tendon insertion site. A ground electrode was inserted at the scruff of the neck. Recordings were made using trains of 10 stimuli at 1, 3, 5, 10 and 20 Hz. Each frequency was performed in triplicate with a 30 second rest between trains to avoid fatigue, and the mean CMAP decrement of the three trains calculated. Data was acquired via Powerlab 4/25 (AD Instruments, UK) with a sampling frequency of 200 kHz and a bandwidth of 1 Hz-5 kHz and analyzed with Clampfit 10.2 (Molecular Devices, USA). Experiments typically lasted 45-60 minutes following which mice were allowed to recover in a heated chamber with a delay of at least 3 days before the inverted screen test was performed.

Chapter 3

A characterization of congenital myasthenic syndromes caused by mutations in *DPAGT1, ALG2, ALG14* and *GFPT1.*

3.1 Introduction

Clinical characterization of congenital myasthenic syndromes encourages accurate diagnosis and thereby the appropriate treatment of patients, as well as improving the quality of prognostic information that can be provided. Within recent decades much work has been done to advance characterization of genetic subtypes. Following the identification of DOK7 CMS in 2006 (Beeson et al. 2006), it was appreciated that a group of patients remained who were suspected of having CMS but who didn't have a mutation in any known CMS gene. Most had predominant proximal muscle weakness and, unlike DOK7 CMS, had the feature of tubular aggregates on muscle biopsy.

Mutations in the four genes discussed herein; *DPAGT1, ALG2, ALG14* and *GFPT1*, account for many of the group described above, and they comprise all genes, with the exception of *AGRN* and *LRP4*, associated with a congenital myasthenic

syndrome to be identified since the discovery of DOK7 CMS. All four encode enzymes in glycosylation pathways and all result in disorders of autosomal recessive inheritance. *GFPT1* was the first to be discovered, the disease locus having been identified by homozygosity mapping (Senderek et al. 2011). A detailed clinical description of a large international group of patients followed (Guergueltcheva et al. 2012). Subsequently *DPAGT1* (Belaya et al. 2012b) and later *ALG2* and *ALG14* (Cossins et al. 2013) were identified using whole-exome and whole-genome sequencing.

GFPT1 (glutamine-fructose-6-phosphate transaminase 1) encodes a protein of the same name which is a key enzyme in the hexosamine biosynthetic pathway (HBP) (Figure 3.1). This metabolic pathway produces amino sugars for the synthesis of glycoproteins, glycolipids and proteoglycans (Senderek et al. 2011). *DPAGT1, ALG2* and *ALG14* all encode early components of the N-linked glycosylation pathway (Figure 3.2). N-linked protein glycosylation is a ubiquitous post-translational modification which can affect protein folding and stability. This metabolic pathway constructs glycan residues in a stepwise manner which are then transferred to nascent protein. The two pathways are related; the main product of the HBP, UDP-GlcNAC (uridine diphosphate N-acetylglucosamine), is a key substrate for N-linked glycosylation.

These four genes differ from the majority of CMS genes identified to date in that they are ubiquitous and have functions that can potentially modify many other proteins, rather than being localized to the NMJ. Both *DPAGT1* (Carrera et al. 2012; Imtiaz, Al-Mostafa, and Al-Hassnan 2012; Iqbal et al. 2012; Timal et al. 2012; Vuillaumier-Barrot 2005; Wu et al. 2003; Würde et al. 2012) and *ALG2* (Thiel et al. 2003) have previously been associated with congenital disorders of glycosylation (CDG). CDGs are an expanding group of disorders which usually present with multisystem disease, are often severe, and usually include a CNS component. Thus, mutations in these genes are an

unexpected cause of a disorder primarily affecting NMJ transmission and their identification has no doubt been aided by the increasing availability of next generation DNA sequencing techniques.

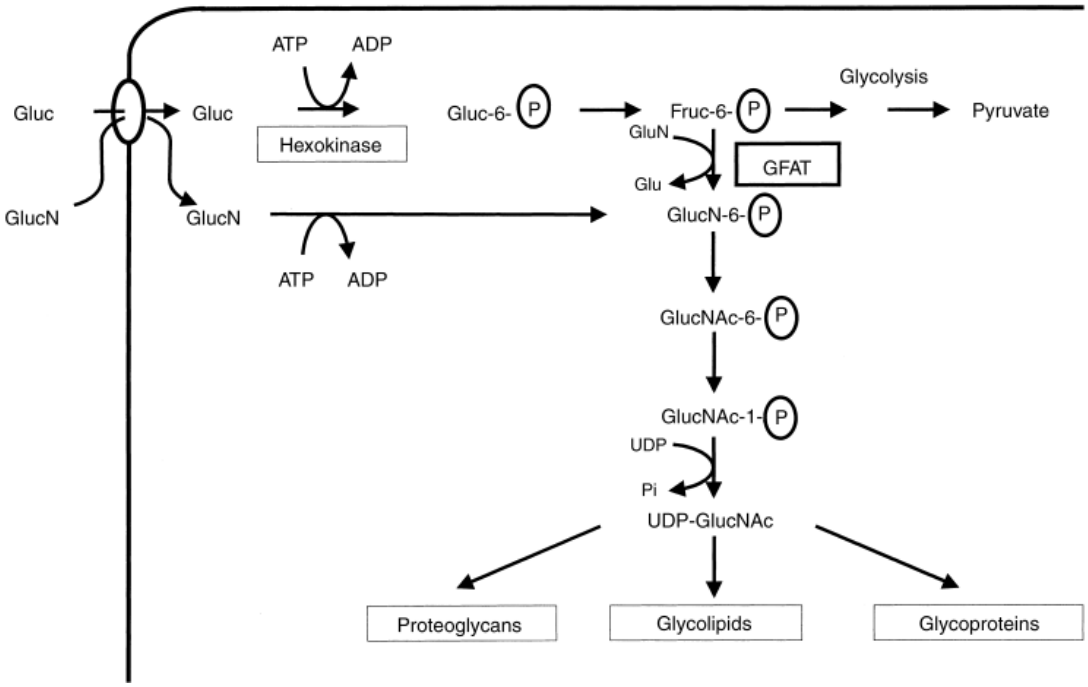

Figure 3.1: The hexosamine biosynthetic pathway: Glucose (Gluc) enters the cell through the glucose transporter and is metabolized. The hexosamine biosynthetic pathway merges from glycolysis using fructose-6-phosphate (Fruc-6-P) to form glucosamine-6-P (GlucN-6-P). Glutamine (GluN) serves as donor of the aminogroup. The reaction is catalyzed by the rate-limiting enzyme glutamine: fructose-6-phosphate-amidotransferase (GFAT). GlucN-6-P is rapidly acetylated, isomerized to N-Acetylglucosamine-6-phosphate (GlucNAc-1-P) and activated to UDP-N-acetylglucosamine (UDP-GlucNAc) that serves as common precursor for all amino sugars used for the synthesis of glycoproteins, -lipids, and proteoglycans. Glucosamine (GlucN) can also enter the cell through the glucose transporter and is rapidly phosphorylated by hexokinase yielding GlucN-6-P, thereby bypassing the rate-limiting first step of the hexosamine biosynthetic pathway. GFAT is synonymous with GFPT1. Reprinted by permission from Macmillan Publishers Ltd: Kidney International, Schleicher and Weigert 2000, Copyright 2000, Nature Publishing Group (URL: http://www.nature.com/ki/).

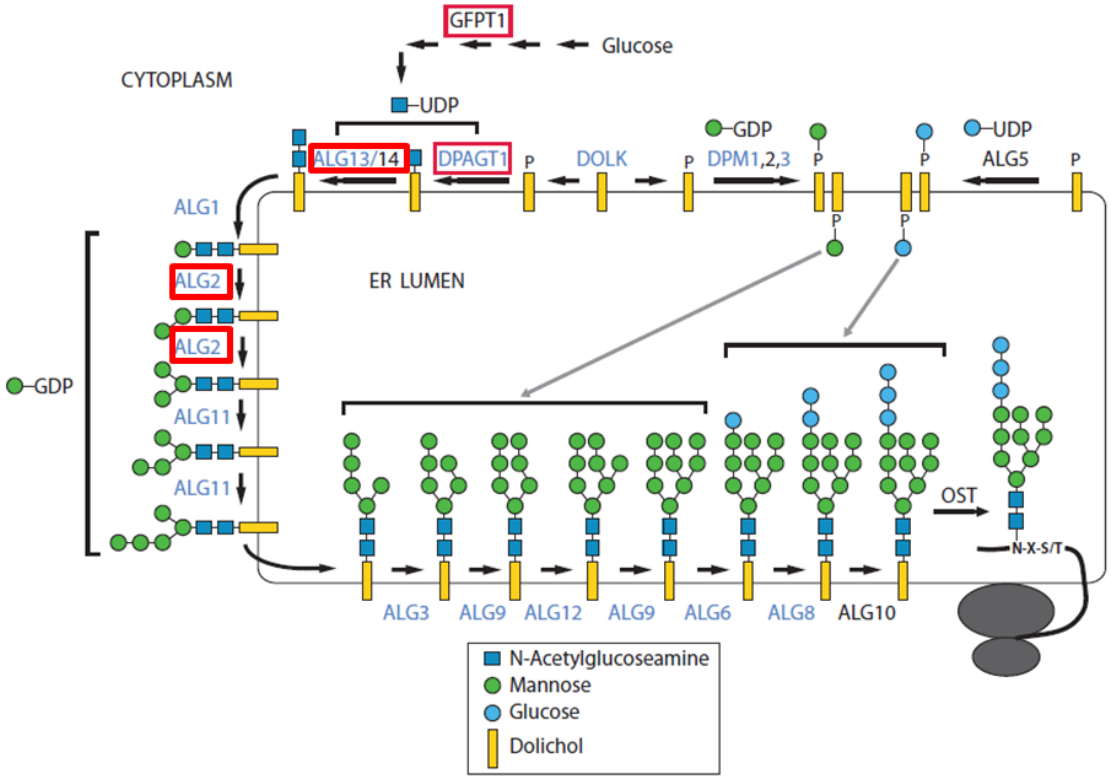

Figure 3.2: N-linked glycosylation pathway: UDP-GlcNAc (or UDP-N-acetylglucosamine), a product of the hexosamine biosynthetic pathway is an essential substrate for N-linked protein glycosylation. DPAGT1 catalyzes the first committed step of N-linked glycosylation in which cytoplasmic UDP-GlcNAc is added to a transmembrane lipid carrier, dolichol phosphate. The core glycan is assembled by enzymatic addition of individual sugar residues (mannose and glucose) in a stepwise manner. During assembly the oligosaccharide is transported across the membrane to the endoplasmic reticulum interior where further sugar residues are added. Once fully assembled, the core glycan is released from dolichol ready to be transferred to an N-linked glycosylation site on nascent protein. Reprinted from Belaya et al. 2012a, Ann. N.Y. Acad. Sci., by permission of John Wiley and Sons. ©2012 New York Academy of Sciences.

3.1.1 Aims

1) The characterization of congenital myasthenic syndromes caused by mutations in *DPAGT1*, *ALG2*, *ALG14* and *GFPT1*.
2) To compare and contrast the phenotype of these syndromes with other forms of CMS.

3.2 Patients and methods

Patient consent for use of data was obtained with ethical approval OXREC B: 04.OXB.017 and Oxfordshire REC C 09/H0606/74.

Cardiac data discussed herein was obtained from a research study run by Dr Andrew Lewis and Professor Stefan Neubauer of the Department of Cardiovascular Medicine, University of Oxford and given ethical approval by Berkshire REC 07/H06076. The study of the patients described here was a collaborative effort though all data acquisition and analysis was performed by the cardiology team.

Patients were identified via the national CMS service based at the John Radcliffe Hospital, Oxford and via the associated research laboratory based at the Weatherall Institute of Molecular Medicine. The genes were identified sequentially and the following kinships have previously been reported elsewhere: 1-4 (Belaya et al. 2012b), 5 (Basiri et al. 2013), 6-8 (Cossins et al. 2013) and 9-10 (Guergueltcheva et al. 2012). All patients in whom mutations in *DPAGT1*, *ALG2*, *ALG14* or *GFPT1* had been identified by the laboratory were included in the study. Because the clinical service and the research laboratory have international reputation as expert in congenital myasthenic disorders clinicians from other centres often request genetic testing as well as management advice. Therefore some patients discussed here have not attended the CMS clinic in Oxford in person and information is based on local reports. Patients were invited to attend for up to date review where practicable. Clinical history, examination and investigation data were collated from case notes review in combination with up to date clinical review where performed.

3.2.1 History

Specific points in the history were recorded. This included neonatal history, motor milestones and development, as well as age and symptoms at onset. Progression of symptoms, the presence of respiratory crises and response to treatment was noted.

3.2.2 Clinical assessment

Neurological examination was recorded including the presence of ptosis, or ophthalmoplegia and the severity and pattern of muscle weakness. Quantitative myasthenia gravis (QMG) scores where performed were also recorded. The QMG score (Figure 3.3) was initially developed for the evaluation of therapy for AIMG and is based on quantitative testing of sentinel muscle groups (Jaretzki et al. 2000). Thirteen parameters are scored from 0-3. Patients can score up to a maximum of 39 points and a higher score reflects greater weakness. The QMG score has also been used in the assessment of CMS (Lashley et al. 2010; Burke et al. 2004).

3.2.3 Investigations

Results of neurophysiological studies were sought. In particular the presence of abnormal (≥10%) CMAP decrement on RNS and the presence of increased jitter or blocking on SFEMG studies were noted.

Single-fibre EMG is considered to be abnormal if either the overall mean jitter is elevated or if >10% of individual recordings are greater than predefined normal limits.

QMG	0	1	2	3	
Lateral diplopia (s)	>60	11-60	1-10	0	
Ptosis(s)	>60	11-60	1-10	0	
Facial muscles (eyelid closure)	Normal	Some resistance to opening	Unable to resist opening	Incomplete lid closure	
Swallowing	Normal	Occasional Choking	Consistent choking	Unable to swallow	
Head lift 45° (s)	>120	30-120	0-30	Unable	
R arm 90° (s) test both arms together	>240	91-240	11-90	0-10	
L arm 90° (s) test both arms together	>240	91-240	11-90	0-10	
Counting 1-50 dysarthria / nasal speech	None	At 30-49	At 10-29	Before 9	
R Leg 45° (s) test separately	>100	31 - 100	1 - 30	0	
L Leg 45° (s) test separately	>100	31 - 100	1 - 30	0	
Vital Capacity	M > 3.5 F >2.5	M 2.6 - 3.5 F 1.9 - 2.5	M 1.5 - 2.5 F 1.2 - 1.8	M < 1.5 F <1.2	
R Grip (kg) gently support dynamometer	M > 45 F > 31	M 16 - 45 F 11 - 31	M 5 - 15 F 5- 10	M < 5 F < 5	
L Grip (kg) elbow at 90°	M > 45 F > 31	M 16 - 45 F 11 - 31	M 5 - 15 F 5- 10	M < 5 F < 5	
				Total	

Figure 3.3: Quantitative myasthenia gravis (QMG) score: Scoring sheet for QMG testing demonstrating the 13 parameters tested and their grading.

Specific normative data exists for different muscles and for volitional and stimulated methods (Kokubun et al. 2011). Because specific muscles tested and reporting practice varied between the centres performing the studies, only the presence of abnormal increased jitter or of blocking was noted.

Muscle biopsy findings were reviewed and the presence of tubular aggregates noted as well as any additional features described in reports. Serum creatine kinase (CK) levels and results of any electrocardiograms (ECGs) performed were noted.

Results of biochemical tests of glycosylation, where performed, were also noted. Transferrin glycoform analysis is used to detect disordered glycosylation and can be used in the evaluation of congenital disorders of glycosylation where it can help to classify CDG syndromes. A number of different laboratory methods exist and in the

patients described here either transferrin isoelectric focusing (IEF), or determination of the percentage of carbohydrate deficient transferrin (% CDT) by immunoturbidimetry, or both were performed. Both methods determine the degree of glycosylation of the serum glycoprotein transferrin (Tf). Under normal circumstances serum transferrin separates into different isoforms depending on degrees of glycosylation, though tetrasialo-Tf (which has four sialic acid residues) is the most abundant form. Aberrant glycosylation causes an increase in hyposialated isoforms. Sialic acid residues are negatively charged and Tf IEF separates the differently charged Tf isoforms into bands on an agarose gel by electrophoresis. The pattern of these bands can help to distinguish between type I and type II CDGs (Figure 3.4). In measuring % CDT by immunoturbidimetry the hyposialated (carbohydrate deficient) isoforms are quantified and the sum of these relative to total Tf is expressed as a percentage.[1]

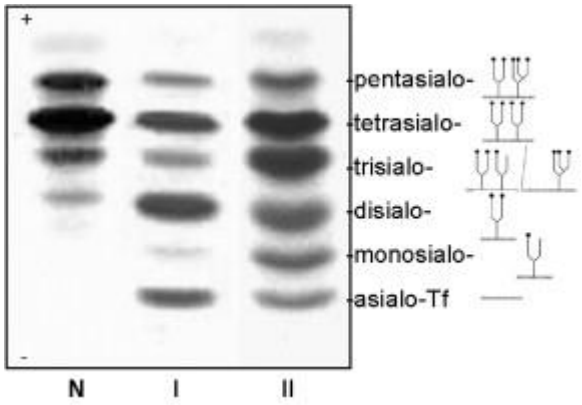

Figure 3.4: Isoelectric focusing of serum transferrin (Tf): The normal profile (N) shows several bands with the highest intensity of the tetrasialo-Tf. CDG type I pattern (I) is characterized by decreased tetrasialo-, and increased asialo- and disialo-Tf bands. CDG type II pattern (II) may present various combinations of elevated asialo-, disialo-, trisialo- and monosialo-bands. Glycan structure of various Tf isoforms are shown to the side.[2]

[1] Paragraph adapted from Finlayson et al. 2013a (URL: http://jnnp.bmj.com/content/84/10/1119).
[2] Reprinted from Clinica Chimica Acta, 385 (1-2), Marklová and Albahri, Screening and Diagnosis of Congenital Disorders of Glycosylation, 6-20, Copyright 2007, with permission from Elsevier.

3.3 Results

Nineteen patients from 11 kinships were identified in total (Table 3.1). These comprise DPAGT1: 9 patients, ALG2: 5 patients, ALG14: 2 patients and GFPT1: 3 patients. Patients 1-4, 10 and 15-19 had been reviewed in Oxford and examined either by myself, or by another clinician in the CMS service. Clinical information on patient 5, who is the sibling of patient 4, was provided by their local clinician Dr S Ignacio Pascual-Pascual, Madrid, Spain. Patients 6-9 and 11-14 had had their DNA tested in the research laboratory and their clinical information was provided by their local clinicians.

3.3.1 Mutations

Mutations identified were as follows.

3.3.1.1 DPAGT1

Patients 1-5 had heterozygous missense mutations with the exception of patient 2 who was heterozygous for a frameshift single-nucleotide duplication, c.699dup, along with a missense mutation. Patients 6-9, from kinship 5, were homozygous for a missense mutation. All kinships had private mutations with the exception of patients 1 and 2 who share the mutation c.349G>A.

3.3.1.2 ALG2

Patient 10 was homozygous for a missense mutation. Patients 11-14 were homozygous for the insertion-deletion mutation c.214_226delinsAGTCCCCGGC.

3.3.1.3 ALG14

Both siblings were heterozygous for a missense mutation (c.194C>T) and one nonsense mutation (c.310C>T) which introduces a premature stop codon truncating the protein by 112 amino acid residues (Cossins et al. 2013).

3.3.1.4 GFPT1

Patients 17 and 18 were both heterozygous for private missense mutations. Patient 19 was heterozygous for a missense mutation and a C>A nucleotide substitution in the 3'UTR of the mRNA, the effect of which remains unclear.

3.3.2 Onset of symptoms and clinical course

Age and symptoms at onset are summarized in Table 3.2. All but one patient reported difficulty with ambulation or hypotonia as a presenting symptom. Except for those with *ALG2* mutations, most patients had a later onset than is typical of many CMS subtypes (after infancy), with normal motor milestones.

In only one patient (7) was onset of symptoms described as abrupt. Patient 6, within the same family, is the only patient to have been affected by respiratory crises. In two (patients 16 and 18) there was a clear history of rapid sustained deterioration in strength during adulthood on a background of milder weakness. Detailed descriptions of clinical course, where available, are given below.

Patient	Kinship	Gene	Mutation 1	Mutation 2	Sex	Ethnicity	Consanguinity
1	1	*DPAGT1*	c.324G>C (p.Met108Ile)	c.349G>A (p.Val117Ile)	M	White European/UK	-
2	2	*DPAGT1*	c.349G>A (p.Val117Ile)	c.699dup (p.Thr234Hisfs*116)	F	White European/UK	-
3	3	*DPAGT1*	c.574G>A (p.Gly192Ser)	c.478G>A (p.Gly160Ser)	F	White European/Zimbabwe	-
4	4	*DPAGT1*	c.358C>A (p.Leu120Met)	c.791T>G (p.Val264Gly)	M	Argentinian	-
5	4	*DPAGT1*			F		
6	5	*DPAGT1*	c.652C>T (p.Arg218Trp)	c.652C>T (p.Arg218Trp)	F	Iranian	+
7	5	*DPAGT1*			F		
8	5	*DPAGT1*			M		
9	5	*DPAGT1*			M		
10	6	*ALG2*	c.203T>G (p.Val68Gly)	c.203T>G (p.Val68Gly)	M	White European/Italian	+
11	7	*ALG2*	c.214_226delinsAGTCCCCGGC	c.214_226delinsAGTCCCCGGC	M	Saudi Arabian	+
12	7	*ALG2*	(p.72_75delinsSPR)	(p.72_75delinsSPR)	F		
13	7	*ALG2*			F		
14	7	*ALG2*			F		
15	8	*ALG14*	c.194C>T (p.Pro65Leu)	c.310C>T (p.Arg104*)	F	White European/ UK	-
16	8	*ALG14*			F		
17	9	*GFPT1*	c.1154G>A (p.Arg385His)	c.1301G>A (p.Arg434His)	M	White European/ UK	-
18	10	*GFPT1*	c.44C>T (p.Thr15Met)	c.1486C>T (p.Arg496Trp)	M	White European/ UK	-
19	11	*GFPT1*	c.238G>A (p.Asp80Asn)	c.2046 + 22C>A	F	White European/ UK	u/k

Table 3.1: Genetic mutations and patient characteristics: F; female, M; male, UK; United Kingdom, +; yes, -; no, u/k; unknown.

Patient	Kinship	Gene	Current age (yrs)	Age when assessed (yrs)	Onset age	Symptoms at onset
1	1	*DPAGT1*	43	43	2.5 yrs	Episodic difficulty walking
2	2	*DPAGT1*	57	57	7 yrs	Falls and unable to keep up with friends
3	3	*DPAGT1*	58	58	2 yrs	Hypotonia and poor head control
4	4	*DPAGT1*	17	25	0.5 yrs	Abnormal gait
5	4	*DPAGT1*	6	6	First year	Hypotonia and delayed motor development
6	5	*DPAGT1*	25 *	20	<7 yrs	Mild and fluctuating proximal lower limb weakness
7	5	*DPAGT1*	28	23	17 yrs	Fluctuating ptosis and muscle cramps
8	5	*DPAGT1*	26	21	3 yrs	Frequent falls
9	5	*DPAGT1*	34	u/k	13 yrs	Difficulty climbing stairs then gait disturbance
10	6	*ALG2*	59	59	4 yrs	Waddling gait, falls
11	7	*ALG2*	23	20	22 months	Hypotonia
12	7	*ALG2*	17	14	Infancy	Delayed motor milestones
13	7	*ALG2*	12	9	Infancy	Delayed motor milestones, hypotonia
14	7	*ALG2*	3	15 months	15 months	Delayed motor milestones, hypotonia
15	8	*ALG14*	62	61	7 yrs	Difficulty climbing steps and hills
16	8	*ALG14*	51	41	Childhood	Difficulty running
17	9	*GFPT1*	26	26	Childhood	Weakness
18	10	*GFPT1*	39	39	6 yrs	Falls and slower than brother
19	11	*GFPT1*	72	71	Childhood	Late walking and last at sport in school

Table 3.2: Age and symptoms at onset: *; deceased, u/k; unknown, yrs; years.

3.3.2.1 DPAGT1[2]

Patient 1 was poor at sports during childhood although was able to run short distances. During childhood his walking deteriorated and he started to use a wheelchair at around 9 years. At that time he had a muscle biopsy and was told he had Werdnig-Hoffman spinal muscular atrophy. It became apparent over subsequent years that this diagnosis was not correct and CMS was suspected. In adult life he has been stable but with long-term fluctuations lasting weeks to months not associated with exacerbating factors such as infection.

Patients 2 and 3, who are now in their sixth decade, report slowly progressive weakness. Patient 2 worsened during adolescence and began to have frequent falls and was noted to waddle when she walked. Around this time she developed difficulty lifting objects above her head and playing netball. Her condition stabilized in her 20s although she had a prolonged apnoea following suxamethonium administration during an operation age 22. Her weakness later progressed and she developed truncal weakness age 30. She reports increasing neck weakness in her fifth and sixth decades.

Patient 3, who is most severely affected, reports worsening around age 7. She was diagnosed with AIMG at that time and underwent thymectomy with no benefit. She continued to deteriorate, and by age 14 was using a wheelchair most of the time. In her 40s she had plasma exchange with no effect. During adult life her weakness has worsened and while at 49 she was able to walk 20 paces, now at age 58 she can transfer independently but is unable to take steps.

The siblings, patients 4 and 5, who are the youngest with *DPAGT1* mutations, report some improvement in their teens and childhood respectively. Following

[2] Section 3.3.2.1 reproduced from Finlayson et al. 2013a (URL:http://jnnp.bmj.com/content/84/10/1119).

improvement in his teens patient 4 was able to walk 5 km without support. He can also climb stairs and run although his running style is abnormal and slower than his peers. Patient 5 has generalized hypotonia though can walk, run and jump.

Patients 6-9 are siblings from a consanguineous Iranian family. Age of onset varies between 3 and 17 years. Two of the siblings (patients 6 and 7) have previously been treated for AIMG.

3.3.2.2 ALG2[3]

Patient 10 was initially diagnosed with muscular dystrophy around 4 years of age when he had symptoms suggestive of proximal muscle weakness and falls. His symptoms worsened at 10 years when he was unable to walk unaided. At 60 years he is now able to walk 15-20 metres but has never been able to run. His weakness is exacerbated by stress and infections.

Patients 11-14 are from a consanguineous Saudi family with onset of symptoms; either hypotonia, delayed motor development or both, ranging from infancy to 22 months. None have achieved independent ambulation (though patient 14 is still only 3 years of age) and slow progressive deterioration is described in patients 11-14.

[3] Sections 3.3.2.2 and 3.3.2.3 adapted from Cossins et al. 2013, Congenital myasthenic syndromes due to mutations in ALG2 and ALG14. © Cossins et al (2013). Published by Oxford University Press on behalf of the Guarantors of Brain. http://brain.oxfordjournals.org/content/136/3/944.article-info. This is an Open Access article distributed under the terms of the Creative Commons Attribution Non-Commercial License (http://creativecommons.org/licenses/by-nc/3.0/).

3.3.2.3 ALG14[3]

Both siblings achieved normal motor milestones. Symptoms became apparent in patient 15 at 7 years of age and progressed until the late teens when she had regular falls. Symptoms have remained generally stable during adult life but with exacerbation of weakness during viral infections. Her younger sister, patient 16 was not investigated until age 40 when she developed proximal limb weakness, struggling to lift objects above her head and climb stairs. In retrospect she had been considerably weaker than her peers during childhood. Both siblings were treated for presumed AIMG before a diagnosis of CMS was made.

3.3.2.4 GFPT1

Patient 17 was thought to have been a little slow in sitting, standing and walking and was described as always a clumsy child. He was noticed to be weak during childhood though the clinical picture was confounded by development of retinitis pigmentosa, diagnosed at the age of 5. He lost the ability to run by age 8 and has progressed from using a wheelchair intermittently at age 10 to using one most of the time as an adult.

Patient 18 was noted to fall frequently by his parents at age 6 and had to climb on all four limbs on a hill walking holiday. He had previously achieved normal motor milestones. At age 12 upper limb weakness became evident when he had difficulty holding his flute. Problems did not progress until age 20 when over period of 1 week there was rapid deterioration in strength in all four limbs without subsequent further progression.

Patient 19 was fostered as a child and details of her early life are unknown. She was late in walking and remembers being last at sport in school. She recalls waking one

day age 15 and being unable to move for 1 week due to weakness which then improved partially. She then describes indolent and fluctuating generalized weakness throughout her life.

3.3.3 Pattern of neuromuscular weakness

A summary of clinical features is presented in Table 3.3. Ophthalmoplegia was absent in all patients. Ptosis was seen in five and in three of these it was mild and asymmetric (patients 2, 16 and 19). None of the patients with *ALG2* mutations have ptosis. Both sisters with *ALG14* mutations have a mild latent divergent squint. Facial weakness was reported in nine patients (with DPAGT1, ALG2 or GFPT1 subtypes) and was described as mild in all but one. Symptoms of bulbar weakness were apparent in five patients and were generally mild and had not required investigation or intervention. While respiratory symptoms were described in six patients, only one (patient 6 who had *DPAGT1* mutations) experienced respiratory crises or required assisted ventilation. This patient had two episodes of respiratory crisis; the first at age 15, and the second age 25 during which she died. Respiratory symptoms in patients 1, 2 and 15 are not clearly related to myasthenic weakness and patients 1 and 15 have co-morbidities that could explain their shortness of breath.

All patients have weakness affecting, but not restricted to, limb-girdle musculature on examination with the exception of patient 19. This patient had mild weakness of finger extensors and ankle dorsiflexors but other limb muscles were strong. Weakness greater in proximal rather than distal muscles was noted in the majority. However, proximal predominance was not seen in either of the patients with *ALG14*

mutations, and in patient 1 with *DPAGT1* mutations distal muscles were weaker than proximal muscles.

Spinal abnormalities are present in four patients. Patients 9 and 10 both have lumbar hyperlordosis. In addition, patient 9 has mild scoliosis. Mild scoliosis was also noted in patients 2 and 4, at 62 and 11 years respectively.

Joint contractures were reported in six patients. Patient 1 has significant flexion contractures of the knees, ankles, elbows and fingers. Patient 17 has contractures of the hamstrings and patient 18 has mild bilateral flexion contractures of both knees and restricted ankle dorsiflexion. The age of developing contractures is unknown in these patients and all three have been dependent on a wheelchair which may have contributed to contracture development. Three patients from kinship seven with *ALG2* mutations have proximal joint contractures and were considered to share a similar phenotype with Ullrich congenital muscular dystrophy. These three patients also have distal joint laxity and a high arched palate.

3.3.3.1 Additional features

Two patients with *DPAGT1* mutations and three siblings with *ALG2* mutations have mild learning disability. Of these five, patients 5, 11 and 12 have had normal brain MRI results. Patient 17 has retinitis pigmentosa of unknown aetiology and is registered blind.

Patients	1	2	3	4	5	6	7	8	9	10	11	12	13	14	15	16	17	18	19
	DPAGT1									ALG2					ALG14		GFPT1		
Ptosis	-	mild	-	-	-	-	+	-	+	-	-	-	-	-	-	mild	-	-	mild
Ophthalmoplegia	-	-	-	-	-	-	-	-	-	-	-	-	-	-	-	-	-	-	-
Facial weakness	-	mild	-	-	mild	-	-	-	+	-	mild	mild	mild	mild	-	-	mild	mild	-
Bulbar symptoms	mild	mild	-	-	-	-	+	-	+	-	-	-	-	-	-	-	mild	-	-
Respiratory symptoms	+	+	-	-	-	+	-	-	-	-	+	+	-	-	+	-	-	-	-
Required ventilation	-	-	-	-	-	+	-	-	-	-	-	-	-	-	-	-	-	-	-
Respiratory crises	-	-	-	-	-	+	-	-	-	-	-	-	-	-	-	-	-	-	-
Limb weakness	+	+	+	+	+	+	+	+	+	+	+	+	+	+	+	+	+	+	+
Muscle wasting	-	-	+	-	-	-	-	+	u/k	-	u/k	u/k	u/k	u/k	-	-	-	-	-
Contractures	+	-	-	-	-	u/k	u/k	u/k	u/k	-	+	+	+	-	+	-	+	+	-
Spinal abnormality	-	+	-	+	-	u/k	u/k	u/k	+	+	-	-	-	-	-	-	-	-	-
Joint laxity	-	-	-	-	-	u/k	u/k	u/k	u/k	-	+	+	+	-	-	-	-	-	-
High arched palate	-	-	-	-	u/k	u/k	u/k	u/k	u/k	-	+	+	+	-	-	-	-	-	-
QMG score	9	18	20	nd	nd	nd	nd	nd	nd	13	nd	nd	nd	nd	15	nd	11	7	13
Learning disability	-	-	+	-	+	-	-	-	-	-	+	+	+	+	-	-	-	-	-

Table 3.3: Clinical features: +; yes, -; no, u/k; unknown, nd; not done.

3.3.4 Investigations

Results of investigations are summarized in Table 3.4 with the exception of muscle biopsy findings which are in Table 3.5.

3.3.4.1 Neurophysiology

Abnormal CMAP decrement was detected in all patients who had repetitive nerve stimulation (n = 16). Detailed results of RNS were available for patients 1, 3, 4, 10, and 17-19. Within the DPAGT1 group, and patient 10 who has *ALG2* mutations, RNS showed greater proximal abnormality. The same was not true of the one patient (18) with GFPT1 CMS who had had both a proximal and a distal muscle tested.

Extra discharges to single stimuli were recorded from the hypothenar muscles of patient 3 during motor nerve conduction study at age 49, but not at age 45 years, and presumed to be a treatment effect. Repetitive discharges were not reported in other patients.

Single-fibre EMG was abnormal in all who had the test performed (n = 11). There was increased jitter and blocking in all but one patient (19), who had abnormal jitter but no potential blocking. In this patient increased jitter was found in extensor digitorum communis despite normal strength of this muscle on clinical examination.

Abnormal spontaneous activity indicative of active denervation (fibrillations and positive sharp waves) were said to be present on standard EMG of all tested muscles, and especially the proximal muscles, of patient 6. This feature was not reported in any other patient.

3.3.4.2 Muscle Biopsy

Tubular aggregates (Figure 3.5) were detected in 7/11 patients who were investigated by muscle biopsy. In some cases tubular aggregates were not detected on initial biopsy but were seen on later repeat biopsies. For example tubular aggregates were seen in the second biopsy of patient 4 performed age 9 years. Although ultrastructural abnormalities were detected in this patient's biopsy at age 5 years these were not identified as TA. Tubular aggregates were detected in some biopsies where electron microscopy (EM) had not been performed. However, they were demonstrated in all but one biopsy where EM is known to have been performed.

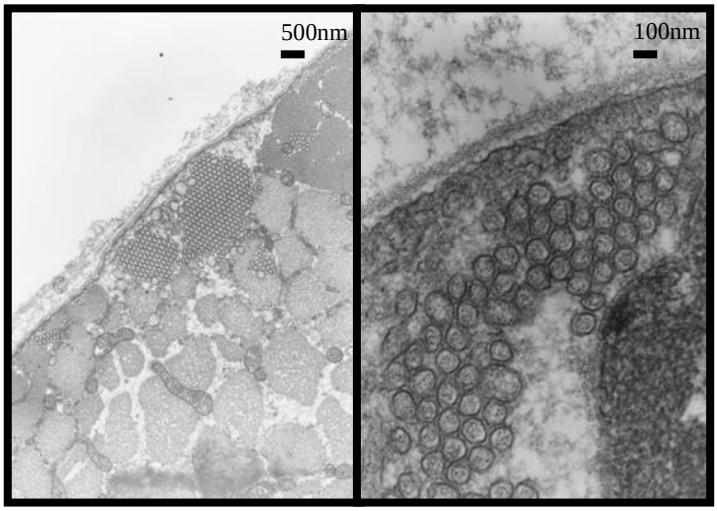

Figure 3.5: Tubular aggregates: Electron micrograph of a muscle biopsy from patient 1 showing tubular aggregates. Reprinted from Belaya et al. 2012b, Mutations in DPAGT1 Cause a Limb-Girdle Congenital Myasthenic Syndrome with Tubular Aggregates, © 2012 The American Society of Human Genetics, by permission of Elsevier under CCPL: http://creativecommons.org/licenses/by/3.0/legalcode.

Except for the first from patient 2, no muscle biopsy was reported as showing completely normal muscle, and a range of other, mostly non-specific, features were reported. These included variation in fibre size, fibre type predominance, internal nuclei, and the presence of vacuoles. A dystrophic pattern was reported in a biopsy of vastus lateralis from patient 7.

The third biopsy from patient 2 was from an intercostal muscle and detailed study of the NMJ indicated a postsynaptic defect. Endplates were of normal size and had a normal amount of acetylcholinesterase activity but showed reduced α-bungarotoxin binding, at 11.2 amol/endplate (normal range 13-30), indicative of receptor deficiency. Electrophysiological studies demonstrated a reduction in miniature endplate potential amplitude to less than 50% of normal also in keeping with receptor deficiency. A motor point biopsy of vastus lateralis from patient 1 has previously been characterized and reported (Slater et al. 2006; Belaya et al. 2012b). This too showed a reduction of α-bungarotoxin binding and in amplitude of synaptic potentials. Ultrastructural studies showed that the amount of postsynaptic folding was five times lower than in control muscle (Figure 3.6).

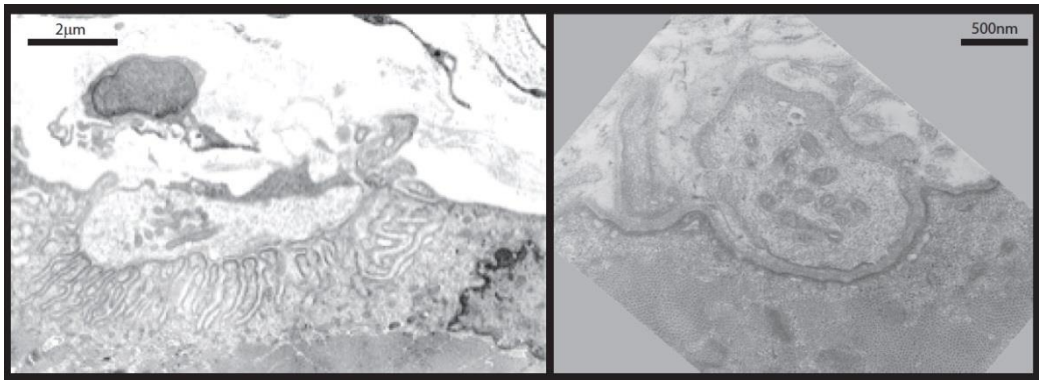

Figure 3.6: Electron micrograph of the motor endplate region in a patient with DPAGT1 CMS: A. An endplate region from a normal control subject. Adapted from Slater et al, Pre- and post-synaptic abnormalities associated with impaired neuromuscular transmission in a group of patients with 'limb-girdle myasthenia', Brain, 2006, 129 (8), 2061-76 by permission of Oxford University Press. © Oxford University Press. **B.** The endplate region in a muscle biopsy from patient 1 shows markedly reduced folding of the postsynaptic membrane. Reprinted from Belaya et al. 2012b, Mutations in DPAGT1 Cause a Limb-Girdle Congenital Myasthenic Syndrome with Tubular Aggregates, © 2012 The American Society of Human Genetics, by permission of Elsevier under CCPL: http://creativecommons.org/licenses/by/3.0/legalcode.

Patient	1	2	3	4	5	6	7	8	9	10	11	12	13	14	15	16	17	18	19
	DPAGT1									ALG2					ALG14		GFPT1		
CK raised	-	-	-	-	-	-	-	-	nd	+/-	-	-	-	+	nd	-	+	+	-
Abnormal biochemical test of glycosylation	nd	-	-	+	+	nd	nd	nd	nd	nd	nd	nd	nd	nd	nd	nd	nd	nd	nd
RNS decrement	+	+	+	+	+	+	+	+	u/k	+	+	+	nd	nd	+	+	+	+	+
SFEMG raised jitter	+	+	+	+	nd	nd	nd	nd	nd	+	+	+	nd	nd	+	nd	+	+	+
blocking	+	+	+	+	nd	nd	nd	nd	nd	+	u/k	u/k	nd	nd	+	nd	+	+	-
Myopathic EMG	nd	+	+	+	nd	+	+	+	u/k	+	nd	nd	nd	nd	nd	nd	nd	+	u/k

Table 3.4: Results of investigations: +; yes, -; no, +/-; variable, u/k; unknown, nd; not done; CK; creatine kinase, RNS; repetitive nerve stimulation, SFEMG; single-fibre electromyography.

Patient	Gene	Age at biopsy (yrs)	Muscle sampled	Tubular aggregates/EM performed	Other findings
1	*DPAGT1*	9	Deltoid	-/-	Unremarkable except for one focus of myonecrosis and phagocytosis
		19	Quadriceps	+/+	Moderate generalized hypertrophy, >25% muscle fibres are 2C
2	*DPAGT1*	16	Deltoid	-/-	Normal to light microscopy
		20	Wrist extensor	+/+	Normal to light microscopy but EM showed TA.
		32	Intercostal	nd	Acetylcholinesterase activity normal. Reduced α- bungarotoxin binding, at 11.2amol/endplate (normal range 13-30). Electrophysiological studies demonstrated a reduction in miniature endplate potential amplitude (<50% normal).
		57	Deltoid	No convincing TA/-	Moderate increase in fibre diameters, some vacuolation, possible necrotic fibre, small and focal increase in endomysial connective tissue, marked predominance of type I fibres, no convincing TA, one fibre expressing developmental myosin.
3	*DPAGT1*	47	Deltoid	+/+	Autophagic vacuoles. Excess of glycogen.
		57	Deltoid	+/-	Similar to earlier biopsy
4	*DPAGT1*	5	u/k	Ultrastructural abnormalities detected though not identified as TA/+	Moderate variation in fibre diameters.
		9	u/k	+/-	Moderate variation in fibre diameters.
6	*DPAGT1*	u/k	Vastus lateralis	-/u/k	Reduced number of muscle fibres. Increase in connective tissue. Fibre size variability. Some central nuclei.
7	*DPAGT1*	u/k	Vastus lateralis	-/u/k	Dystrophic pattern

Table 3.5: Muscle biopsy findings: +; yes, -; no, +/-; u/k; unknown, nd; not done, EM; electron microscopy, TA; tubular aggregates, yrs; years.

Table 3.5: (continued)

Patient	Gene	Age at biopsy (yrs)	Muscle sampled	Tubular aggregates/EM performed	Other findings
10	*ALG2*	50	u/k	+/+	Moderate variation in fibre size and shape. Increase in internal nucleation. Myopathic.
12	*ALG2*	6	Quadriceps	-/u/k	Variation in fibre size. Type 1 predominance. Myopathic
15	*ALG14*	52 58	Quadriceps u/k	-/- -/-	Significant fibre type disproportion. Variation in fibre size and shape, scattered atrophic fibres, no grouped atrophy, occasional hypertrophic fibres, slight increase in internal nuclei, occasional split fibres.
17	*GFPT1*	21	Deltoid	+/-	Variation in fibre size. Many atrophic fibres, some degenerating. Rare atrophic fibres express developmental myosin, many small fibres express neonatal myosin. Multiple internal nuclei. Features consistent with denervation
18	*GFPT1*	20 34	Quadriceps Deltoid	+/+ 'probably'/-	Marked type II fibre predominance. Similar to earlier biopsy. Myopathic and consistent with myasthenia. Several fibres have multiple small rimmed vacuoles.

3.3.4.3 Creatine kinase levels

In the DPAGT1 group creatine kinase (CK) levels were normal in all patients tested (n = 8). Of the five patients with *ALG2* mutation, CK was raised in two. In patient 10 this was variable and was slightly elevated when tested at age 53 years [=267 international units/litre (IU/L, normal range 24−195)] but within normal limits at age 59 years [= 123 IU/L, (normal range 55−170)]. In patient 14 the CK level was raised at 269 IU/L (normal range 38−174 IU/L). One patient with *ALG14* mutations had CK levels checked and this was normal. CK was raised in two of the three patients with *GFPT1* mutations. In patient 17 the CK level was mildly elevated (415 IU/L) but in patient 18 it was moderately raised at age 20 years [= 1744 IU/L, (normal range 75-200 IU/L)].

3.3.4.4 Biochemical tests of glycosylation

Results of biochemical tests of glycosylation were available for patients 2-5 (all with *DPAGT1* mutations). The sera of patients 2 and 3 tested by isoelectric focusing were normal. The sera of patients 4 and 5 were tested by immunoturbidimetry and later by isoelectric focusing and were abnormal in both assays. Patient 4 had 8.5%, and patient 5 had 5.9% CDT measured by immunoturbidimetry (normal range 1.39-2.65%). On IEF the sera of patients 4 and 5 both showed a profile compatible with a CDG type I syndrome, with increased asialo- and disialo- isoforms and decreased tetrasialotransferrin.

3.3.4.5 Cardiac investigations

Four patients (2 with DPAGT1 and 2 with GFPT1 CMS) were found to have an abnormal 12 lead ECG. In patients where old ECGs were available these changes were noted to be longstanding (n = 3). All patients had repolarization abnormalities including ST segment flattening and/or inversion of T waves. In addition patient 17 had left ventricular hypertrophy by voltage criteria (Figure 3.7). These four patients have undergone further investigation by echocardiography and cardiac MRI as part of a collaborative cardiology research study to assess for cardiomyopathy (Lewis et al. 2014). The main findings of the study are reported as follows. Despite normal biventricular volumes and systolic function in all, late gadolinium enhancement suggestive of areas of mild (patient 1) or patchy (patients 3, 17 and 18) fibrosis were seen on MRI with a preponderance of enhancement in the basoinferolateral wall. Additional 31P MRI spectroscopy was abnormal in patients 2 and 3 indicating impaired energetics in cardiac muscle, and in three patients there was evidence of diastolic dysfunction. Thus, overall there was no evidence of overt cardiac failure but some features suggestive of incipient cardiomyopathy in the patients studied (Lewis et al. 2014).

ECG results were also available for patients 1, 10 and 19, none of which showed a repolarization abnormality. In patient 1 (DPAGT1) the ECG showed borderline first degree heart block, in patient 10 (ALG2) there was complete right bundle branch block, and in patient 19 (GFPT1) the ECG was normal.

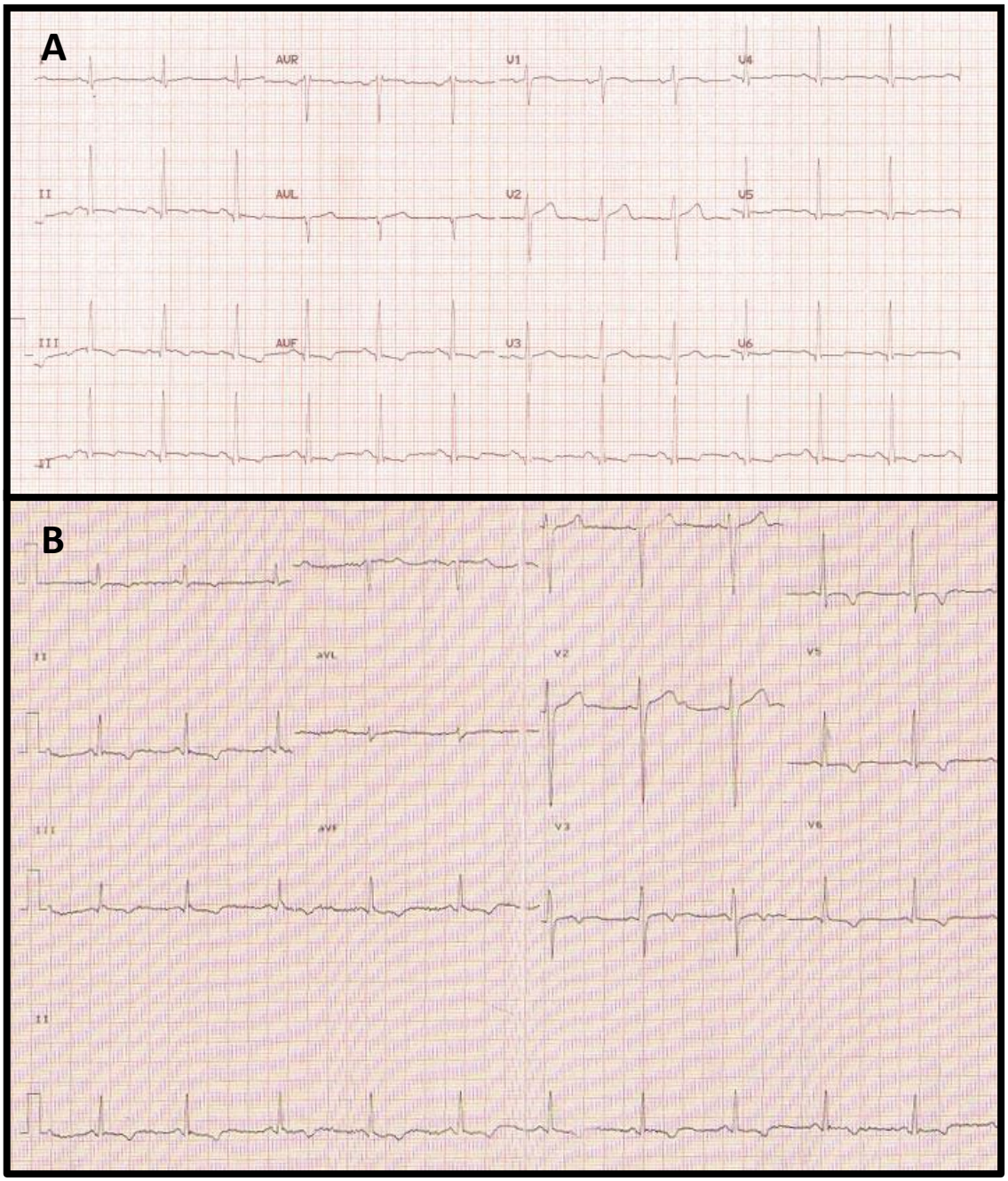

Figure 3.7: ECG abnormalities: A. From patient 2 with *DPAGT1* mutations showing ST segment flattening/T wave inversion in leads II, III, AVF and V4-V6. **B.** From patient 17 with *GFPT1* mutations showing T wave inversion in leads I, II, III, AVF, and V3-6 as well as left ventricular hypertrophy by voltage criteria.

3.3.5 Response to treatment

Response to treatment is summarized in Table 3.6.

3.3.5.1 Pyridostigmine

Thirteen patients have tried pyridostigmine of which 12 have responded to it (DPAGT1: patients 1-6, ALG2: patient 10, ALG14: patient 15, GFPT1: patients 17-19). The response in patient 16 (with *ALG14* mutations) was unclear. Patient 5 who has DPAGT1 CMS does not take pyridostigmine regularly because she is so mildly affected. Patient 2 described feeling like "Wonder Woman" after initial pyridostigmine though, like patient 19, reports that its effect has diminished over time.

3.3.5.2 3,4-diaminopyridine

The addition of 3,4-DAP to pyridostigmine therapy has been beneficial in four of the five patients who have had an adequate therapeutic trial (DPAGT1: patients 1 and 3, and GFPT1: patients 17 and 18). In one patient (patient 15 with *ALG14* mutations) 3,4-DAP caused worsening of symptoms. Patient 2 was unable to tolerate 3,4-DAP due to side effects including tingling in the extremities.

3.3.5.3 Oral salbutamol and ephedrine

Two patients (15 and 17) have been treated with ephedrine. Patient 15 did not respond to two separate trials of the drug, while patient 17 reports a modest improvement in symptoms.

Three patients, two with *DPAGT1* and one with *GFPT1* mutations, have been treated with oral salbutamol and report improvement in muscle strength. For patient 1 oral salbutamol has prevented major fluctuations, improved his grip and has enabled him to go from wheelchair bound to walking within his home. Patient 3 reported improvement in her strength and stability when transferring from bed to chair. Although this patient remains very limited in mobility, the improvement in strength has led to significant functional improvement and she is now more independent in some aspects of personal care. This patient felt improvement within the first few weeks of treatment and was continuing to improve at 6 months. Patient 18 showed improvement in QMG score from 12/39 pre-salbutamol to 7/39 after 2 years of salbutamol treatment as an adjunct to pyridostigmine and 3,4-DAP. The most significant improvement was seen in the arm raise component of the QMG which improved from 16 seconds to the test ceiling of 240 seconds.

Side effects of salbutamol were reported by two patients. Patient 1 has experienced an increase in muscle cramps but is prepared to tolerate these in view of the benefit to his strength. Patient 2 experienced marked side effects, including palpitations, insomnia, sweating and chest pain on starting salbutamol. The drug was discontinued as a result and the patient had an inadequate therapeutic trial of the drug.

Patient	1	2	3	4	5	6	7	8	9	10	11	12	13	14	15	16	17	18	19
					DPAGT1							ALG2			ALG14			GFPT1	
Pyridostigmine	+	+	+	+	+	+	u/k	+	u/k	+	nt	nt	nt	nt	+	+/-	+	+	+
3,4-diaminopyridine	+	s	+	nt	nt	nt	nt	nt	nt	nt	nt	nt	nt	nt	--	nt	+	+	nt
Ephedrine	nt	nt	nt	nt	nt	nt	nt	nt	nt	nt	nt	nt	nt	nt	-	nt	+	nt	nt
Oral salbutamol	+	s	+	nt	nt	nt	nt	nt	nt	nt	nt	nt	nt	nt	nt	nt	nt	+	nt

Table 3.6: Response to treatment: +; benefit, +/-; unclear response, -; no benefit, --; worsened, nt; not tried, s; unable to tolerate due to side effects.

3.4 Discussion[4]

3.4.1 Clinical features compared with other forms of CMS

The four subtypes described here share a number of features. Typical of CMS these patients have an autosomal recessive pattern of inheritance and present with muscle weakness early on in life which in most cases responds to anticholinesterase medication. Features that may be more specific to these subtypes, and could help to differentiate them from other forms of CMS, are a delayed onset beyond infancy, a limb-girdle pattern of weakness, relative sparing of the ocular and facial muscles and a myopathy associated with tubular aggregates. Lack of, or very minimal, ptosis in particular is a clinical feature of these new subtypes which sets them apart from the overwhelming majority of other forms of CMS. Although DOK7 CMS presents at a similar onset age, causes a limb-girdle pattern of weakness and spares extraocular muscles, it does not respond to pyridostigmine and tubular aggregates are not seen on muscle biopsy. The absence of respiratory crises, which are seen typically in fast channel syndrome, rapsyn and ChAT deficiency and in just one of the patients described here, may also help to differentiate from some forms of CMS.

A 3,4-DAP add-on was beneficial in most of the small number who had tried the drug. However, a patient with *ALG14* mutations reported worsening of symptoms with 3,4-DAP. So far therapeutic trials of ephedrine or oral salbutamol are limited to a few patients making it difficult to draw definite conclusions. However, it appears to be beneficial in all but one of the patients (again with *ALG14* mutation) who have had an adequate therapeutic trial. One DPAGT1 patient in particular reported dramatic

[4] Adapted from Finlayson et al. 2013a (URL:http://jnnp.bmj.com/content/84/10/1119).

functional improvement with oral salbutamol. Oral salbutamol and ephedrine are used effectively in some other forms of CMS with prominent myopathic features including CMS due to mutations in *DOK7* and *COLQ* and are thought to exert their effect by stimulating muscle β_2-adrenergic receptors. This may help maintain postsynaptic structure, thereby conserving the safety factor.

Similar to patients with other forms of CMS many patients described here had initially been wrongly diagnosed and treated for AIMG. It is likely that some patients with these new subtypes will be misdiagnosed as simple myopathy given the limb-girdle phenotype and abnormal findings on muscle biopsy. The myopathic EMG potentials often encountered in myasthenic disorders, seen in all eight patients who underwent a standard EMG study, may also contribute to an erroneous diagnosis of myopathy.

It is not clear whether any features can help to distinguish between the four subtypes described here. At present the numbers of cases with each subtype are too small to establish this or to make genotype-phenotype correlations. However, the finding of normal CK levels in all DPAGT1 patients described here and elsewhere (Selcen et al. 2014), but elevated levels in some GFPT1 patients may indicate that this could be used to differentiate between these two subtypes. In a previous study 50% of a large group of patients with GFPT1 CMS had elevated CK levels (Guergueltcheva et al. 2012).

Few additional cases of CMS secondary to mutations in these genes have been reported. Since the identification of the *ALG2* mutation in the large Saudi family described here, the same insertion-deletion mutation has been detected in one further family, who probably share a common founder (Monies et al. 2014). The three affected

patients from the second family have a similar phenotype to the patients described here, with a limb-girdle pattern of weakness and sparing of ocular and bulbar muscles. In contrast to the four Saudi patients described here, contractures were not a feature, and neither joint laxity, a high arched palate nor learning disability were reported.

Details of three further patients from two kinships with DPAGT1 CMS have also very recently been published (Selcen et al. 2014). Four novel mutations are described. The first, Met1Leu, reduces protein expression, while the second, His375Tyr, decreases enzyme activity. One patient carries two novel mutations, one which abolishes enzyme activity; Val264Met, in combination with a synonymous mutation; Leu120Leu, which results in exon skipping. There was a range in severity of weakness, but again the clinical phenotype was broadly similar to the patients described here. One difference of note is that trace limitation of lateral gaze was described in one patient, whereas eye movements were unaffected in all patients previously described. In addition to electrophysiological evidence of neurotransmission defect, muscle biopsies from patients were abnormal, demonstrating tubular aggregates and other myopathic features also seen in some of the patients described here, such as fibre-type disproportion and an autophagic myopathy.

3.4.2 Possible mechanisms of myasthenia

DPAGT1, ALG2 and ALG14 are involved in the first steps of the core glycan assembly before it is transferred onto the asparagine residue of nascent proteins (Bretthauer 2009; Jackson, Kukuruzinska, and Robbins 1993; Lu et al. 2012; Zhu and Lehrman 1990). ALG2 and ALG14 have been shown to be enriched at motor endplates (Cossins et al. 2013). The muscle acetylcholine receptor is a glycoprotein with all subunits

known to undergo N-linked glycosylation (Shoji et al. 1992). It has been proposed that mutations in *DPAGT1* impair AChR subunit glycosylation leading to reduced assembly and transport of the AChR into the postsynaptic membrane, and thus reduced endplate AChR number (Belaya et al. 2012b). In support of this, findings from muscle biopsies subject to detailed studies including ultrastructural, electrophysiological and bungarotoxin-binding studies from patients 1 and 2, and in other reports (Selcen et al. 2014), have been consistent with reduced endplate AChR. There is also evidence that DPAGT1 is required for cell-surface AChR expression from *in vitro* studies. In cell culture experiments, in the presence of tunicamycin, a specific DPAGT1 inhibitor, α-bungarotoxin binding was partially restored by overexpression of wild type *DPAGT1* but not *DPAGT1* c.699dup mutant (Belaya et al. 2012b). Similarly, expression of ALG14 mutant p.Pro65Leu in HEK293 cells resulted in reduced AChR expression, measured by α-bungarotoxin binding (Cossins et al. 2013). Reduced endplate AChR is likely to be the major mechanism for impaired neuromuscular transmission, although impaired glycosylation of other proteins located at the neuromuscular junction may also contribute to these disorders. Furthermore, ultrastructural studies of endplate from patients harbouring *DPAGT1* mutations have shown a combination of pre-, as well as postsynaptic abnormality, with small and sometimes degenerating nerve terminals (Selcen et al. 2014).

GFPT1 is a key enzyme in the biosynthetic pathway that provides amino sugars for the synthesis of glycoproteins, glycolipids, and proteoglycans. Although the underlying mechanism of GFPT1 congenital myasthenic syndrome is not fully elucidated, the similarity of clinical features shared between patients with *GFPT1* mutations and those with *DPAGT1, ALG2* or *ALG14* mutations suggests that the same N-linked glycosylation pathway is involved. In support of this hypothesis experiments

with cultured muscle cells from two patients with *GFPT1* mutations have shown significant reduction in cell-surface AChR expression (Zoltowska et al. 2013).

The presence of tubular aggregates on muscle biopsy is a useful distinguishing feature from other forms of CMS although these were not seen in early biopsies from the DPAGT1 patients suggesting they accumulate over time. Another explanation could be that repeat biopsies were more likely to be subject to ultrastructural studies which are more sensitive in detecting TA. Tubular aggregates were not seen in the only patient with *ALG14* mutations who has had a biopsy so it is not possible to conclude whether they could be a feature in that particular subtype. While tubular aggregates were detected in biopsies from the patients with *GFPT1* mutations reported here, they were present in only 13/18 biopsies from the 14 families described in a large case series (Guergueltcheva et al. 2012), in which patients 17 and 18 are included. In that series it is not clear whether electron microscopy analysis was performed in addition to histology in those biopsies where tubular aggregates were not detected.

Tubular aggregates visualized by electron microscopy are inclusions of tubules of variable appearance within muscle fibres (Pavlovicová, Novotová, and Zahradník 2003). It is generally accepted that these structures derive from the sarcoplasmic reticulum (SR), although the mechanism of their formation has not been elucidated. It has been suggested that reshaping of the SR and TA formation is initiated by aggregation of misfolded proteins (Schiaffino 2012). Where glycan residues have a critical contribution to the structural integrity of a protein, it follows that disordered glycosylation due to mutations in glycosylation pathway genes could lead to protein misfolding and predispose to TA formation.

Tubular aggregates have been observed in some cases of myotonia, myotonic dystrophy, and muscle channelopathies. Additionally a poorly defined ‘tubular aggregate myopathy’ (TAM) is described (Engel, Bishop, and Cunningham 1970; Niakan, Harati, and Danon 1985; Rosenberg, Neville, and Ringel 1985; Schiaffino 2012) associated with myalgia and cramps. Recently mutations in *STIM1*(stromal interaction molecule 1), which encodes a calcium sensor in the endoplasmic reticulum, were detected in families with an autosomal dominant form of TAM (Böhm et al. 2013). However, most described cases are recessive and it is probable that TAM represents a number of different disorders.

3.4.3 Congenital disorders of glycosylation

Previously, mutations in *DPAGT1* have been reported in connection with a very different clinical picture: congenital disorder of glycosylation type Ij. Congenital disorders of glycosylation are a group of disorders caused by defects in the formation (type I) or processing (type II) of glycoproteins or glycolipids. The majority are recessive, often present with multisystemic disease, and great variability in clinical features is reported (Jaeken 2011). Type Ij is an infrequent CDG with just eleven individuals (seven families) with an identified genetic mutation found in the literature (Carrera et al. 2012; Imtiaz, Al-Mostafa, and Al-Hassnan 2012; Iqbal et al. 2012; Timal et al. 2012; Vuillaumier-Barrot 2005; Wu et al. 2003; Würde et al. 2012). In nine of these patients clinical details have been reported (Table 3.7) and clear multisystem involvement is described in the majority. In six of the nine, symptom onset was within the first day of life with death occurring before 3 years of age in five individuals. Some clinical features are shared, with six having had seizures (three refractory), seven had

hypotonia, and five had microcephaly. However, there is significant variation in clinical features and severity with two siblings (patients x and xi, Table 3.7), aged 34 and 32 years at the time of the report (Iqbal et al. 2012), presenting with a relatively mild phenotype. A severe fetal hypokinesia phenotype was described in patient ix with no spontaneous movements and very little movements with stimuli (Carrera et al. 2012). Absence of intra-uterine movements was reported by his mother and he had joint contractures. Fetal hypokinesia and contractures are associated with some forms of CMS (particularly rapsyn CMS and mutation of the AChR γ-subunit). In addition, contractures and a high arched palate, both features suggestive of fetal akinesia, were reported in three of the four patients with *ALG2* mutations from kinship 7.

Patient	Reference and year reported	Mutations	Sex/Onset age /Onset symptoms/Age at death	Clinical features
i	Wu et al, 2003	c.660A>G (p.Tyr170Cys) and unspecified splicing defect	F/4 months/infantile spasms/alive at 6 years	Developmental delay, microcephaly, arched palate, micrognathia, exotropia, fifth finger clinodactyly, single flexion creases, skin dimples on upper thighs, severe hypotonia, refractory seizures
ii **iii**	Vuillaumier-Barrot, 2005	c.890A>T (p.Ile297Phe) and c.162-8G>A (splicing defect)	Not reported	Not reported
iv	Imtiaz et al 2011	homozygous c.902G>A (p.Arg301His)	M/birth/respiratory distress/5 years	Developmental delay, hypotonia, microcephaly, cyanotic spells, elevated ALT, elevated CK, delayed myelination on brain MRI, seizures, muscle biopsy showed fibre type disproportion
v			M/birth/hypotonia, poor feeding, choking/7 months	Decreased fetal movement, microcephaly, elevated ALT
vi	Wurde et al, 2012	homozygous c.341C>G (p.Ala114Gly)	F/day 1/hyperexcitability/8 months	Developmental delay, reduced spontaneous movement, hypocalcaemia, hypotonia, refractory seizures, bilateral cataracts, mild hepatomegaly, inverted mammillae, nystagmus, strabism, hypertrichosis, progressive microcephaly, cerebral atrophy, long eyelashes, slight elevation of liver enzymes
vii			F/day 1/ tremor, fasciculations, abnormal movements/1 year	Developmental delay, reduced spontaneous movement, hyperreflexia, pathological fat pads, shortened Achilles tendons, bilateral cataracts, refractory seizures, progressive microcephaly, strabism, nystagmus, slight elevation of liver enzymes

Table 3.7: Previously reported cases of CDG-Ij: CK; creatine kinase, ALT; alanine aminotransferase, IQ; intelligence quotient. Reproduced from Finlayson et al. 2013a (URL: http://jnnp.bmj.com/content/84/10/1119).

Table 3.7: (continued)

Patient	Reference and year reported	Mutations	Sex/Onset age /Onset symptoms/Age at death	Clinical features
viii	Timal et al, 2012	c.206T>A (p.Ile69Asn) and c.161 + 5G>A (splicing defect)	M/birth/asphyxia/2.5 years	Respiratory insufficiency, apnoeas, jaundice, elevated liver enzymes, bilateral nuclear cataract, cryptorchidism, dysmorphia, hypertonia of extremities, joint contractures, tremor, feeding difficulties
ix	Carrera et al, 2012	c.901C>T (p.Arg301Cys) and c.1054T>G (p.Leu385Arg)	M/birth/abnormal fetal monitoring – emergency C-section-mechanical ventilation/1.5 months	No intra-uterine movements felt, fetal hypokinesia phenotype, unexpressive face without nasolobial grooves, soft long ears, U-shaped vermillion of upper lip, thick skin, hypertrichosis, hand camptodactyly, moderate multiple contractures, hypotonia, severe hypokinesia
x	Iqbal et al, 2012	c.85A>T (p.Ile29Phe) and c.503T>C (p.Leu168Pro)	F/5 years/ epilepsy, hypotonia, aggressive behaviour/alive at 34 years	Mild atypical facial dysmorphism, night blindness, moderate IQ (35-49), abnormal speech, balance problem
xi			M/2 years/ epilepsy, hypotonia, aggressive behaviour/alive at 32 years	Mild atypical facial dysmorphism, moderate IQ (35-49), abnormal speech, balance problem

None of the mutations in the DPAGT1 CMS patients were shared by the CDG-Ij cases. The first four kinships diagnosed with DPAGT1 CMS had a missense mutation in exon 3, and it has been suggested that this exon may be especially important for a function related to neuromuscular transmission (Belaya et al. 2012b). However, two siblings with CDG-Ij reported to have severe multisystem disease were both homozygous for the exon 3 mutation c.341C>G (Würde et al. 2012). In the CDG-Ij cases with hypotonia, including one of the siblings with exon 3 mutations, details of whether SFEMG or RNS was performed are not reported. Therefore, it is not known whether there was any a defect of neuromuscular transmission and this remains a possibility.

A sole patient with a multisystem CDG caused by mutation in *ALG2*; CDG type Ii, has been reported previously. The patient was said to be normal at birth but within the 1st year of life developed a multisystemic disorder with mental retardation, seizures, coloboma of the iris, hypomyelination, hepatomegaly, and coagulation abnormalities (Thiel et al. 2003). The patient was heterozygous for mutations different to those reported here and was known to be alive at 3 years of age. Neither *ALG14* nor *GFPT1* have been reported to be associated with a CDG.

Why the patients reported here have symptoms largely restricted to a NMJ disorder is not understood, though there are a number of potential possibilities. Different mutations may be expected to result in different levels of functional enzymatic activity and it is possible that those with disease restricted to the NMJ have higher levels of enzyme function and thus a milder phenotype than those with multisystem disease. Alternatively it may be that appropriate glycosylation of AChR subunits (or other NMJ proteins) is more critical to normal function than in proteins of other tissues, thus making the NMJ more susceptible to a modest impairment of

glycosylation. A further possibility is that these genes have an uncharacterized muscle-specific function and these patients' mutations specifically disrupt that function while the protein can function adequately in other cell types. Of note a number of patients have symptoms unrelated to the NMJ disorder. Six of the cases reported here, with either DPAGT1 or ALG2 CMS, have mild learning disability, and in recent report of three patients with DPAGT1 CMS, intellectual impairment was described in two, whereas the third was previously diagnosed with an autistic spectrum disorder (Selcen et al. 2014). Furthermore, one patient described here with GFPT1 CMS has retinitis pigmentosa. While cognitive impairment and retinal disease may be incidental in these cases the possibility that these features are related to disordered glycosylation should be considered. With the discovery and study of additional patients this should become clearer.

3.4.4 Cardiac findings

The mild abnormalities seen in cardiac investigations of the small group of patients studied with *GFPT1* and *DPAGT1* mutations may be suggestive of incipient cardiomyopathy, and give further support to the possibility of multisystem involvement in these patients. Other published cases of DPAGT1 CMS describe prolonged or borderline prolonged QTc interval on ECG (Selcen et al. 2014). The normal systolic function in the four patients studied here is reassuring. Cardiomyopathy is a reported feature in many CDG subtypes (Footitt et al. 2009) and mutations in dolichol kinase (*DOLK*), another early N-linked glycosylation pathway component, have been reported to cause non-syndromic dilated cardiomyopathy (Lefeber et al. 2011) as well as cardiomyopathy as part of a severe multisystem disorder (Lieu et al. 2013). Cardiac

abnormalities are not known to be a feature of any other genetically defined CMS. Even in DOK7 CMS, where the protein is known to be expressed in rat cardiac muscle, cardiac investigations were normal in all but one patient of a large cohort (Palace et al. 2007). One report of similar ECG abnormalities in CMS was available in the literature (Dobkin and Verity 1978). This paper describes a family of three siblings affected by a limb-girdle form of CMS who have similar ECG abnormalities to the patients described here. The patients reported also had a similar phenotype to those described here, including tubular aggregates on muscle biopsy, and it is highly possible they too had a mutation in a glycosylation pathway gene. Given the small numbers of asymptomatic patients in whom cardiac assessment has been performed, it may be prudent to screen all patients with mutations in a glycosylation pathway. This may be especially relevant where long term β_2- agonists are used.

3.4.5 Biochemical tests of glycosylation

Biochemical tests may help identify some patients with glycosylation pathway mutations as they were abnormal in 2/4 patients with *DPAGT1* mutations described here and in 2/3 described in a recent report (Selcen et al. 2014).

In the six families of patients with CDG type Ij with clinical details reported, hypoglycosylation of serum transferrin on IEF was demonstrated in all. As not all patients reported here had abnormal studies, this is in keeping with the suggestion that the reduction of DPAGT1 enzymatic activity is less marked in those patients with CMS compared with patients with multisystem disease diagnosed as CDG Ij. Although results were not available or not performed in patients described here with a genotype other than *DPAGT1*, it is possible these tests could be helpful in those conditions as

well. In support of this %CDT has been reported to be elevated in one, and borderline in two patients, with ALG2 CMS reported elsewhere (Monies et al. 2014). Thus in patients with a limb-girdle phenotype and CMAP decrement, testing for abnormal glycosylation should be considered and may bypass the need for more invasive investigation.

Chapter 4

Muscle MRI in congenital myasthenia

4.1 Introduction

Muscle MRI has played an increasing role in the diagnosis of many neuromuscular disorders (Mercuri et al. 2007; Straub, Carlier, and Mercuri 2012). It is non-invasive, quick, generally well tolerated and can identify muscles most suitable for biopsy. So far most studies have concentrated on lower limb imaging, where most clinical experience lies, but whole-body MRI or MRI of the truncal and upper limb muscles is beginning to be explored (Straub, Carlier, and Mercuri 2012; Faridian-Aragh et al. 2014). The majority of findings described relate to hyperintensity on T1-weighted (T1w) images reflecting fatty infiltration of muscle. Another finding is hyperintensity on fat-suppressed T2-weighted sequences such as short-tau-inversion-recovery (STIR), likely reflecting increased water content due to inflammation or increased blood flow (Lovitt, Moore, and Marden 2006). It is postulated that STIR imaging may be able to show earlier changes than T1w imaging, before fatty infiltration has had a chance to develop or become evident (Mercuri et al. 2007).

Analysis in published reports is often undertaken using semi-quantitative descriptive rating scales of T1w findings (Mercuri et al. 2002b; Fischer et al. 2008; Kim et al. 2010; Faridian-Aragh et al. 2014). However, in muscle disorders a main focus has been on identifying patterns of muscle involvement (Figure 4.1) because of the sometimes striking differences seen between conditions, which can help direct genetic testing in inherited myopathies and dystrophies (Straub, Carlier, and Mercuri 2012). Bethlem myopathy, where the pattern of central sparing of the vasti muscles (Figure 4.2) is considered almost pathognomonic, is a prime example of the utility of muscle imaging (Mercuri et al. 2005; Mercuri et al. 2002c; Morrow et al. 2013a).

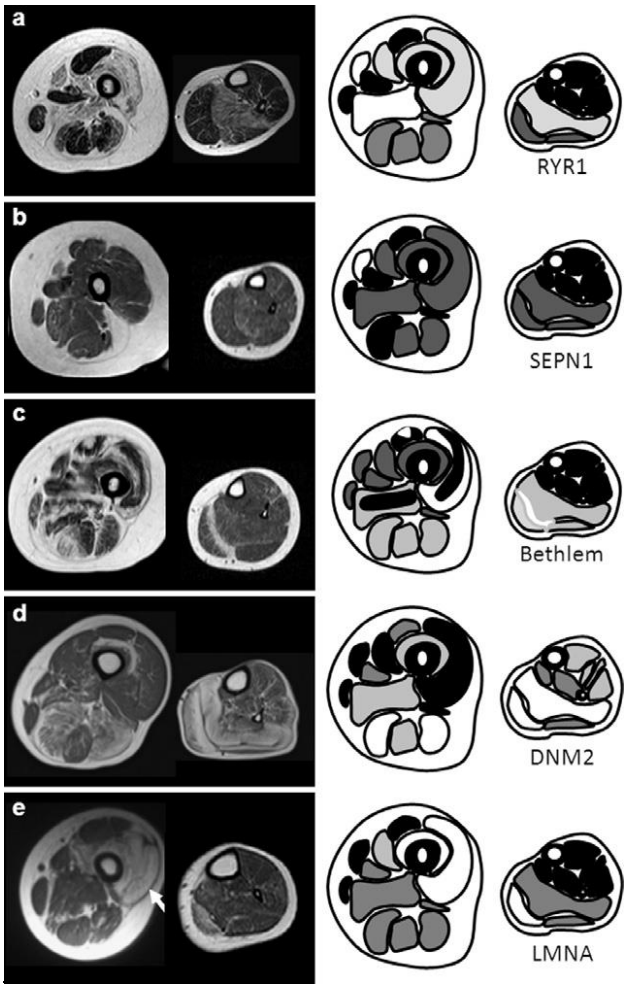

Figure 4.1: Patterns of muscle pathology in congenital myopathies: The figure shows panels of axial T1w MR images through the left thigh and calf of various myopathies and corresponding drawings that illustrate the selective muscle involvement in shades of grey, with white being most severely affected and black being normal. RYR1, autosomal dominant ryanodine receptor 1 associated myopathy; SEPN1, selenoprotein 1 associated congenital myopathy; Bethlem, autosomal dominant Bethlem myopathy caused by collagen VI mutations; DNM2, dynamin 2 associated centronuclear myopathy, LMNA, laminopathy. The MR images provide examples of selective muscle pathology in individual patients, whereas the drawings summarize typical patterns of muscle pathology according to current knowledge.[1]

[1] Reprinted from Neuromuscular Disorders, 22 Suppl 2, Straub, Carlier, and Mercuri, TREAT-NMD workshop: Pattern recognition in genetic muscle diseases using muscle MRI, S42-53, Copyright 2012, with permission from Elsevier.

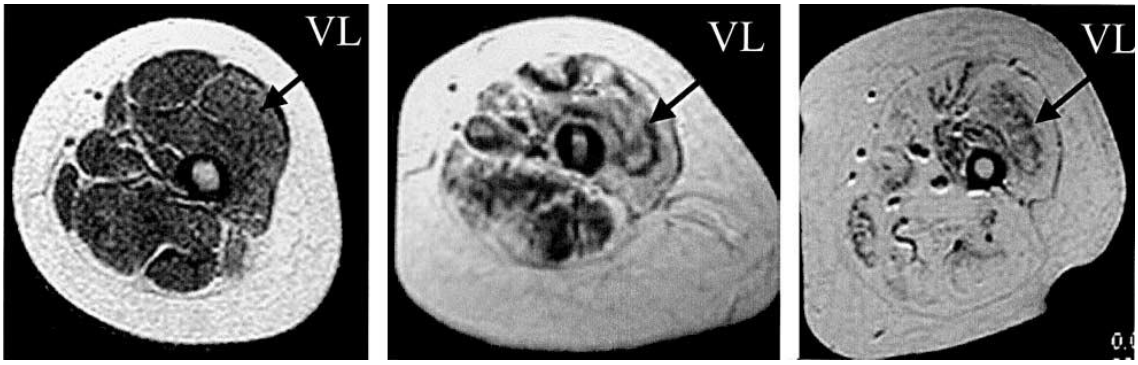

Figure 4.2: T1w thigh muscle MRI findings in three generations of a family with Bethlem myopathy: Images show the characteristic pattern of muscle involvement in this condition as well as more marked fatty infiltration seen with increasing disease duration. Note that the vastus lateralis (VL) is only marginally affected at its periphery in the 6-year-old young girl (left). The periphery of the same muscle is also more markedly affected in her mother (middle) and in her grandmother with obvious sparing of the central part (right).[2]

Muscle MRI findings in DOK7 CMS have been reported in brief (Klein et al. 2013). This study described the findings of retrospective clinical scans in six children with DOK7 CMS, and reported that MRI was abnormal in 2/6 showing mild, non-specific, and non-selective atrophic, changes. With the exception of this study, no other reports of muscle MRI appearance in CMS have been published to date. Although most CMS subtypes have been associated with mild myopathic features on muscle biopsy (Kinali et al. 2008) some subtypes have specific pathophysiological features that suggest they are likely to have greater secondary muscle damage. Slow channel syndrome (Engel et al. 1982) and COLQ CMS (Hutchinson et al. 1993) are associated with an excitotoxic endplate myopathy with degeneration of postsynaptic junctional folds. Similar degeneration, as well as other myopathic features, have been described in DOK7 CMS (Selcen et al. 2008; Klein et al. 2013), which can mimic a limb-girdle myopathy, and GFPT1 (Guergueltcheva et al. 2012) and DPAGT1 (Belaya et al. 2012b) subtypes are associated with tubular aggregates, inclusions within muscle fibres thought to represent aggregations of misfolded proteins. Therefore it is possible that some CMS

[2] Reprinted from European Journal of Paediatric Neurology, 6, Mercuri et al, Muscle MRI findings in a three-generation family affected by Bethlem myopathy, 309-14, Copyright 2002, with permission from Elsevier.

patients could have abnormal muscle MRI signal, and there may be a diagnostically useful difference between subtypes which could enable institution of early and appropriate symptomatic treatment and direct genetic testing. Additionally, patients on CMS treatments aimed at reducing muscle damage over time might be assessed for their sub-clinical efficacy using longitudinal muscle MRI. Furthermore, an appreciation of typical MRI findings in CMS would add to the growing body of knowledge of the spectrum of muscle MRI features in neuromuscular disease which would broadly be of benefit in the investigation of patients.

4.1.1 Aims

1) Define the nature of any abnormalities on lower limb muscle MRI in different congenital myasthenic syndromes.

2) Correlate muscle MRI findings with clinical parameters including CMS subtype.

4.2 Methods

4.2.1 Recruitment of participants and ethical approval

A prospective imaging study was designed and the study granted ethical approval by South Central Research Ethics Committee A (11/SC/0157). Patients with genetically confirmed congenital myasthenia were recruited via the nationally commissioned CMS service. Approximate age and sex matched healthy controls were also recruited.

4.2.2 Clinical parameters

Patient clinical data was collected including genetic subtype, age at onset and current treatment. Concurrent clinical assessments included QMG score (Figure 3.3), timed 10 metre walk, myasthenia gravis activities of daily living (MGADL) score and MRC scoring of lower limb muscle strength. The MGADL scale is an eight question survey designed to grade clinical severity in AIMG (Figure 4.3), where it has been shown to correlate with the QMG score (Wolfe et al. 1999). The mean of right and left leg raise times, which are clinically useful to monitor response to treatment, was extracted from the QMG score.

Grade	0	1	2	3	Score
Talking	Normal	Intermittent slurring or nasal speech	Constant slurring or nasal, but can be understood	Difficult to understand speech	
Chewing	Normal	Fatigue with solid food	Fatigue with soft food	Gastric tube	
Swallowing	Normal	Rare episode of choking	Frequent choking necessitating changes in diet	Gastric tube	
Breathing	Normal	Shortness of breath with exertion	Shortness of breath at rest	Ventilator dependence	
Impairment of ability to brush teeth or comb hair	None	Extra effort, but no rest periods needed	Rest periods needed	Cannot do one of these functions	
Impairment of ability to arise from a chair	None	Mild, sometimes uses arms	Moderate, always uses arms	Severe, requires assistance	
Double vision	None	Occurs, but not daily	Daily, but not constant	Constant	
Eyelid droop	None	Occurs, but not daily	Daily, but not constant	Constant	

Total score _____

Figure 4.3: Myasthenia gravis activities of daily living scale.

4.2.3 MRI sequences

Subjects were scanned at 3T (Siemens TIM Trio, Erlangen, Germany) lying feet first in a supine position with a spine matrix coil, and two surface array coils; one a peripheral angiography coil, to receive the signal from the thighs and calves of both limbs.

Scanning sequences were based on a clinical imaging protocol from the Queen Square Muscle Imaging Centre, London, UK. This comprised T1w axial imaging (typical parameters: repetition time (TR)/echo time (TE) = 575/9.7 ms) and axial STIR imaging (typical parameters TR/TE/inversion time (TI) = 5200/38/220 ms) both with 4 mm slice thickness and 2 mm slice gap.

4.2.4 MRI analysis

Patient and control scans were intermixed and analyzed by two experienced assessors blinded to clinical details (Dr Jasper Morrow and Professor Tarek Yousry from the Muscle Imaging Centre in Queen Square). The following muscles were analyzed bilaterally: rectus femoris, vastus lateralis, vastus intermedius, vastus medialis, biceps femoris long head, biceps femoris short head, semitendinosus, semimembranosus, adductor magnus, adductor longus, sartorius, gracilis, tibialis anterior, extensor hallucis longus, peroneus longus, lateral gastrocnemius, medial gastrocnemius, soleus and tibialis posterior.

These 38 muscles were assessed on T1w sequences for the presence of fatty infiltration using the semi-quantitative Mercuri score (Mercuri et al. 2002b) (Table 4.1). The same muscles were assessed on STIR sequences and were graded on a previously

described three point scale as follows: 0 -normal, 1 -mild or 2 -marked hyperintensity (Morrow et al. 2013b).

The T1w (Mercuri) and STIR scoring were analyzed to look for any pattern of selective muscle involvement.

Mercuri grade	Description
0	Normal appearance
1	Early moth-eaten appearance, with scattered small areas of increased signal.
2a	Late moth-eaten appearance, with numerous discrete areas of increased signal with beginning confluence, comprising less than 30% of the volume of the individual muscle.
2b	Late moth-eaten appearance, with numerous discrete areas of increased signal with beginning confluence, comprising 30–60% of the volume of the individual muscle.
3	Washed-out appearance, fuzzy appearance due to confluent areas of increased signal.
4	End-stage appearance, muscle replaced by increased density connective tissue and fat, with only a rim of fascia and neurovascular structures distinguishable.

Table 4.1: Mercuri grades for T1 sequences. From Mercuri et al. 2002b.

4.2.4.1 Categorizing severity of muscle involvement for each subject

Taking control data into account, an overall categorization for the two sequences was created (Table 4.2). The severity of both T1w and STIR findings in each subject's thigh and calf muscles were then categorized.

In addition a mean T1 score was established for each subject. To calculate this Mercuri scores for each muscle were first modified to contain only numerical values as follows: Grade 0 = 0, Grade 1 = 1, Grade 2a = 2, Grade 2b = 3, Grade 3 = 4, Grade 4 = 5. The mean was then calculated by dividing the sum of modified Mercuri scores by the total number of muscles analyzed.

Categorization	Symbol	T1w results	STIR results
Normal	-	All muscles Mercuri grade 0-1	All muscles normal intensity
Mild limited changes	+/-	≤50% muscles Mercuri grade 2a	Mild hyperintensity in ≤25% of muscles
Mild extensive changes	+	>50% muscles Mercuri grade 2a	Mild hyperintensity in >25% of muscles
Marked changes	++	Any muscles Mercuri grade 2b or more	Any muscles with marked hyperintensity

Table 4.2: Severity categorization of T1 and STIR scores.

4.2.4.2 Statistical analysis

Statistical analyses were performed using GraphPad Prism version 6, GraphPad Software, California. Spearman's rank correlation coefficient (rho) was used to assess correlation between mean T1 score and clinical parameters. The overall mean T1 scores of different subtypes were compared to control using an unpaired t-test with Welch's correction on logarithmically transformed (to base-e) scores. It is important to note that the small group sizes, due to the rarity of CMS, limits meaningful additional statistical analysis and therefore much of the analysis is descriptive.

4.3 Results

4.3.1 Patient and control demographics

Twenty one subjects with eight CMS subtypes and ten healthy controls were recruited (Table 4.3). Scanning was incomplete in four because of either technical issues or inability to tolerate lying flat: subject 10 (DOK7) only had thigh imaging, subject 12 (SCS) had the right thigh and both calves imaged, subject 14 (SCS) only had calf imaging, and subject i (control) did not have calf STIR imaging.

	Number	M/F	Mean age and range (years)
Control	10	4M/6F	35.70 (18-54)
All CMS	21	12M/9F	39.10 (16-66)
CMS by subtype			
• **AChR def**	4	2M/2F	24 (16-34)
• **Rapsyn**	3	2M/1F	51.3 (41-63)
• **DOK7**	4	2M/2F	39.8 (25-62)
• **SCS**	4	3M/1F	50.3 (24-66)
• **COLQ**	1	F	16
• **ChAT**	1	M	16
• **GFPT1**	2	2M	32 (25-39)
• **DPAGT1**	2	2F	57.5 (57-58)

Table 4.3: Subject demographics: AChR def; acetylcholine receptor deficiency due to ε-subunit mutation, SCS; slow channel syndrome, M; male, F; female.

4.3.2 T1w sequences

All control muscles were Mercuri grade 0, 1 or 2a (Figure 4.4). Fatty infiltration in controls (i.e. muscles of Mercuri grade 1 or above) was found in 180/240 (75%) of thigh and 122/140 (87%) of calf muscles (Table 4.4). In the CMS cohort fatty infiltration was found in 410/468 (87.6%) of thigh and 239/280 (85.4%) of calf muscles and Mercuri grades were either 0, 1, 2a, 2b or 3 (Table 4.4). No muscles in the CMS cohort were assigned an overall maximum Mercuri grade of 4 though focal areas of fat equivalent to Mercuri grade 4 were identified in 15 muscles (7 peroneus longus) of five patients (with GFPT1, DPAGT1, rapsyn and SCS subtypes) and in one peroneus longus muscle of one control subject (e). No selective pattern of muscle involvement was identified in any of the eight CMS subtypes. The numbers were too small within subtype groups to demonstrate definite differences. However abnormalities not seen in controls were identified most consistently in the DPAGT1 and GFPT1subtypes where Mercuri scores grade 2a or higher were seen in all calf muscles and in two of these subjects the thigh muscles were similarly affected.

	CONTROL						CMS					
	Thigh			Calf			Thigh			Calf		
Mercuri grade	**Number (%) of muscles**	**Number of subjects**	**Comments**	**Number (%) of muscles**	**Number of subjects**	**Comments**	**Number (%) of muscles**	**Number of subjects**	**Comments**	**Number (%) of muscles**	**Number of subjects**	**Comments**
Grade 0	60 (25%)	8		18 (12.8%)	3		58 (12.4%)	10		41 (14.6%)	7	
Grade 1	169 (70.4%)	9		111 (79.3%)	10		250 (53.4%)	18		108 (38.6%)	15	
Grade 2a	11 (4.6%)	3	Includes 2 eldest controls	11 (7.9%)	4	Includes 2 eldest controls	118 (25.2%)	14		80 (28.6%)	18	
Grade 2b	nil			nil			36 (7.7%)	6	GFPT1, DPAGT1, SCS and rapsyn.	25 (8.9%)	5	GFPT1, DPAGT1, SCS.
Grade 3	nil			nil			6 (1.3%)	4		26 (9.3%)	5	GFPT1, DPAGT1, SCS and rapsyn.

Table 4.4: Number of muscles by Mercuri grade in the control and CMS cohort.

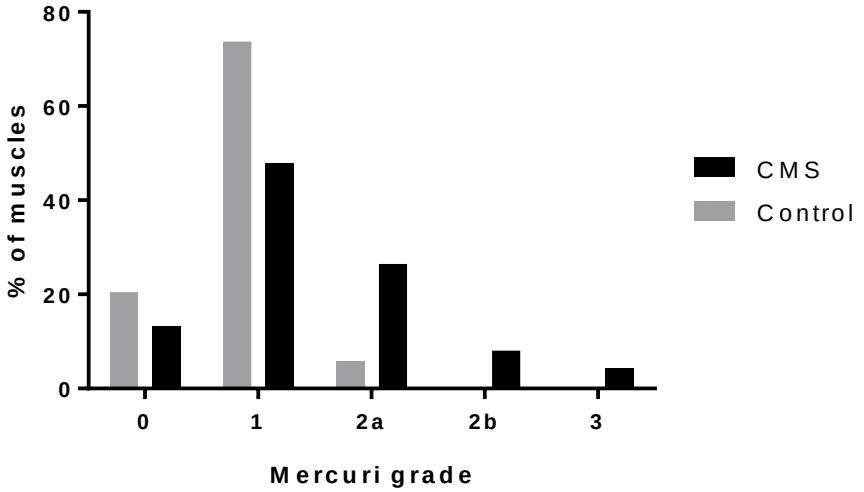

Figure 4.4: Proportions of muscles by Mercuri grade: combined data from thigh and calf muscles are shown.

The overall mean T1 score of the control group was 0.85 compared with 1.46 in the CMS cohort. Mean T1 scores varied by CMS subtype (Figure 4.5). Mean T1 scores for individual control subjects (Table 4.5) and CMS subjects (Table 4.6) are given alongside their severity categories for T1w and STIR imaging. Clinical parameters for each CMS subject and the mean values for CMS subtypes are also presented in Table 4.6.

The most striking difference from healthy controls is seen in the GFPT1 and DPAGT1 groups which had mean T1 scores almost treble that of the control group, while the mean T1 score of the slow channel syndrome group was over double that of the control group. Despite the small group numbers this is reflected in statistical analysis which found the mean T1 score of these three subtypes to be significantly different from the control population (Table 4.6). By contrast the AChR deficiency group had a very similar mean T1 score to the control group at 0.80.

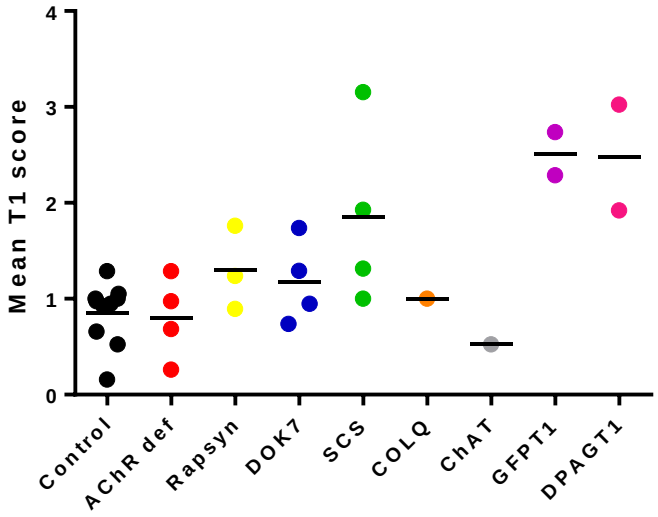

Figure 4.5: Mean T1 scores by subtype: Values for individual subjects (dots) and the overall mean for each group (black bars) are shown. AChR def; acetylcholine receptor deficiency, SCS; slow channel syndrome.

Control subject ID	Thigh		Calf		Mean T1 score
	T1	STIR	T1	STIR	
a	-	-	-	-	0.95
b	+/-	-	+/-	-	1.05
c	+/-	-	+/-	+/-	1
d	-	-	-	+	0.53
e	+/-	-	+/-	+/-	1.29
f	-	-	+/-	+/-	0.97
g	-	-	-	+/-	0.16
h	-	-	-	-	0.92
i	-	-	-	nd	0.66
j	-	-	-	+/-	1.00

Table 4.5: Control group T1 and STIR imaging: nd; not done, -; normal, +/-; mild limited changes, +; mild extensive changes, ++; marked changes.

Subject ID	Age at onset (months) /current age (years)	MGADL score	QMG score	Leg raise time (s)	MRC score HF/KF/KE/AD	Timed 10m walk (s)	Treatment	MRI severity categorization Thigh		MRI severity categorization Calf		Mean T1 score
								T1	STIR	T1	STIR	
AChR def												
1	2/16	6	13	38	4+/4+/5/4	5.87	**P, D**	-	-	-	-	0.26
2	4/30	9	16	3.5	4-/4/4+/4	unable	**P, D**	+/-	-	+/-	+/-	1.29
3	0/34	9	17	19.5	4+/4+/4+/4-	unable	**P, D**	+/-	-	+/-	-	0.68
4	2/16	9	24	0	4-/4/4+/4	unable	**P, D**	+/-	-	+/-	-	0.97
mean	**2/24**	**8.25**	**17.5**	**15.25**								**0.80 (p = ns)**
Rapsyn												
5	576/63	2	14	19	5/5/5/4	7.5	**P**	++	-	+	-	1.76
6	120*/41	5	6	56	5/5/5/5	6.6	**P**	-	-	+/-	+/-	0.89
7	0/50	4	7	49	5/5/5/5	6.78	**P**	+/-	-	++	+/-	1.24
mean	**232/51.3**	**3.7**	**9**	**41.3**		**6.96**						**1.3 (p = ns)**
DOK7												
8	0/40	10	16	87.5	5/5/5/5	7.6	**D, S**, E	+	-	+	+/-	1.74
9	252/25	0	3	100	5/5/5/nd	6	**S**, E	-	-	+/-	-	0.95
10	36/62	5	16	24.5	5/5/5/5	11.5	**D, E**	+/-	-	nd	nd	1.29
11	0/32	11	16	19.5	5/5/nd/5	8.26	**E**	-	-	+/-	+/-	0.74
mean	**72/39.8**	**6.5**	**12.75**	**57.88**								**1.18 (p = ns)**

Table 4.6: Clinical parameters and MRI findings: *; at least, MRC score; Medical Research Council strength score, HF; hip flexion, KF; knee flexion, KE; knee extension, AD; ankle dorsiflexion, m; metres, s; seconds, nd; not done, P; pyridostigmine, D; 3,4-diaminopyridine, S; salbutamol, E; ephedrine, F; fluoxetine, Q; quinidine (bold indicates ongoing treatment), -; normal, +/-; mild limited changes, +; mild extensive changes, ++; marked changes (as defined in the methods), p; p value (unpaired t-test with Welch's correction on logarithmically transformed (to base-e) scores), ns; not significant.

Table 4.6: (continued)

Subject ID	Age at onset (months) /current age (years)	MGADL score	QMG score	Leg raise time (s)	MRC score HF/KF/KE/AD	Timed 10m walk (s)	Treatment	MRI severity categorization Thigh		MRI severity categorization Calf		Mean T1 score
								T1	STIR	T1	STIR	
SCS												
12	36/54	8	7	37	5/5/5/5	12.3	**F**, Q	++	-	++	+/-	3.15
13	36/57	8	22	85.5	5/5/5/5	7.2		+/-	-	+	+/-	1.32
14	72/66	3	14	29	4+/5/5/3+	7.62	**P, F, S**	nd	nd	++	+	1.93
15	216/24	3	3	100	5/5/5/5	4.94	**F**	-	-	+/-	+/-	1
mean	**90/50.3**	**5.5**	**11.5**	**62.88**								**1.85 (p = 0.0399)**
COLQ												
16	84/16	1	7	41	nd	8.46	**E**	+/-	-	+/-	-	1
ChAT												
17	4/16	6	13	3	5/5/5/4+	5.7	**P, S**	-	-	+/-	+/-	0.53
GFPT1												
18	72/39	3	7	20	4/5/5/4+	6.9	**P, D, S**	++	-	++	++	2.74
19	16/25	2	13	12.5	4-/4/4/4+	9.42	**E**	++	-	++	+/-	2.29
mean	**44/32**	**2.5**	**10**	**16.25**		**8.16**						**2.51 (p = 0.0003)**
DPAGT1												
20	84/57	8	18	33.5	4+/5-/4/4	nd	**P**	++	-	+	+/-	1.92
21	24/58	3	18	0	3-/5/5/4	unable	**P, D, S**	++	-	++	+	3.03
mean	**54/57.5**	**5.5**	**18**	**16.75**								**2.47 (p = 0.0346)**

	Normal	Mild limited changes	Mild extensive changes	Marked changes
Thigh control	7/10 (70%)	3/10 (30%)		
Calf control	6/10 (60%)	4/10 (40%)		
Thigh all CMS	6/20 (30%)	7/20 (35%)	1/20 (5%)	6/20 (30%)
Calf all CMS	1/20 (5%)	9/20 (45%)	4/20 (20%)	6/20 (30%)
Thigh AChR def	1/4	3/4		
Calf AChR def	1/4	3/4		
Thigh rapsyn	1/3	1/3		1/3
Calf rapsyn		1/3	1/3	1/3
Thigh DOK7	2/4	1/4	1/4	
Calf DOK7		2/3	1/3	
Thigh SCS	1/3	1/3		1/3
Calf SCS		1/4	1/4	2/4
Thigh COLQ		1/1		
Calf COLQ		1/1		
Thigh ChAT	1/1			
Calf ChAT		1/1		
Thigh GFPT1				2/2
Calf GFPT1				2/2
Thigh DPAGT1				2/2
Calf DPAGT1			1/2	1/2

Table 4.7: T1 severity categorization summary: The number of subjects in each category/the total number of subjects in each group is shown.

All control subjects were in the normal or mild limited category, whereas in the entire CMS cohort 35% of thighs and 50% of calves were in a more severely affected category with either mild extensive or marked fatty infiltration. The following CMS subtypes had at least one subject with mild extensive or marked fatty infiltration: rapsyn, DOK7, SCS, GFPT1 and DPAGT1. The latter two subtypes had the most severe fatty infiltration out of all: all four subjects with either GFPT1 or DPAGT1 CMS were categorized as having marked or mild extensive changes in both thighs and calves (Table 4.7).

In five subjects MRI appearances suggested a degree of muscle atrophy. Global atrophy was definite and marked in subject 21 (DPAGT1 CMS). A patient with SCS had localized atrophy of right lateral gastrocnemius (12). Three patients with AChR deficiency had possible atrophy of the anterior compartment of the thigh (2 and 3) or posterior compartment of the calf (4). Patient 2 was also thought to have atrophy of the posterior superficial compartment of the calf.

Example T1w and STIR images from control subjects (Figure 4.6) and T1w images from subjects with different CMS subtypes (Figure 4.7) are shown below.

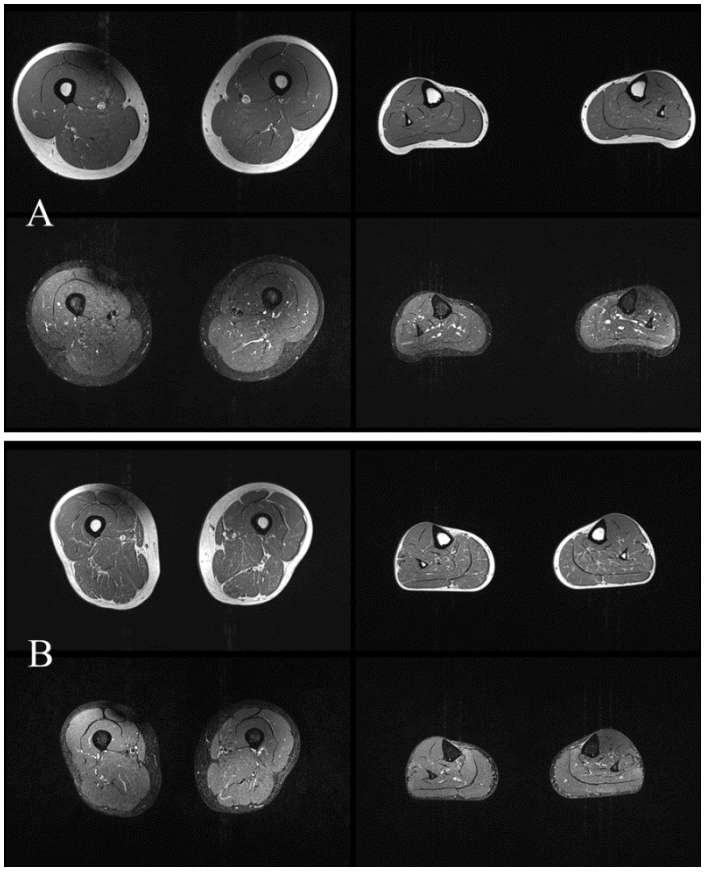

Figure 4.6: MR images from control subjects: T1w images on the top and STIR images on the bottom row are shown from healthy control subjects with **(A)** the lowest mean T1 score (subject g) and **(B)** the highest mean T1 score (subject e). Axial thigh images are shown on the left and calf on the right. On T1w images muscle has a dark grey appearance and fat, as well as bone, is white. On STIR images the fat signal is suppressed and white is indicative of other tissue types with high water content including blood vessels and areas of 'oedema' within muscles.

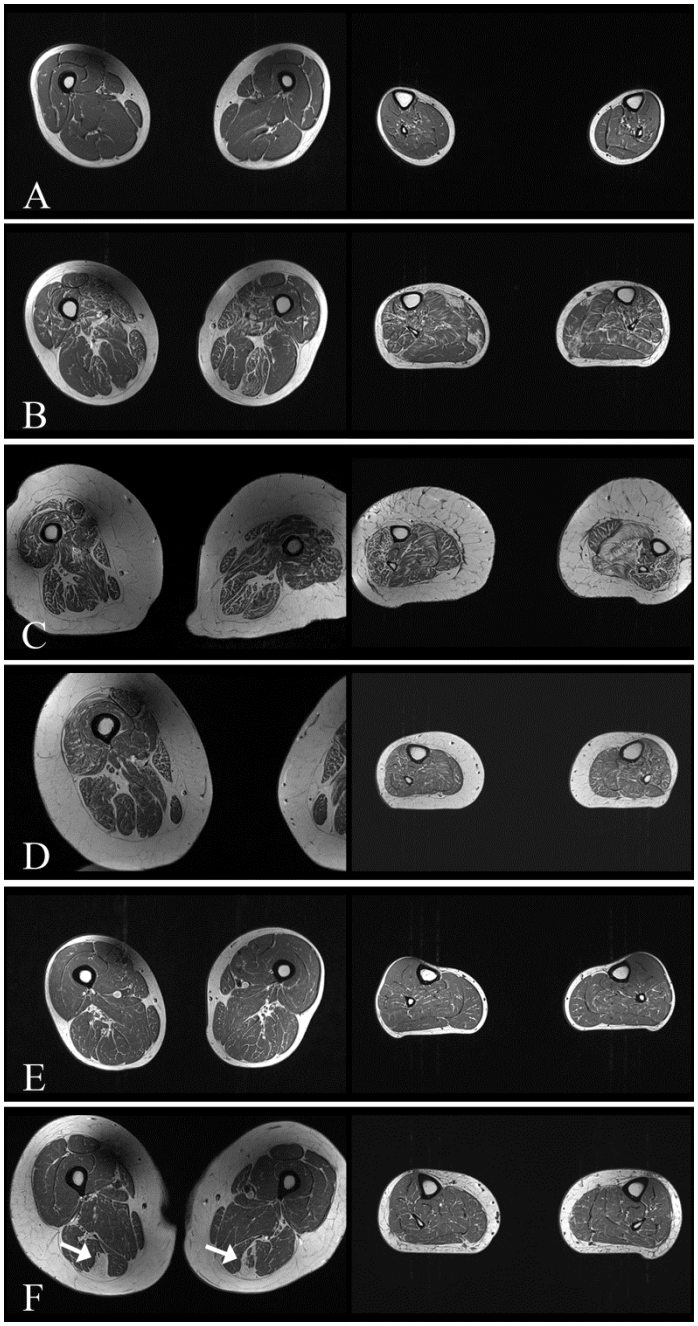

Figure 4.7: T1w MR images from CMS subjects: Axial thigh images are shown on the left and calf images on the right from individual subjects with **(A)** AChR deficiency (3), **(B)** GFPT1 (18), **(C)** DPAGT1 (21), **(D)** slow channel syndrome (12), **(E)** DOK7 (8) and **(F)** rapsyn (5) CMS. Note the focal areas of fat equivalent to Mercuri grade 4 bilaterally in semitendinosus muscles in **F** (arrows). Subject ID in brackets. Note the field imhomogeneity artefact that can be seen predominantly affecting the anterior region of the right thigh. This was present to some degree on all scans, though did not significantly interfere with Mercuri scoring.

4.3.3 STIR sequences

STIR sequence findings are shown for individual control subjects (Table 4.5) and CMS subjects (Table 4.6) according to the categories defined in the methods. A summary of STIR findings is shown below (Table 4.8).

STIR feature	Number of CMS subjects	Number of control subjects
Any STIR abnormality of thighs	0	0
Any STIR abnormality of calves	14/20	6/9
All abnormal muscles show mild hyperintensity	13/14	6/6
Any muscles show marked hyperintensity	1/14	0/6
Calf categorized as		
• **Normal**	6/20	3/9
• **Mild limited**	11/20	5/9
• **Mild extensive**	2/20	1/9
• **Marked**	1/20	0/9
Medial gastrocnemius findings		
• **Unilateral STIR abnormality**	6/20	0/9
• **Bilateral STIR abnormality**	5/20	6/9
• **Distal portion only affected**	9/16 muscles	12/12 muscles

Table 4.8: Summary of STIR findings.

Generally STIR imaging did not show any overt differences between the CMS and control groups and was completely normal in all thigh muscles. Mild hyperintensity of some calf muscles was seen in 14/20 CMS subjects and 6/9 controls. Just one subject (18), with GFPT1 CMS, had marked STIR hyperintensity in medial gastrocnemius bilaterally. Medial gastrocnemius was the most common muscle in which mild hyperintensity was detected, affecting 11 CMS subjects and all six controls. One difference between CMS and control groups was that STIR hyperintensity only affected the distal portion of medial gastrocnemius in controls, but was also seen proximally in 7/16 CMS muscles. In two CMS subjects (3 and 7) and two control

subjects (c and e) a STIR hyperintense ‘central stripe’ corresponding to the muscle endplate region of medial gastrocnemius was noted. In subject 3 this feature was also seen in soleus bilaterally and in the two control subjects was described as faint (Figure 4.8).

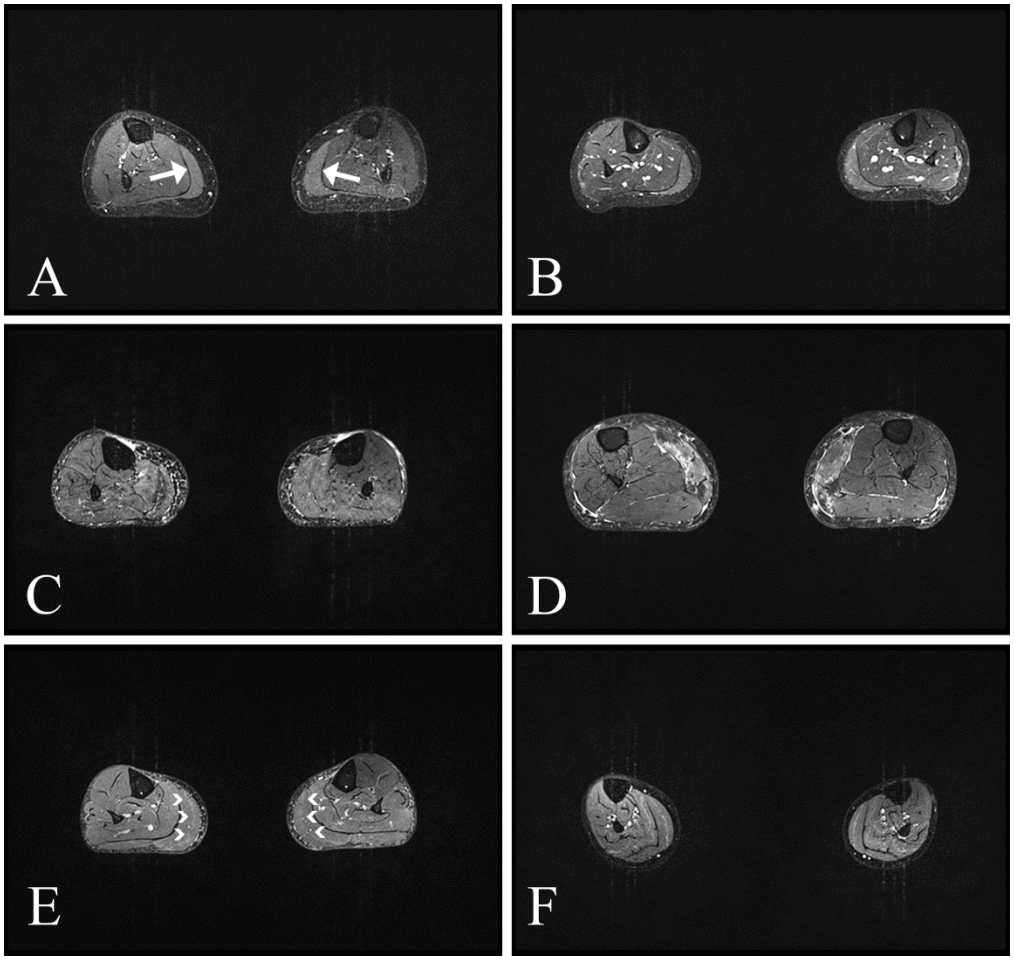

Figure 4.8: STIR imaging in calf muscles: **(A)** Mild hyperintensity seen bilaterally in distal medial gastrocnemius (arrows) in a subject with ChAT CMS (17) and **(B)** in a healthy control (g). **(C)** More extensive mild STIR hyperintensity in a subject with SCS (14); involvement of lateral and medial gastrocnemius as well as soleus is evident. **(D)** Marked STIR hyperintensity in medial gastrocnemius bilaterally in a subject with GFPT1 CMS (18). **(E)** A ‘central stripe’ can be seen bilaterally in medial gastrocnemius of this healthy control (e) (small arrows) and **(F)** in this subject with AChR deficiency (3) (a central stripe is also seen bilaterally in soleus). Subject ID in brackets.

4.3.4 Correlation with clinical parameters

Mean T1 score correlated with age in the CMS group as a whole (Figure 4.9). A trend towards correlation with age was seen in the control group though this was not statistically significant. Correlation between the QMG and MGADL scores was evident (Figure 4.10).

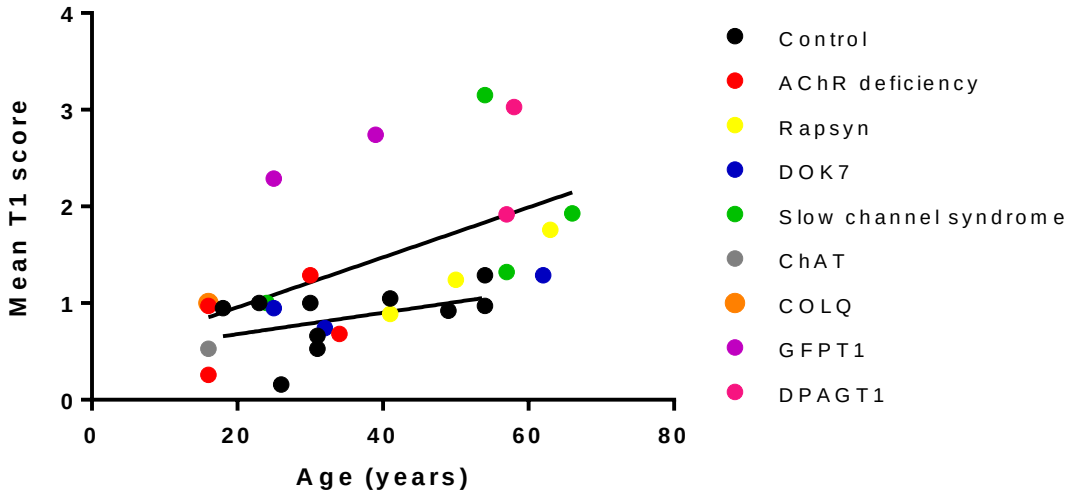

Figure 4.9: Mean T1 score and age: A significant correlation between mean T1 score and age of subject is seen in the CMS cohort (Spearman rho = 0.6237, p= 0.0025), but not in the control group (Spearman rho = 0.3058, p = ns).

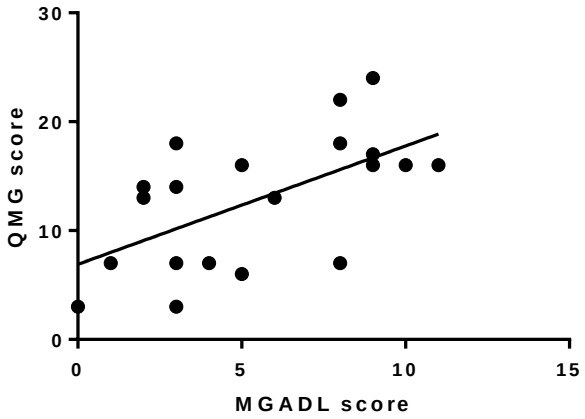

Figure 4.10: Correlation of QMG and MGADL scores: Significant correlation is seen between quantitative myasthenia gravis (QMG) and myasthenia gravis activities of daily living **(**MGADL) scores (Spearman rho = 0.5825, p = 0.0056).

No statistically significant correlation was evident between mean T1 score and any of the following clinical parameters: leg raise time, QMG score, MGADL score or MRC muscle strength grades, when the CMS cohort was examined overall. When only those subtypes which had abnormal T1w imaging (i.e. showed mild extensive or marked changes by severity categorization) were analyzed then statistically significant correlations are seen with some parameters (Figure 4.11). Whichever of the following mean T1 scores was most relevant to the clinical parameter in question was used in these analyses: whole leg, thigh, or calf. For example, the mean T1 score of the calf was used to correlate with ankle dorsiflexion strength. The proximal hip flexors were not imaged and so hip flexion and leg raise time were correlated with mean T1 of the thigh. The strongest inverse correlation was seen between thigh mean T1 score and hip flexion strength and leg raise, followed by calf mean T1 score and ankle dorsiflexion strength. Although a statistically significant correlation was also demonstrated between thigh mean T1 score and knee flexion and extension, in both analyses this appears to be an effect of just two subjects (with GFPT1 and DPAGT1 subtypes) and therefore may not be clinically relevant. No correlation was seen between mean T1 score and either the QMG or the MGADL score in this subgroup analysis.

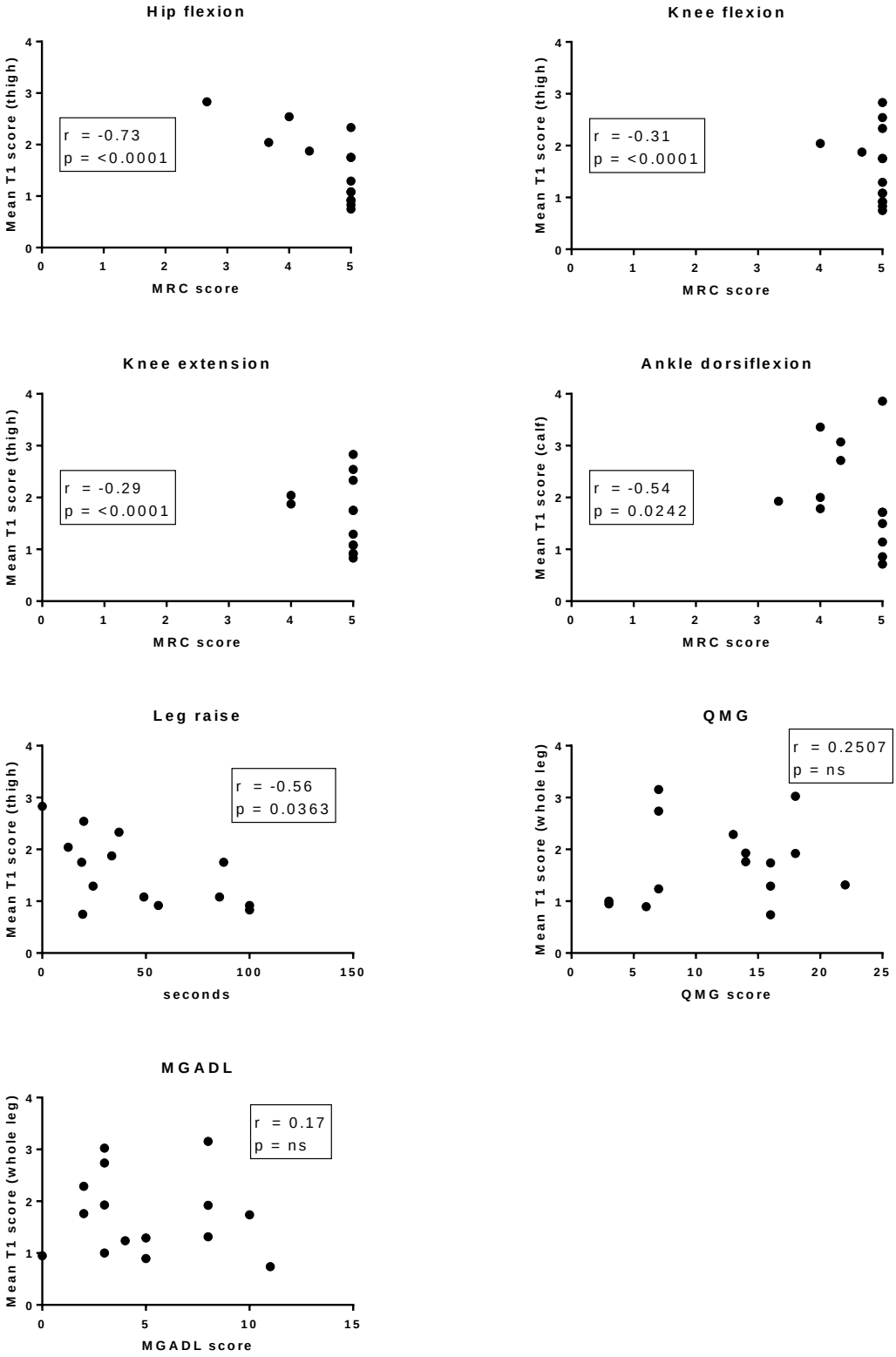

Figure 4.11: Correlation of mean T1 score and clinical severity in subtypes showing abnormal MRI: Subtypes included in analysis are: rapsyn, DOK7, SCS, DPAGT1 and GFPT1. Mean T1 of thigh or calf was used where most relevant to the measured parameter. r; Spearman's rho, p; p value (two tailed t-test), ns; not significant; MRC score; Medical Research Council strength score.

4.4 Discussion

4.4.1 Main findings

It is acknowledged that, like most other published studies of muscle MRI findings in rare inherited neuromuscular disorders, this study is limited by small patient numbers as well as the variation in age and hence disease progression between subjects. Even within subtype groups the duration, dose and age at starting treatment varies. It is unlikely that these variations can be fully eliminated mainly because the congenital myasthenic syndromes are collectively and individually rare.

In this study difference compared with control muscle imaging was evident within some CMS subtypes. The main differences were seen on T1w imaging which detects fatty infiltration of muscles suggesting progressive muscle damage. While some fatty infiltration on T1w imaging was seen in all healthy controls as well as all patients, differences were seen in the extent (number of muscles) and severity of fatty infiltration in some CMS subtypes. No selective pattern of muscle involvement was observed.

A notable finding of this study is that some fatty infiltration was seen in all healthy controls and over half had mild STIR hyperintensity in predominantly distal gastrocnemius. Semi-quantitative MRI analysis of healthy controls is rare and just two studies which have employed similar methods were identified (Torriani et al. 2012; Morrow et al. 2013b). Both studies, one including adults and the other children, demonstrated mild fatty infiltration in their healthy controls on T1w imaging and the latter study also reported mild STIR hyperintensity, predominantly in distal gastrocnemius muscles. The latter study also documented the appearance of a STIR hyperintense ‘central stripe’ corresponding to the muscle endplate region of medial gastrocnemius in some patients with non-dystrophic myotonia and postulated this to be

a diagnostic feature. However, this feature was seen in two of the CMS cohort; one with rapsyn mutations and the second in a subject with AChR deficiency as well as faintly in two of the control group. This underscores the importance of establishing normal control data prior to assigning mild MRI hyperintensity as abnormal.

4.4.2 T1w findings

Scans from the four subjects with glycosylation pathway subtypes (GFPT1 or DPAGT1 CMS) had the most severe fatty infiltration of the entire CMS cohort. Thigh and calf images from these subjects were unequivocally abnormal even in the youngest patient of this group, who was 25 years old, and their mean T1 scores were almost three times that of the control group. In both GFPT1 and DPAGT1 subtypes the myasthenic disorder is thought to arise from aberrant glycosylation of synaptic components. Glycosylation is a ubiquitous post-translational modification known to be biologically significant in muscle, with more than 200 known glycosyltransferases residing in the Golgi apparatus (Brown and Jimenez-Mallebrera 2010, 38). Therefore, it is possible mutations in these genes could have additional direct pathological effects in extrasynaptic regions. Furthermore, unlike any of the other subtypes imaged in this study, GFPT1 and DPAGT1 CMS are associated with the appearance of tubular aggregates on muscle biopsy suggesting some underlying myopathic process.

No difference from control group T1w imaging was apparent in the four subjects with AChR deficiency, or in either of the single subjects with COLQ and ChAT CMS. Despite their essentially normal MRI scans the patients with AChR deficiency were amongst the weakest in the entire cohort. This group had the lowest mean leg raise time, the highest mean MGADL score and the second highest mean QMG score

compared with any other subgroup with two or more subjects. Additionally, of the four subjects in the entire cohort who could not attempt a 10 m walk because of severe weakness, three have AChR deficiency syndrome. It may be significant that this group were the youngest compared to any other subgroup with two or more subjects. Further imaging of older patients with AChR deficiency CMS is desirable to investigate whether fatty infiltration may develop over a longer period of time.

In the remainder of subtypes (slow channel syndrome, rapsyn and DOK7) the findings were mixed. Some subjects fell into the categories of mild extensive or marked T1w fatty infiltration and others fell in the normal or mild limited categories that encompassed all healthy controls. However, the degree of fatty infiltration was always less compared with that observed in the glycosylation pathways subtypes and in one subject with slow channel syndrome.

The correlation of mean T1 score and age would suggest that fatty infiltration increases over time and is related to disease duration. Although a statistically significant correlation was not seen in the control group, a recent study of lower limb muscles in healthy volunteers has shown correlation between a quantitative fat fraction assessment and age (Morrow et al. 2014). Other than with age the degree of T1w abnormality did not correlate with clinical parameters in the CMS cohort as a whole. This likely reflects the pathophysiological heterogeneity of the different syndromes, with weakness caused by myopathic changes more in some subtypes than in others. In support of this, some degree of inverse correlation was seen between T1 score and muscle weakness (MRC grade) and timed leg raise when those subtypes with abnormal T1 imaging were analyzed as a separate group. Despite the proximal hip flexors not being included in the study, the strongest correlation was seen with hip flexion then timed leg raise.

4.4.3 STIR findings

Only minor differences in STIR imaging between the CMS and control cohorts were observed. Marked STIR hyperintensity was seen in just one subject who has GFPT1 CMS and therefore also had markedly abnormal T1 imaging. When mild STIR hyperintensity of gastrocnemius was detected it was limited to the distal portion of the muscle in all control subjects but in just over half of CMS subjects. Therefore proximal STIR hyperintensity of the gastrocnemius may be more likely to be associated with pathology than limited distal involvement. However, this finding is fairly subtle.

It has been postulated that STIR sequences may have the potential to show abnormalities early in the disease course of many myopathic conditions, and earlier than T1w sequences which have been said to frequently be unhelpful early in the clinical course of neuromuscular illnesses (Lovitt, Moore, and Marden 2006). However, STIR sequences did not add significant information to T1w images in a group of children with various muscular dystrophies (Mercuri et al. 2002a). The minimal STIR findings in the majority of CMS patients in this study, even in those with long disease duration and established T1w abnormalities suggests that STIR sequences would be unlikely to help identify changes in children with CMS.

STIR hyperintensity results from prolongation of T2 relaxation times and is typically referred to as muscle oedema or inflammation although the underlying molecular basis of this is poorly understood (Lovitt, Moore, and Marden 2006). Increased T2 relaxation time, and hence T2 hyperintensity, has been demonstrated in healthy muscles post-exercise and has been argued to be due to an overall increase in water mobility within tissue (Ababneh et al. 2008). Therefore the demonstration of STIR hyperintensity in two thirds of the control group may be explained by normal

physiological mechanisms and has previously been reported in a healthy control population (Morrow et al. 2013b). By this rationale it may be expected that in syndromes where there is overstimulation of the muscle, such as COLQ and slow channel syndrome, then STIR hyperintensity would be pronounced. However, this was not the case.

4.4.4 Findings compared with other neuromuscular disorders

No prospective studies of muscle MRI in CMS have been published to date. The range of imaging appearance, from normal to mild, non-specific findings and atrophy, described in a retrospective study of children with DOK7 CMS sounds similar to the mixed findings in DOK7 subjects here (Klein et al. 2013). However, it is difficult to directly compare results of these two studies, as one includes a paediatric and the other an adult population, and the imaging sequences used and the age when MRI was performed in the DOK7 study are both unknown.

There are few published reports on MR imaging in autoimmune myasthenic disorders and these concentrate on cranial muscle imaging. In 2006 a study of patients with MuSK-MG and a group with AChR-MG, matched for pattern and severity of muscle weakness, found bulbar and facial muscle weakness and wasting to be associated with significant muscle atrophy and fatty replacement in MuSK-MG. Although there was some evidence for similar findings in the AChR-MG patients this was not significantly different from controls and, taking neurophysiological data and other evidence into account, the authors concluded that the differences between the two groups appeared to be quantitative (Farrugia et al. 2006). A subsequent report of two patients with MuSK-MG also found facial and bulbar muscle atrophy and fatty

replacement (Zouvelou et al. 2011). Most recently a case report documented marked muscle atrophy and fatty replacement on cervical and bulbar muscle MR imaging in a patient with late onset AChR-MG prior to treatment (Zouvelou et al. 2012). Although a combination of T1w and T2w imaging was used in these three studies, the T2 fat suppression technique is different from the fat-suppressing STIR imaging used in this study, and no comment on muscle oedema or inflammation is made. While atrophy was reported in these patients with AIMG, it was infrequent in this CMS population. In only one patient was it global and marked and in most cases where seen it was suspected only. There is large normal inter-individual variation in muscle bulk and defining abnormality is not straightforward, particularly if not using a quantitative technique in combination with well-defined control data. Furthermore, when seen, atrophy is unlikely to be of use in differentiating from other forms of neuromuscular disease.

The range in findings seen in different forms of CMS in this study in some ways parallels the broad range of findings described in myopathic disorders with different underlying pathology. The main difference being that in myopathies preferential involvement of specific muscles is common in some disorders. In congenital myopathies, a large and clinically heterogeneous group of disorders with significant clinical overlap, and which may mimic CMS, the pattern of muscle involvement on muscle MRI can be diagnostically useful. For example atrophy of the sartorius muscle is considered the hallmark of SEPN-1 related myopathies, whereas in Bethlem myopathy the periphery of the muscles, especially the vasti, is more affected than the central part. Conversely, in laminopathies the muscle MRI findings are reported to be fairly unspecific (Straub, Carlier, and Mercuri 2012). Another difference is the degree of fatty infiltration reported in some myopathies which often appears more severe than

observed in this CMS cohort. Published images of typical axial T1w slices of thigh or calf often show muscles of Mercuri grade 4 appearance (Straub, Carlier, and Mercuri 2012; Lovitt, Moore, and Marden 2006; Mercuri et al. 2005). Although patches of grade 4 appearance were observed in 15 muscles (of 5 CMS subjects) in this study no individual muscles were scored overall with this grade.

A recent study of lower limb MRI findings in a cohort of 13 patients with tubular aggregate myopathy demonstrated T1w abnormality (Mercuri grade 1 or higher) in 59% of muscles imaged, whereas STIR abnormalities were minimal (Beltrame et al. 2014). The study found the posterior compartment of the calf (gastrocnemius and soleus) to be the region most severely affected. In addition, a disparity in severity of fatty infiltration between the long and short head of biceps femoris (with a greater degree of fatty replacement observed in the long head) was suggested as a possible diagnostic feature. Such a disparity was not observed in any of the four subjects with glycosylation pathway abnormalities included in this study, all of whom had tubular aggregates on muscle biopsy.

4.4.5 Clinical implications

This study suggests that muscle MR imaging may be of some diagnostic utility in the investigation of congenital myasthenia. Although no specific pattern of muscle involvement was identified, results would suggest that some comments can be made based on the severity of T1 hyperintensity in thigh and calf muscles.

First a normal scan does not exclude a congenital myasthenic syndrome. Rather, in a weak patient whose scan falls into the normal or mild limited category a diagnosis of AChR deficiency should be considered. Second, severe abnormality is suggestive of

a glycosylation pathway gene abnormality (*GFPT1* or *DPAGT1*). The small group sizes make definitive comment on findings in other subtypes difficult especially as there were varied findings within these groups. However, it is possible to say that an abnormal amount of T1 hyperintensity (though probably less than that seen in GFPT1 or DPAGT1 CMS) may be seen slow channel syndrome, rapsyn or DOK7 CMS. Theoretically scanning a larger number of patients should clarify this further but given the rarity of some of the subtypes this may prove challenging.

Overall this study suggests STIR imaging to be of much lower clinical utility than T1w imaging in congenital myasthenia and if the patient is known to have CMS then a simple short T1 imaging protocol may be sufficient. This may be important for children or some adults who find lying flat for prolonged periods challenging. The scanning protocol used in this study required patients to be in the scanner for a half hour period but this could potentially be halved if just T1w sequences were acquired.

While MRI findings in a variety of neuromuscular disorders have been reported, the majority are small descriptive case series, and with time overlap between different clinical syndromes has become more evident. It is thought muscle MRI could potentially be used to monitor disease progression, perhaps as an indicator of response to treatment (Mercuri et al. 2007). However, many questions identified in a recent workshop of an international group of experts remain; including the spectrum of findings within individual disorders, whether degree of pathology is mutation specific and whether ethnic or gender differences exist (Straub, Carlier, and Mercuri 2012). A recent study examining reproducibility, and age, body-weight and gender dependency of selected skeletal muscle MRI outcome measures in healthy volunteers has begun to address some of these questions (Morrow et al. 2014).

Whether muscle MRI could be used to monitor the effect of treatment in CMS subtypes where there is MRI abnormality cannot be answered by this study. Previous studies have demonstrated correlation of reversal of T2w hyperintensity and clinical improvement with reduction in creatine kinase levels in inflammatory myopathies (Lovitt, Moore, and Marden 2006). The correlation between some clinical severity parameters and imaging findings, in those where the muscle MRI is affected more than controls, suggests muscle MRI may provide a biomarker for disease progression and treatment efficacy.

In summary, this study has shown a wide range of MRI appearance from normal imaging to marked abnormality depending upon CMS subtype. T1w images seem to be especially abnormal in glycosylation pathway CMS subtypes, but were normal in AChR deficiency syndrome; the most common form of CMS. Muscle MRI could have an adjunctive role in the investigatory approach to CMS, and specifically in differentiating CMS subtypes. Its future use in monitoring disease progression and treatment efficacy requires further longitudinal studies.

Chapter 5

Evaluating lamotrigine as a treatment for slow channel congenital myasthenic syndrome

5.1 Introduction and aims

5.1.1 Slow channel congenital myasthenia

Slow channel congenital myasthenic syndrome accounts for around 11% of congenital myasthenia in the UK and is the only dominantly inherited form of CMS (Finlayson, Beeson, and Palace 2013). The underlying pathology is prolonged activation of the AChR ion channel, thought to impair neuromuscular transmission by various mechanisms including desensitization blockade of the receptor as well as depolarization block at the muscle endplate (Engel et al. 2010).

The AChR pore is formed of five subunits each consisting of four helical segments which coil around one another to form an outer (M1, M3 and M4 domains) and an inner ring (M2 domains) (Figure 5.1). The channel gate is a constricting hydrophobic girdle formed by weak interactions between neighbouring helices of the inner ring. ACh binding to the extracellular ligand-binding domain triggers rotation of protein chains at the entrance to the pore, which is communicated through the inner

helices and opens the pore by breaking the girdle apart (Miyazawa, Fujiyoshi, and Unwin 2003) (Figure 5.2). Although around 70% of UK cases, including the patient described later in this chapter, are affected by the α-subunit missense mutation G153S, mutations in all adult AChR subunits have been described. Some mutations (including the αG153S mutation which lies near the extracellular ACh binding site) act mainly to increase the receptor's affinity for ACh, while others, often in the pore-lining M2 domain, stabilize and prolong the open state (Engel et al. 2010).

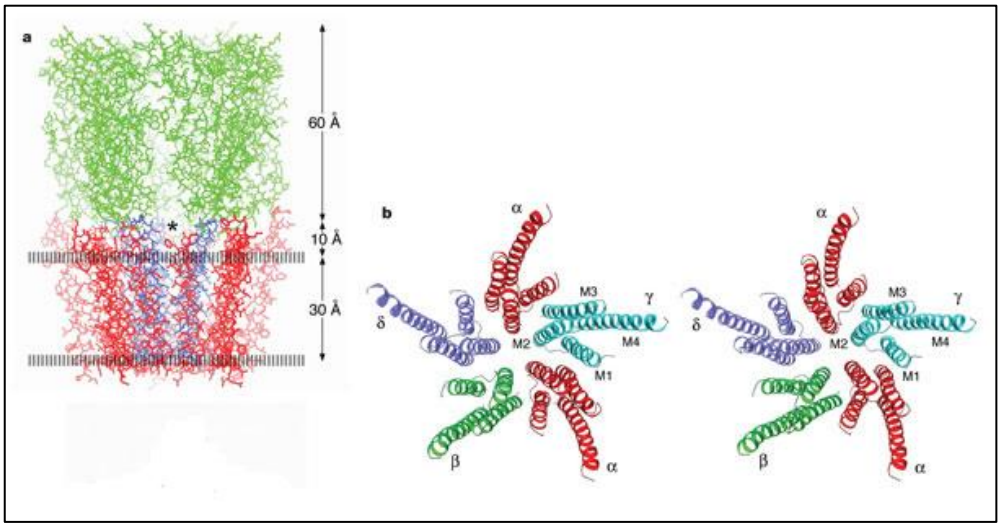

Figure 5.1: Pentameric structure of the AChR pore: a. View normal to the receptor axis showing the α-helical pore structure (blue, pore-facing; red, lipid-facing helices) in relation to the membrane surfaces (broken lines) and the β-sheet structure (green) comprising the ligand-binding domain; the asterisk denotes open space at a subunit interface. **b.** Stereo view of the pore, as seen from the synaptic cleft, with subunits shown in different colours (α, red; β, green; γ, cyan; δ, blue). Adapted by permission from Macmillan Publishers Ltd: Nature, Miyazawa, Fujiyoshi, and Unwin 2003, Copyright 2003, Nature Publishing Group (URL: http://www.nature.com/nature/index.html).

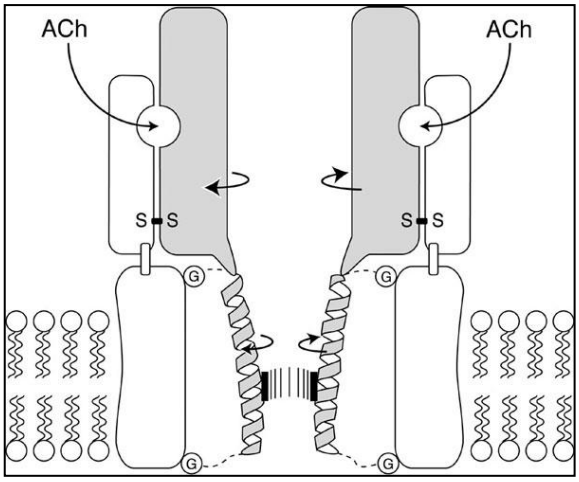

Figure 5.2: Gating mechanism of the AChR pore: The ACh-induced rotations in the alpha-subunits are transmitted to the gate—a hydrophobic barrier to ion permeation—through the M2 helices. The rotations destabilize the gate, causing the helices to adopt an alternative configuration which is permeable to the ions. The helices move freely during gating because they are mainly separated from the outer protein wall and connected to it by flexible loops, containing glycine residues (G). S-S is the disulphide-bridge pivot in the ligand-binding domain, which is anchored to the fixed outer shell of the pore. The relevant moving parts are shaded. Reprinted by permission from Macmillan Publishers Ltd: Nature, Miyazawa, Fujiyoshi, and Unwin 2003, Copyright 2003, Nature Publishing Group (URL: http://www.nature.com/nature/index.html).

The net result of either category of mutation is the prolongation of endplate potential decay which can be measured by *ex vivo* microelectrode studies (Engel et al. 1982). Figure 5.3 shows a typical prolonged miniature endplate potential (MEPP) recording from a slow channel model mouse aside that of a wild type animal for comparison. Prolonged ion channel activation, resulting in high intracellular Ca^{2+} concentration leads to an excitotoxic endplate myopathy. The myopathy is characterized by a loss of structural integrity of the endplate including destruction of the junctional folds with a loss of AChRs, degeneration of postsynaptic organelles, and apoptosis of the junctional nuclei. These features predispose to failure of the EPP to reach threshold and thereby compromise the safety factor of neurotransmission. Degeneration of endplate structures can be visualized by electron microscopy (Figure 5.4). This secondary damage probably accounts for much of the weakness and the progressive deterioration experienced by patients. Predictably, pyridostigmine and 3,4-diaminopyridine exacerbate the underlying pathology, usually cause deterioration, and should be avoided. Treatments that block the AChR ion channel in its open state without causing depolarization, such as fluoxetine or quinidine, are routinely used

(Harper and Engel 1998; Harper, Fukodome, and Engel 2003) and recently clinical and electrophysiological improvement in one patient treated with quinine, a stereo-isomer of quinidine was reported (Peyer et al. 2013).

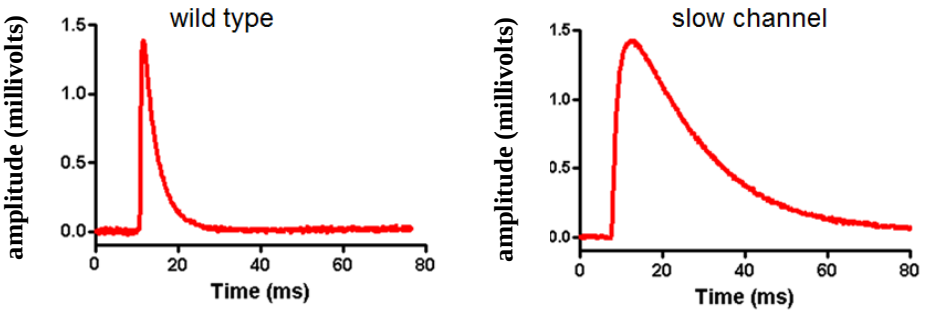

Figure 5.3: Miniature endplate potentials recorded by microelectrode studies of phrenic nerve-hemidiaphragm preparations: The recording on the right is from a slow channel transgenic mouse model harbouring the mutation εL221F and shows prolonged decay compared to the wild type recording on the left. Endplate potentials also show prolonged decay.

5.1.2 Lamotrigine

Lamotrigine was chosen for study following reports from a patient with slow channel syndrome, due to αG153S mutation, that her myasthenic symptoms improved when she took the drug as a treatment for epilepsy. Symptom onset was in infancy with hypotonia and a droopy head. Treatment with quinidine since age 12 has had a partial effect, though dose escalation had been limited by prolongation of the QT interval, a recognized cardiac side effect. In her teens she began having generalized seizures, commenced lamotrigine at age 16 and is maintained on a relatively high total daily dose of 400 mg.

Lamotrigine (3, 5-diamino-6-(2,3-dichlorophenyl)-1,2,4-triazine) is thought to exert antiepileptic activity primarily by inhibition of neuronal voltage-sensitive sodium channels (Cheung, Kamp, and Harris 1992). However, it is known to have an effect on other targets, including a dose-dependent blocking effect on human muscle nicotinic AChR. A study of acetylcholine receptor function at the single-channel level demonstrated a reduction in mean open time of the AChR pore with increasing lamotrigine concentration (Vallés, Garbus, and Barrantes 2007). This suggests lamotrigine may reduce the prolonged channel openings that characterize slow channel syndrome and therefore could be a potential treatment option.

5.1.3 Transgenic mouse models of slow channel syndrome

A number of transgenic mouse models of slow channel syndrome have been reported (Gomez et al. 1996; Gomez et al. 2002; Gomez et al. 1997; Chevessier et al. 2012). Such models provide a system in which the effects of potential treatments may be studied in more detail than would be possible in patients. More recently a detailed description of the mouse model used in this study was published (Webster et al. 2013), in which the effect of ephedrine was studied. This mouse is homozygous for the missense mutation L221F in the ε-subunit of the acetylcholine receptor. The mice mirror the clinical syndrome and exhibit mild fatigable weakness and neurophysiological evidence of myasthenia. Microelectrode analysis of muscle endplates of these mice demonstrates the prolonged endplate potential decay characteristic of the slow channel syndrome. A repetitive CMAP to single nerve stimulation has been reported in some transgenic models (Gomez et al. 1996; Gomez et al. 1997) but not in the model used in this study. Ultrastructural analysis of endplates

has revealed variable degeneration of the junctional folds, similar to findings described in patients with slow channel syndrome (Figure 5.4).

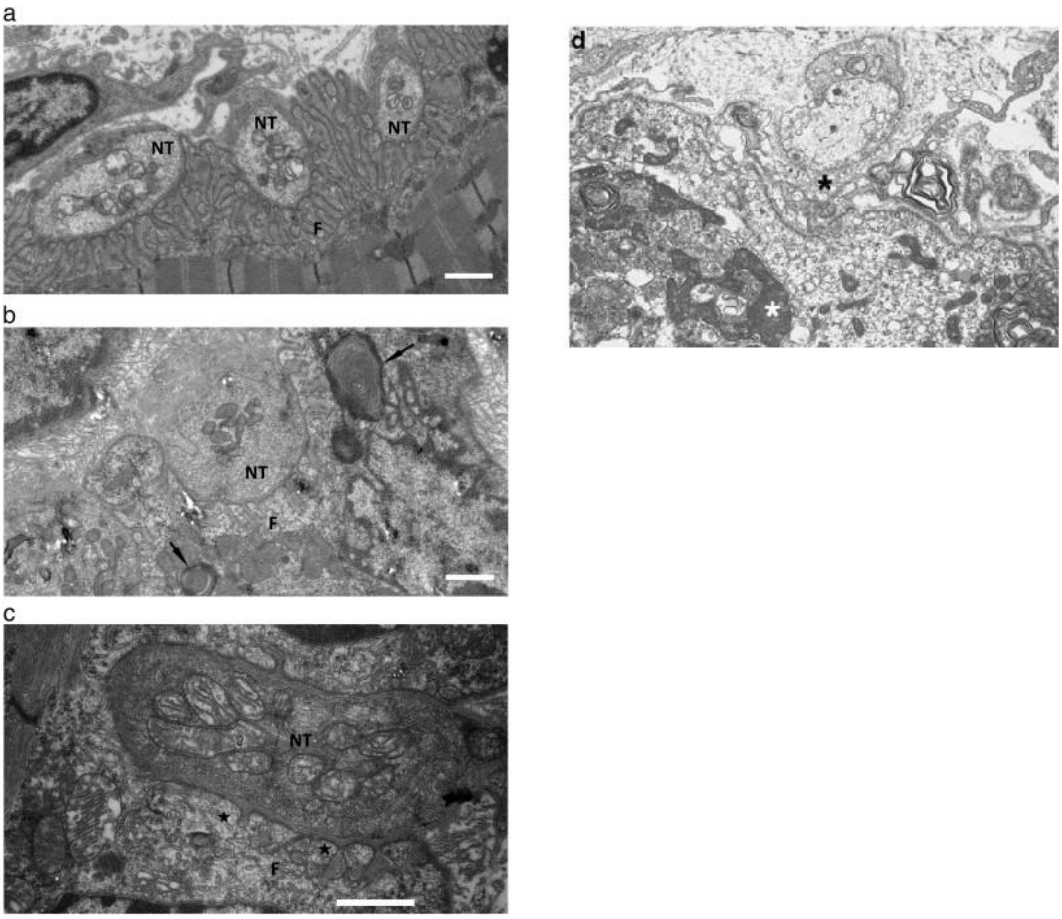

Figure 5.4: Electron microscopic pictures of neuromuscular junction structure in slow channel syndrome: (a-c) Pattern of degeneration of endplate structure. Electron microscopic pictures of neuromuscular junction structure of slow channel model mice from tibialis anterior muscles with varying degree of pathology. **(a)** A proportion of synaptic boutons were associated with normal presynaptic and postsynaptic regions while others **(b and c)** show simplified postsynaptic regions, damaged folds (asterisks) and myeloid structures (arrows) in junctional sarcoplasm. NT = nerve terminal area, F = folding area. Scale bars represent 1 μm.[1] **(d)** Electron microscopy of muscle endplate from a patient with slow channel syndrome. The junctional folds have disintegrated and the synaptic space is filled with debris (black asterisk). The junctional sarcoplasm displays fragmented apoptotic nuclei (white asterisk) and myeloid structures. Reprinted from J. Mol. Neurosci., 40, 2010,143-53, What Have We Learned from the Congenital Myasthenic Syndromes, Engel et al, figure 3d, copyright Springer 2010; with kind permission from Springer Science and Business Media.

[1] Reprinted from Experimental Neurology, 248, Webster et al, A mouse model of the slow channel myasthenic syndrome: Neuromuscular physiology and effects of ephedrine treatment, 286-98, Copyright 2013, with permission from Elsevier.

5.1.4 Aims

The aim of this chapter is to evaluate whether lamotrigine could be a potential treatment for slow channel syndrome by:

a) Examining the electrophysiological effect of lamotrigine on NMJ transmission in a slow channel mouse model by microelectrode studies of *ex vivo* phrenic nerve-hemidiaphragm tissue. Duration of AChR channel opening is the major determinant of endplate potential decay time. Therefore, if lamotrigine blocked open mutant AChR channels an increase in the rate of MEPP and EPP decay would be expected.

b) Assessing the effect of lamotrigine *in vivo*, in a transgenic mouse model of slow channel syndrome using the following techniques:

   i) The inverted screen test; a test of sustained muscle effort.

   ii) Repetitive nerve stimulation, an electrophysiological measurement of transmission failure at the neuromuscular junction.

Improvement in NMJ transmission is expected to lead to an increase in the time a mouse can hold on to the inverted screen as well as a reduction in the degree of abnormality seen on RNS.

5.2 Approaches

Detailed methods are given in Chapter 2. In brief, the approaches in this chapter are as follows.

5.2.1 *Ex vivo* diaphragm electrophysiology

Lamotrigine is very poorly soluble in water and therefore a water soluble salt of the drug, lamotrigine isethionate (Tocris Bioscience, Bristol, UK), was used as active drug in the *ex vivo* microelectrode studies (Section A.1.2). Control experiments with the salt vehicle (isethionic acid; Section A.1.3) were also performed to ascertain that the vehicle had no effect on neurotransmission. Control experiments with wild type diaphragm tissue and a high concentration of lamotrigine were also performed.

The following MEPP and EPP parameters were measured at baseline and with increasing concentrations of drug or vehicle control in the bath solution: amplitude, rise time, half width, area, decay time (τ), quantal content and MEPP frequency. Recordings were made at each concentration of drug or vehicle control after the solution had been applied to the bath for 10 minutes.

5.2.2 *In vivo* treatment trials

Lamotrigine doses for the *in vivo* treatment trials were determined by testing serum lamotrigine concentration in groups of mice treated with different lamotrigine doses. Once suitable doses were established treatment trials were undertaken. Repetitive nerve stimulation was performed pre-treatment and again at the end of a 6 week treatment period. The inverted screen test was performed pre-treatment and at regular intervals during the trial. Two doses of lamotrigine were tested in separate groups of 10 week old model animals. Control experiments were performed in age-matched untreated slow channel mice and in age-matched wild type mice treated with the higher dose of lamotrigine.

5.2.3 Statistical analysis

Statistical analyses were performed using GraphPad Prism version 6, GraphPad Software, California.

5.3 Results

5.3.1 *Ex vivo* diaphragm electrophysiology

Typical raw traces of spontaneous MEPPs and stimulated EPPs recorded from individual endplates at different lamotrigine concentrations (Figure 5.5) show a concentration dependent increase in the rate of endplate potential decay. In the figure this is evident as a reduction in the duration of potentials and concomitant increase in steepness of the falling phase of the potential, and can be seen more clearly in Figure 5.6 where the raw data has been normalized for amplitude and superimposed. Even with the highest concentration of lamotrigine, the endplate potentials did not decay as fast as the typical wild type recordings also shown in Figure 5.6 for comparison.

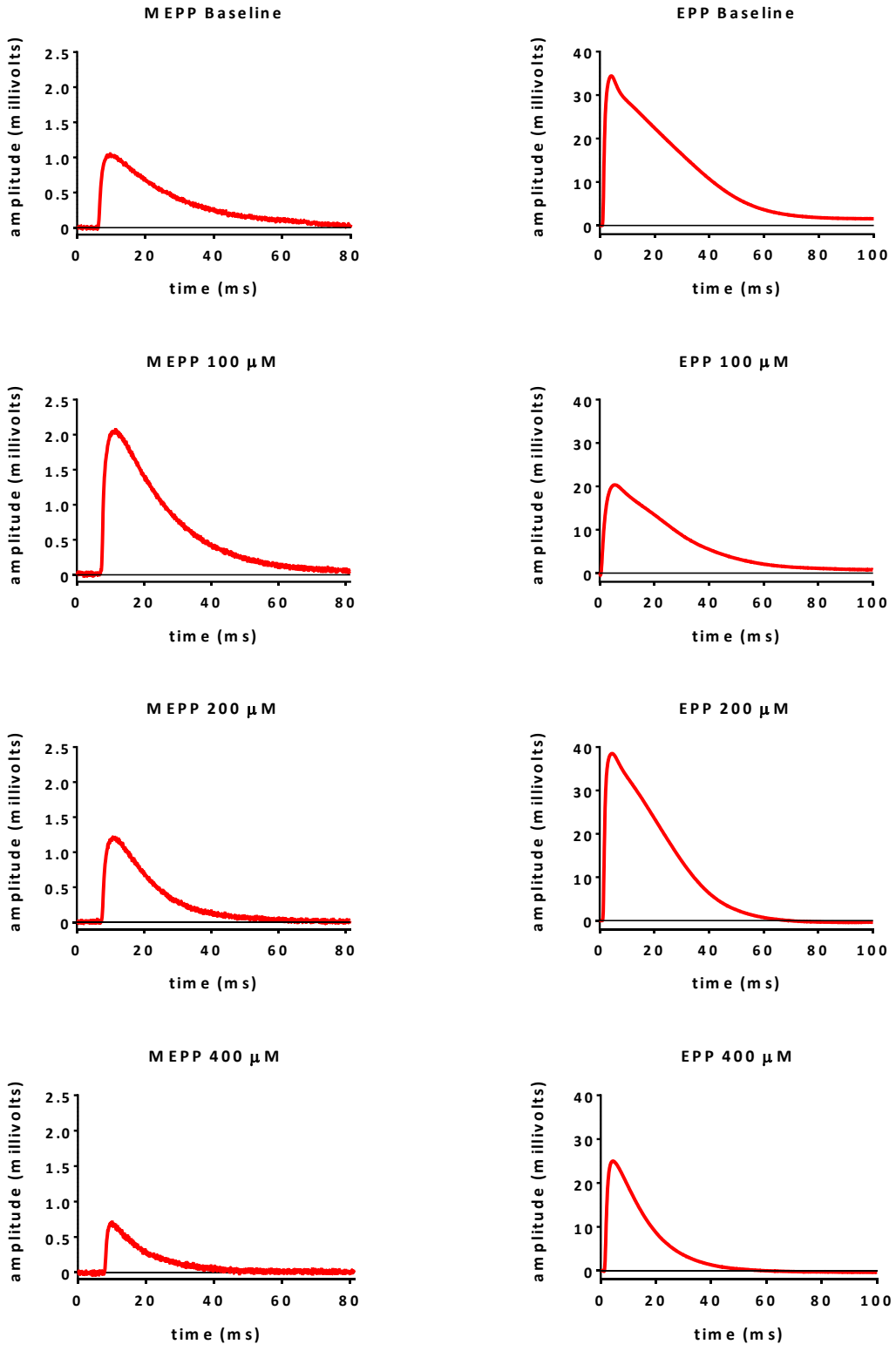

Figure 5.5: Lamotrigine *ex vivo* diaphragm electrophysiology: raw traces: Miniature endplate potentials are shown on the left and endplate potentials on the right at baseline and at different lamotrigine concentrations. An increase in the rate of decay of MEPPs and EPPs is seen with increasing lamotrigine concentration.

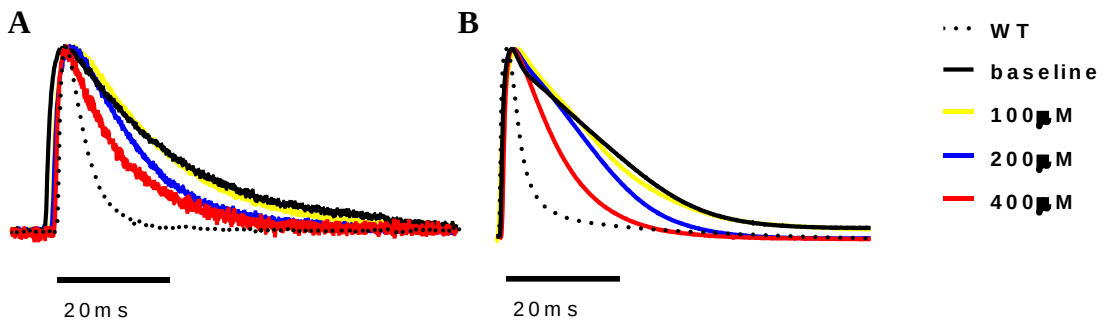

Figure 5.6: Normalized MEPP and EPP data: Superimposed traces from Figure 5.5 normalized for amplitude showing prolonged decay of **A.** miniature endplate potentials (MEPPs) and **B**. endplate potentials (EPPs). As lamotrigine concentration increases so does the rate of endplate potential decay. Black dotted lines indicate wild type recordings in the absence of lamotrigine for comparison.

Generally MEPP waveforms were more consistent than EPP waveforms and were more reliably measured. EPP waveform morphology was more variable between impalements usually because of interference from muscle twitch. At times EPP waveforms had a notched appearance thought to indicate additional, possibly potassium channel, currents within the membrane (an example of this can be seen in the top right panel of Figure 5.5).

Figure 5.7 shows additional MEPP and EPP parameters in detail, including half width, area and rise time as well as MEPP frequency and quantal content. Mean values from three experiments are shown (equates to 15 endplates) at different lamotrigine concentrations and at equivalent concentrations of vehicle control. The vehicle control, isethionic acid, had no significant effect on any MEPP or EPP parameter at any concentration tested. A description of the main findings of the effects of lamotrigine isethionate will now follow.

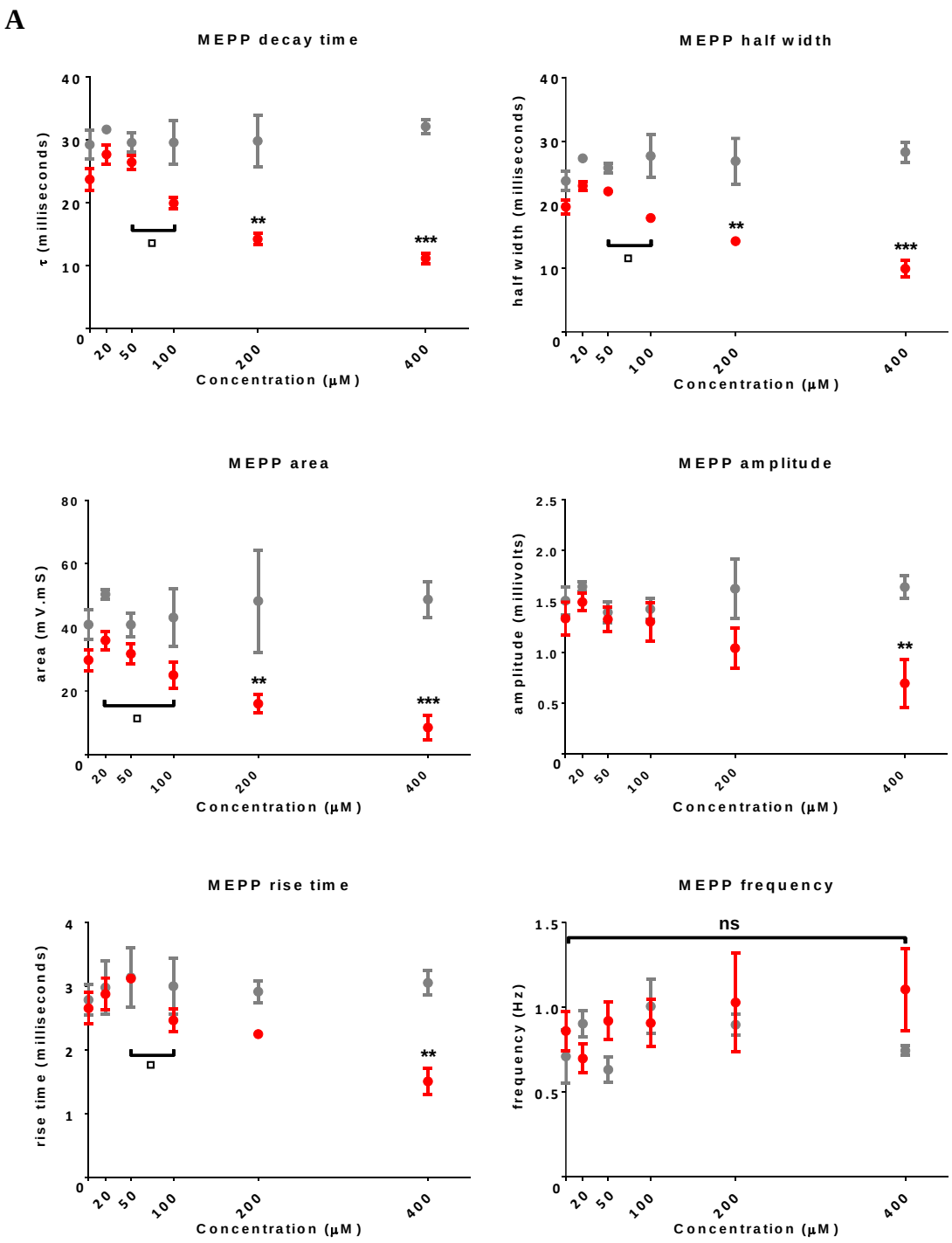

Figure 5.7: Lamotrigine *ex vivo* diaphragm electrophysiology: MEPP and EPP parameters: A: MEPP data (this page), **B:** EPP data (overleaf). Data from experiments with lamotrigine isethionate are shown in red. Vehicle control experiments with isethionic acid in grey. The mean (dot) and SEM (bars) of three experiments are shown. Typically five endplates were sampled at each concentration during each experiment. Repeated measures one-way ANOVA with post-test Tukey's Multiple Comparison was performed. No significant effect in any parameter was noted in control experiments. Stars indicate statistically significant differences between lamotrigine concentration and baseline recording. *: p = 0.01-0.05; **: p = 0.001-0.01; ***: p = <0.001. Squares indicate a significant difference between two indicated lamotrigine concentrations (only the lowest concentrations with a significant effect are indicated by squares), □: p = 0.01-0.05, ns = not significant.

Figure 5.7: (continued)

B

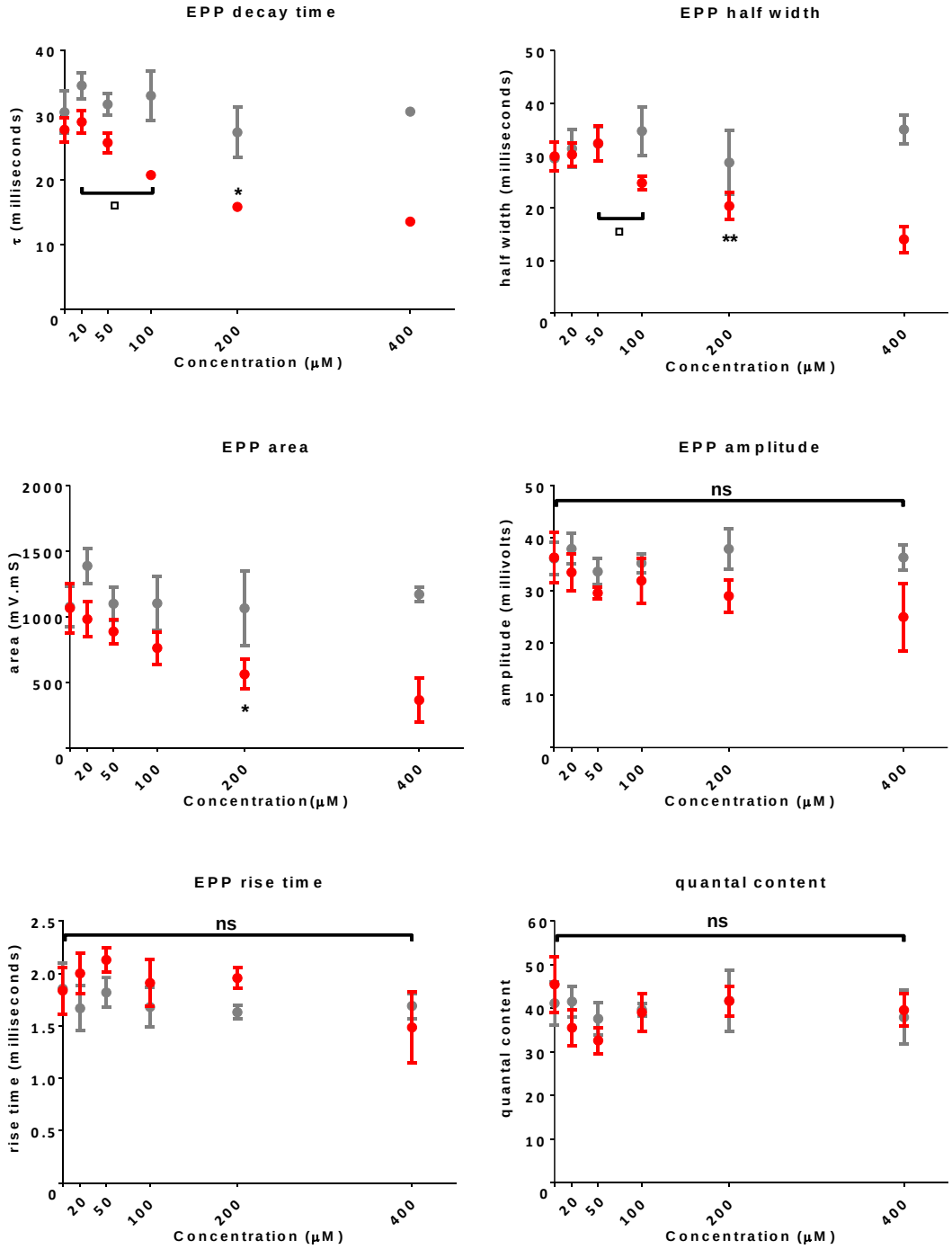

Lamotrigine isethionate reduced MEPP and EPP decay time in a dose dependent manner (Figure 5.7) such that MEPP and EPP decay was just over twice as fast as baseline at the highest concentration of lamotrigine tested (400 μM). The decrease in decay time was statistically significant at a concentration of 200 μM lamotrigine compared with no drug for both MEPPs and EPPs. However, the drug appears to have an effect at lower concentrations than 200 μM, as when decay times are compared between different concentrations rather than to baseline MEPP decay time was significantly reduced at 100 μM (compared with 50 μM lamotrigine) and EPP decay time was significantly reduced at 100 μM (compared with 20 μM lamotrigine). This effect being significant when compared to low lamotrigine concentrations but not when compared to baseline may be explained by dissociation of conotoxin caused by rinsing the drug into the bath, as the conotoxin itself slightly reduces endplate potential decay time. In keeping with this is the trend seen of a small increase in those parameters related to potential decay (including MEPP τ, half width and area, as well as EPP τ) at 20 μM compared to baseline which was also observed in vehicle control experiments. Potential half width and area are significantly influenced by the decay time as well as by amplitude. As expected, there was significant reduction in MEPP half width and area, and in EPP half width, at similar lamotrigine concentrations as affected the decay time. Overall these findings are in keeping with lamotrigine exerting a blocking effect on the AChR ion channel.

Another finding is a significant reduction in MEPP rise time at a high lamotrigine concentration (400 μM) compared with baseline. The endplate potentials of these SCS model mice are known to have a slower rise time than that of wild type mice and, although the mechanism for this is unclear, at 400 μM this is reduced to a value

approaching typical wild type MEPP rise times. A significant effect on EPP rise time was not demonstrated.

Further effects of lamotrigine were seen that are likely at least partially attributable to an effect out with the AChR pore itself. At high concentrations of lamotrigine (400 μM) an almost 50% reduction in MEPP amplitude compared with baseline was seen. No significant effect was seen on the amplitude of recorded EPPs. However, in one of the experiments EPPs were completely unrecordable at this concentration (and therefore EPP data at this concentration couldn't be included in ANOVA). Visible twitch of the muscle was reduced in all experiments at 400 μM and during one at 200 μM compared with lower concentrations of lamotrigine. In some cases an EPP could be generated by increasing the voltage stimulus. This pattern was different to the control experiments, where degree of twitch increased over time because the effect of conotoxin wears off, and is most likely due to block of nerve conduction by block of neuronal sodium channels.

Changes in MEPP frequency are often observed when there is damage to the nerve-diaphragm tissue and can be a surrogate marker of the quality of the preparation. However, a change in frequency could also represent presynaptic modulation of ACh release. No effect on MEPP frequency was seen at any lamotrigine concentration, and furthermore there was no effect on quantal content to suggest presynaptic neurotransmitter release had been modulated by the drug.

Experiments applying 300 μM lamotrigine isethionate to wild type diaphragm tissue showed no reduction in endplate potential decay time compared with baseline recordings (Figure 5.8). In two of these experiments, in the presence of lamotrigine, finding regions where EPPs could be recorded was challenging, which raises the

possibility that some EPPs were blocked. No significant effect on MEPP amplitude was observed (paired t-test).

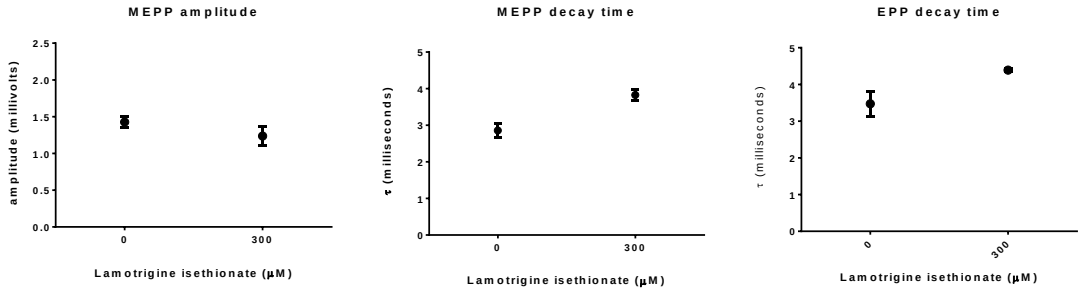

Figure 5.8: Lamotrigine *ex vivo* diaphragm electrophysiology in wild type tissue: No reduction in MEPP or EPP decay time is seen. The mean (dot) and SEM (bars) of three experiments are shown.

5.3.2 Treatment trials

The following three sections present results from serum lamotrigine concentration testing as well as results of the inverted screen test and repetitive nerve stimulation studies.

5.3.2.1 Serum lamotrigine concentration

Serum lamotrigine concentration was tested to establish an optimal treatment dose equivalent to that typically seen in treated human subjects and which may be physiologically relevant. Lamotrigine was detected in the serum of all mice and the concentration was dose dependent (Figure 5.9 and Table 5.1). All dosages administered yielded serum concentrations grossly similar to those typically measured in human

subjects, but because those achieved by 20 mg/kg/day and 30 mg/kg/day were closest to the upper limit of 'target' levels they were chosen for use in the *in vivo* treatment trials.

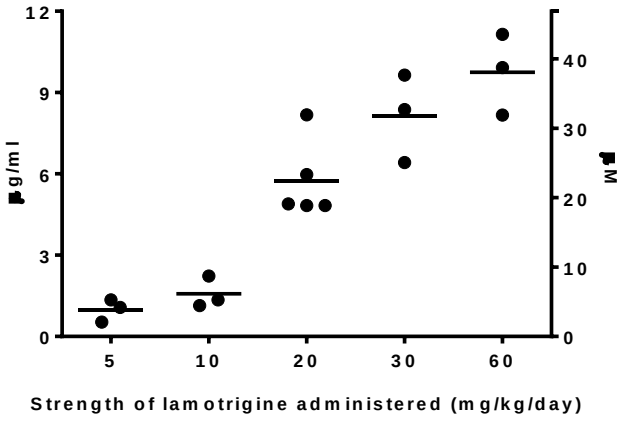

Dose mg/kg/day	Mean µg/ml	Mean µM
5	0.98	3.84
10	1.57	6.14
20	5.74	22.42
30	8.14	31.80
60	9.75	36.46

Figure 5.9 &Table 5.1: Serum lamotrigine concentration: Serum lamotrigine concentrations from mice treated with different strengths of the drug. Concentration in µg/ml on left Y-axis, equivalent in µM shown on right Y-axis. Each data point is from the pooled serum of two mice. Horizontal lines indicate the mean. Numerical values are given in the table.

5.3.2.2 The inverted screen test

All model mice were unable to hold on to the screen for the set maximum period of 600 s, although a wide range of performance was observed over the entire group (ranging from 55-389 s at baseline). The SCS mice treated with either dose of lamotrigine did not show an improvement in performance (Figure 5.10 and Table 5.2).

Performance worsened in the group treated with the higher dose, which showed reduction in mean duration from 196.2 s at baseline to 83.8 s after 6 weeks of treatment ($p=0.0235$ repeated measures one way ANOVA). There was no significant change in performance in either untreated SCS mice or those treated with 20 mg/kg/day. All wild type mice achieved the set maximum of 600 s with the exception of one at week six.

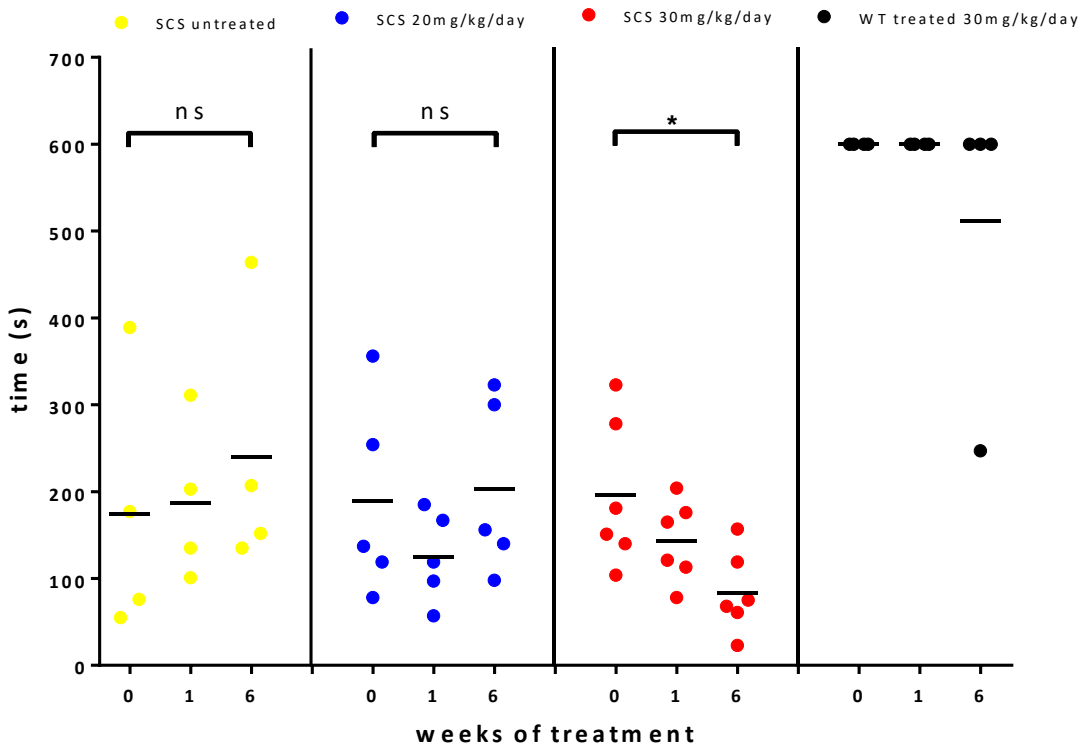

Group	Mean Time (s)		
	Baseline	**1 week**	**6 weeks**
SCS untreated	174.3	187.5	239.5
SCS 20 mg/kg/day	188.8	125.0	203.4
SCS 30 mg/kg/day	196.2	142.8	83.83
Wild type	600.0	600.0	511.8

Figure 5.10 &Table 5.2: Lamotrigine: Inverted screen test results: Inverted screen test results showing time held on to the inverted screen in seconds at 0 (baseline), 1 and 6 weeks of continuous treatment. Data from individual mice (dots) and the mean value (black bar) are shown at each time point. Numerical values are given in the table. The numbers of mice in each group were: slow channel syndrome (SCS) 30 mg/kg/day n = 6; SCS 20 mg/kg/day n = 5; SCS untreated n = 4; WT (wild type) 30 mg/kg/day n = 4. * = p value of 0.0235 on repeated measures one way ANOVA, with Tukey's multiple comparison post-test showing significant difference between 0 and 6 weeks; p = 0.001-0.01.

5.3.2.3 Repetitive nerve stimulation

Almost all (14/15) model mice had CMAP decrement ≥10% on repetitive nerve stimulation and all had a decrement of ≥5%. Figure 5.11 shows an example of abnormal CMAP decrement during one train of RNS. The ten sequential CMAP recordings from gastrocnemius shown here have been superimposed. The CMAP amplitude is measured from the peak to peak of each trace, and decrement calculated by comparing the amplitude of the fifth CMAP to that of the first.

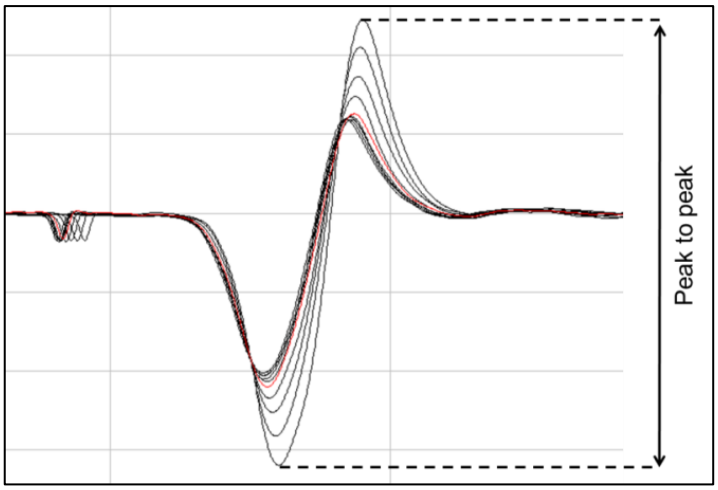

Figure 5.11: Example of CMAP decrement: A superimposed train of ten CMAP recordings from a slow channel model mouse gastrocnemius at 5 Hz stimulation. CMAP amplitude is measured from peak to peak of each trace. The largest waveform is the 1st CMAP with the 5th CMAP in red.

As described in the human slow channel syndrome the degree of CMAP decrement observed was greater at higher rates of stimulation probably indicating greater depolarization block and/or AChR desensitization at higher stimulation frequencies (Figure 5.12). The association between stimulation frequency and decrement was not linear, however, with proportionally more decrement seen between lower stimulation frequencies than between higher rates of stimulation. For example, at

5 Hz stimulation CMAP decrement measures approximately 25% by the tenth stimulus, whereas at 10 Hz the corresponding CMAP shows just over 30% decrement, i.e. only an additional ~5% decrement occurs despite a doubling of stimulation frequency. Furthermore, at a stimulation frequency of 20 Hz, and probably also 10 Hz, the degree of decrement has not reached a plateau by the tenth stimulation, as it appears to have at 3 and 5 Hz. Thus CMAP decrement would probably increase further with ongoing stimulation at 10 and 20 Hz.

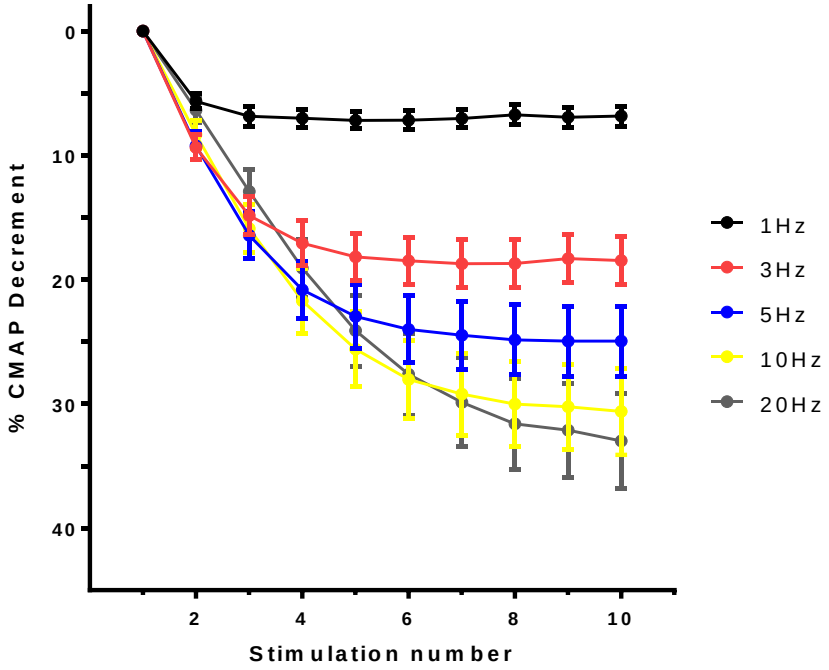

Figure 5.12: CMAP decrement at different stimulation frequencies in the mouse model of slow channel syndrome: The mean (dot) and SEM (bars) of CMAP decrement for all slow channel model mice is shown for ten consecutive stimuli at each stimulation frequency tested.

Results prior to and following 6 weeks of treatment with lamotrigine are shown in Figure 5.13 and Table 5.3. While some variation in baseline decrement was observed between the three SCS groups, there was no significant change in CMAP decrement

following treatment in any group. The group of wild type mice, including the mouse that did not achieve the set maximum on the inverted screen test, had no abnormal decrement at baseline or post treatment. Degree of decrement was not shown to correlate with inverted screen performance. No repetitive CMAP to single nerve stimulation was observed.

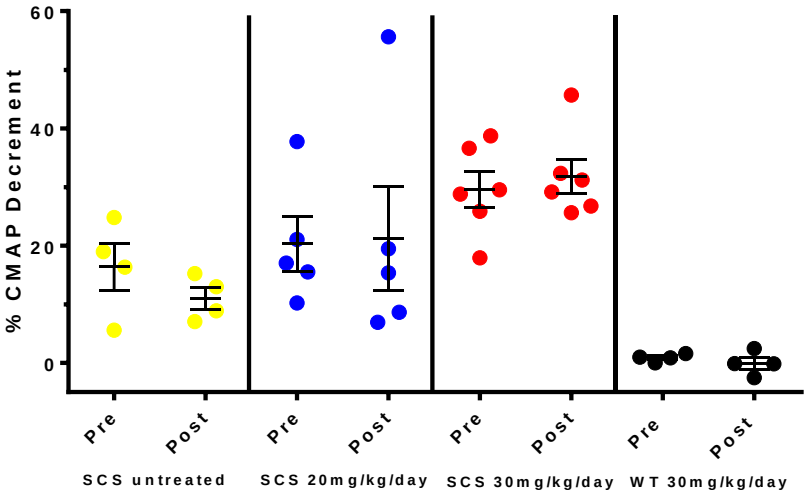

Group	% Mean decrement (+/- SEM)	
	Pre	**Post**
SCS untreated	12.90 (2.67)	9.36 (2.00)
SCS 20 mg/kg/day	16.68 (2.83)	15.56 (6.5)
SCS 30 mg/kg/day	24.27 (2.51)	25.50 (1.73)
Wild type	-1.12 (0.22)	0.10 (1.02)

Figure 5.13 &Table 5.3: Lamotrigine: Repetitive nerve stimulation results: CMAP amplitude decrement comparing 1st to the 5th response at a stimulation frequency of 5 Hz pre- and post- treatment is shown for three groups of slow channel syndrome (SCS) mice; untreated, treated with 20 mg/kg/day and treated with 30 mg/kg/day. Results for wild type (WT) mice treated with 30 mg/kg/day are also shown. Dots indicate data from individual mice. Mean values and the SEM are shown (black bars). Numbers of mice in each group are: SCS 20 mg/kg/day n = 5; SCS 30 mg/kg/day n = 6; SCS untreated controls n = 4, WT 30 mg/kg/day n = 4. Numerical values are given in the table.

5.4 Discussion

As expected lamotrigine isethionate (but not the vehicle control) reduced the prolonged decay of endplate potentials in the *ex vivo* hemidiaphragm experiments in slow channel model animals. This effect was dose dependent and reached statistical significance at a concentration of 200 µM lamotrigine. The effect may occur at least as low as 100 µM, as the difference in MEPP decay time between 50 µM and 100 µM was statistically significant. At the highest concentration tested MEPP decay was just over twice as fast as at baseline. Decay times were not reduced to wild type values, with the fastest rate being around four times slower than that of wild type, even at the highest lamotrigine concentration tested. While decay time may be influenced by the input resistance of the muscle, this is not expected to alter significantly, and the major determinant is AChR channel opening time. Therefore the results of *ex vivo* electrophysiological studies are in keeping with, and most likely represent, lamotrigine blocking the AChR channel. The blocking effect observed here occurred at a concentration similar to that reported in a previous study in which concentrations as low as 50 µM lamotrigine blocked wild type AChR in single-channel patch clamp experiments (Vallés, Garbus, and Barrantes 2007). However, the control experiments with wild type diaphragm tissue showed no such effect with a high lamotrigine concentration (300 µM). It is probable that single-channel analysis is more sensitive at detecting altered channel function than microelectrode studies of endplate potentials.

The main finding of the treatment trial is that, at either dose, treated slow channel mice did not show improvement in either parameter measured: time holding on to the inverted screen or CMAP decrement. The group treated with the lower dose showed no change in inverted screen performance, however, the performance of the group treated

with the higher strength of drug deteriorated. Although one wild type mouse did not hold on for the set maximum at 6 weeks of treatment, it is not possible to be certain that this mouse was truly weak as on occasion strong wild type mice may purposefully drop.

One possible explanation for the lack of improvement is that the drug dosages used to treat the mice were not high enough. Notably, all serum lamotrigine concentrations in treated mice were lower than 50 μM (the minimum concentration at which lamotrigine had been reported to block single-channel recordings). While serum lamotrigine concentrations were grossly similar to those typically seen in treated human subjects it is possible that this may not be physiologically relevant in mice. However, a treatment trial at a higher dose was not undertaken because of the deterioration in inverted screen performance observed in the group treated with 30 mg/kg/day. Another factor to consider is that treatment may not have been given for long enough to see an improvement. Secondary endplate myopathy is thought to account for much of the weakness in the clinical syndrome and this may well take longer than 6 weeks to recover. In support of this mechanism is the progressive nature of improvement in muscle strength typical of patients with slow channel syndrome treated with fluoxetine (Harper, Fukodome, and Engel 2003) or quinidine (Harper and Engel 1998).

The cause of the deterioration in inverted screen performance in the model animals treated with the higher dose is unclear. The lack of an associated deterioration in CMAP decrement would suggest a mechanism out with the NMJ causing deterioration. Lamotrigine is a sodium channel blocker and a possible mechanism for the observed deterioration is that the drug also blocked sodium channels elsewhere, either in the nerve or muscle tissue itself. There is recent evidence to support both of these mechanisms. One study has shown that lamotrigine inhibited $Na_v1.4$ Na^+ current in whole-cell patch clamp experiments with HEK293 cells expressing mouse $Na_v1.4$

channels (Nakatani, Masuko, and Amano 2013). Inhibition was concentration-dependent with a 40% decrease in current observed at 100 µM lamotrigine. A separate study has shown that lamotrigine reduced the peak amplitude of the compound action potential in frog sciatic nerve (Uemura et al. 2014). Again this inhibition was concentration-dependent with a >50% reduction in nerve action potential amplitude observed at the highest lamotrigine concentration tested (500 µM). There is also some evidence from the *ex vivo* microelectrode studies to suggest that lamotrigine was blocking sodium channels in nerve or in muscle, as higher concentrations of lamotrigine (400 µM) sometimes blocked EPPs and diminished or abolished stimulated muscle twitch. These effects, however, were seen at concentrations roughly ten-fold higher than the serum lamotrigine concentrations of treated mice.

Whether the deterioration could be explained by physiological differences between mouse and human is another possibility. Whereas human skeletal muscle is composed of both of fast and slow type fibres, mouse limb muscle is composed almost exclusively of fast twitch muscle fibres which have a sodium channel density four-fold greater than slow twitch fibres (Milton and Behforouz 1995). The higher channel density is thought necessary to maintain action potential amplitude. This may make mouse muscle more susceptible to sodium channel blockade than human limb muscle and could underlie the deterioration. This raises the possibility that a beneficial effect may have been effected by a lower dose, perhaps given for a longer duration. Further differences exist in the mouse model of SCS used in this study compared with the human condition. The slow channel mouse model is homozygous for the εL221F mutation, and expresses no normal ε-subunit, and so all channels are mutant with abnormal kinetics (Webster et al. 2013). By contrast, the mutations causing human slow channel syndrome have a dominant effect, and affected patients have a population of

non-mutated AChRs encoded by the normal allele in addition to a population with abnormal channel function. It is therefore possible the mouse model and the human condition could respond differently to a drug that alters channel kinetics. Although expression levels of the transgene were sufficient for the AChR at the neuromuscular junctions to be visualized by fluorescence microscopy (Webster et al. 2013), another possibility is that there is lower expression of mutant AChR in the slow channel mouse model exacerbated by a degree of endplate myopathy, which is revealed by blockade by lamotrigine. It is also possible that nerve or muscle function and neuromuscular transmission were unaffected by lamotrigine but that poorer inverted screen performance was caused by non-specific side effects.

Overall *ex vivo* and *in vitro* experiments gave no clear indication of the ability of lamotrigine to limit the abnormal function of the AChR channel at physiologically attainable levels. However, the results of the treatment trial in mice should be extrapolated to human subjects with caution. Physiological differences between the mouse model and the human condition may be relevant and as such may not indicate that the drug is expected to cause worsening of weakness in patients.

Chapter 6

Evaluating metoclopramide as a treatment for acetylcholine receptor deficiency syndrome

6.1 Introduction

Metoclopramide was chosen for study following a clear description of improvement of myasthenic symptoms in a child with fast channel congenital myasthenia, due to mutation of the AChR ε-subunit, after taking the drug on four separate occasions. The child was 3-4 years old at the time and had been prescribed the drug for nausea. The patient's mother described improvement in ptosis and general strength within an hour of taking metoclopramide. The patient was also taking regular pyridostigmine and 3,4-diaminopyridine (3,4-DAP) although the improvement was not thought to follow either of these medications because they had not changed.

6.1.1 Metoclopramide and its potential role at the neuromuscular junction

In addition to the nicotinic acetylcholine receptor, several local signalling molecules are active at the skeletal muscle neuromuscular synapse, including muscarinic, adenosine, and neurotrophin receptors (Garcia et al. 2010). Serotonergic receptors have also been postulated to be present at the nerve muscle junction (Wood and Slater 2001; Das et al. 1989). Muscarinic acetylcholine receptors present on the presynaptic nerve terminal (Santafé et al. 2003) are thought to modulate ACh release and both enhancement and reduction coupled to muscarinic mechanisms have been described (Santafé et al. 2003). Furthermore, presynaptic muscarinic modulation of ACh release has been described to be controlled by acetylcholinesterase activity (Minic et al. 2002).

While their individual presence may be known or suspected, the current understanding of the orchestration of these signalling mechanisms and the net effect on neurotransmission remains ill-defined. For example, uncertainty exists over how these signalling mechanisms interact and modulate one another, as well as whether one signalling pathway could have multiple roles which may vary under different physiological conditions.

Metoclopramide hydrochloride is a widely used anti-emetic and pro-kinetic drug. It exerts its anti-emetic action through central inhibition of dopamine (D2) and serotonergic (5HT-3) receptors within the chemoreceptor trigger zone (Rao and Camilleri 2010). In addition, it affects multiple receptor systems within the gut wall to promote gastric motility. Along with pre- and postsynaptic dopaminergic (D2) inhibition, mechanisms include stimulation of presynaptic excitatory 5-HT4 receptors and antagonism of presynaptic inhibition of muscarinic receptors, both of which

promotes ACh release from intrinsic motor neurons (Rao and Camilleri 2010). Metoclopramide is also able to inhibit butyl- and acetylcholinesterase (Petroianu et al. 2003).

Although it is reasonable to expect that the pro-kinetic effect of metoclopramide could improve myasthenic weakness in the index case described above, by encouraging absorption of pyridostigmine and 3,4-DAP, it is worth considering whether it could also have a direct beneficial effect by modulating neurotransmission in myasthenia.

No studies of the effect of metoclopramide on skeletal muscle neurotransmission were identified. However, some evidence of neurotransmission being modulated by serotonin is available. Of the few studies that have examined the effect of serotonin on skeletal muscle some report facilitatory effects while others report depressant effects (Teerapong and Harvey 1979). One study, which looked at twitch tension and endplate potential parameters in mouse phrenic nerve-hemidiaphragm preparations, demonstrated both augmentation and blockade of contractions at lower and higher concentrations respectively. Serotonin reduced the amplitude of MEPPs and EPPs but as quantal content was unaffected it was not thought to augment acetylcholine release. Rather, the findings were thought to suggest that serotonin facilitates transmission by an anticholinesterase action and, at higher concentrations, inhibits by blockade of receptor ion channels (Teerapong and Harvey 1979).

In clinical practice metoclopramide can be taken orally, or by injection, as required for nausea and vomiting. The standard maximum daily dose for adults is 30 mg in 24 hours, although higher doses are used for nausea caused by cytotoxic chemotherapy. Serum levels are not used to monitor treatment in humans although some data is available from pharmacological studies. In one study blood levels were

measured in six healthy adults following a single oral 10 mg dose of metoclopramide (Teng, Bruce, and Dunning 1977). The study found the drug was metabolized quickly with maximum blood levels reached within two hours, a half-life of four hours and approximately 78% of the drug excreted within 24 hours. The maximum serum concentration in these six subjects was approximately 40 ng/ml. Another study found mean plasma metoclopramide concentrations of 37 ng/ml at one hour falling to 7.3 ng/ml at eight hours in a group of six adults also given 10 mg of metoclopramide orally (Bateman, Kahn, and Davies 1979). Toxicity studies in mice have shown an oral LD_{50} of 280 mg/kg with signs of overdose including drowsiness, disorientation, and extrapyramidal reactions (DrugBank 2013).

An important side effect of metoclopramide is its ability to induce acute dystonic reactions, as well as tardive dyskinesia; a persistent and untreatable movement disorder associated with prolonged administration. Caution is recommended when treating the young or elderly in whom dystonic effects are more common. Therefore it would be necessary to establish a clear beneficial effect in myasthenia rather than treating on the basis of anecdotal evidence alone.

6.1.2 Fast channel congenital myasthenic syndrome

Fast channel congenital myasthenic syndrome accounts for around 5% of CMS in the UK. The condition typically presents as the most severe form of CMS with patients at risk of death from life-threatening respiratory crises despite treatment (Palace et al. 2012). Thus, there is a real need for additional treatments for patients with this subtype. Weakness in fast channel syndrome is caused by AChR channel openings that are abnormally brief because of rapid closure of the channel, or reduced probability of the

channel opening. The treatments available for fast channel syndrome, pyridostigmine and 3,4-DAP, indirectly affect channel opening by increasing synaptic ACh availability. These drugs also form the mainstay of treatment in AChR deficiency syndromes due to ε-subunit mutation and rapsyn CMS. If metoclopramide were to augment neurotransmission then it is possible that, like the drugs currently used, it may have an effect on ACh availability rather than directly affecting the kinetic properties of the channel. The presence of multiple signalling mechanisms which metoclopramide could potentially influence at the nerve muscle junction, although fairly undefined, provides some theoretical basis to consider this as a possibility. While a transgenic mouse model of AChR deficiency syndrome has previously been developed (Cossins et al. 2004) a model of fast channel syndrome has not. As both human conditions respond to similar treatments testing the effect of metoclopramide in a receptor deficiency syndrome model is considered a pragmatic approach.

6.1.3 Aims

The aim of this chapter is to evaluate whether metoclopramide can augment NMJ transmission by:

a) Examining the electrophysiological effect of metoclopramide on NMJ transmission using microelectrode studies on *ex vivo* AChR deficiency mouse model phrenic nerve-hemidiaphragm tissue. Because of the potentially numerous and varied local signalling mechanisms that metoclopramide could influence at the NMJ a clear expected outcome on endplate potential parameters is difficult to anticipate. However, any effect expected to translate into clinically relevant

improved muscle strength, should exhibit some effect on stimulated endplate potentials (EPPs), rather than miniature endplate potentials (MEPPs) alone.

b) Assessing the effect of metoclopramide *in vivo*, in a transgenic mouse model of AChR deficiency syndrome. The following techniques were used:

   i. The inverted screen test

   ii. Repetitive nerve stimulation

6.2 Approaches

Detailed methods are given in Chapter 2. In brief, the approaches in this chapter are as follows.

6.2.1 *Ex vivo* diaphragm electrophysiology

Initially MEPP and EPP recordings were made with an increasing concentration of metoclopramide sequentially washed in to the bath solution. Recordings with no drug, then at metoclopramide concentrations of 50 nM, 100 nM, 1 μM and 100 μM were made (Section A.1.4). Recording began 10 minutes after the tissue was exposed to each concentration tested. Experiments were performed on diaphragm tissue from both AChR deficiency mice and wild type mice as a control. Subsequent experiments were performed using tissue from AChR deficiency mice with one selected metoclopramide concentration over a longer period of time to limit any effect of washing in different solutions. In particular, the repeated washing in of solutions can rinse off the conotoxin used to suppress muscle twitch. Control experiments using plain buffer solution to

replicate the effect of washing in the drug solution were also performed. Recordings were made before the drug or buffer was added, then at regular intervals over a two hour period, and finally after the drug or buffer had been washed out and replaced with fresh buffer solution. Part of the purpose of control experiments was to control for the possibility that the optimal locations for EPP recording were learnt with repeated impalements during one experiment, as this could result in an apparent improvement in EPP amplitude. Any such erroneous improvement should be evident in both standard and control recordings.

The following MEPP and EPP parameters were measured at baseline and at each recording point: amplitude, rise time, half width, area, decay time (τ), quantal content and MEPP frequency.

6.2.2 *In vivo* treatment trials

Metoclopramide doses for *in vivo* treatment trials were determined by extrapolating from human doses as described in Section 2.4.1.4. Serum levels were tested in groups of mice treated at the two doses calculated (6 and 12 mg/kg/day) to confirm that the drug was delivered to the mice and was in a range roughly similar to that described in human pharmacological studies. Three separate groups of 10 week old model animals were assigned to receive either of two strengths of metoclopramide or no treatment. Repetitive nerve stimulation was performed pre-treatment and again at the end of a 4 week treatment period. The inverted screen test was performed pre-treatment and at regular intervals during the trial.

6.2.3 Statistical analysis

Statistical analyses were performed using GraphPad Prism version 6, GraphPad Software, California.

6.3 Results

6.3.1 *Ex vivo* diaphragm electrophysiology

6.3.1.1 Studies with varying metoclopramide concentration

Figure 6.1 shows MEPP and EPP parameters at a range of metoclopramide concentrations for both AChR deficiency and wild type mice. Some baseline differences between AChR deficiency and wild type mice are to be expected and are evident in these graphs. This includes the lower amplitude MEPPs and EPPs observed in AChR deficiency mice which is previously described (Cossins et al. 2004) and also seen in recordings from patients with AChR deficiency (Ohno et al. 1997; Vincent et al. 1997). Endplate potential decay is slightly slower in the model mice than in wild type, thought to reflect the expression of fetal type receptors containing the γ-subunit, which have different kinetic properties than adult type receptors (Ohno et al. 1997). As a result of these slower decaying potentials MEPP area is also greater. Similarly, the rise time of potentials is modestly slower in model animals than in wild type.

With the addition of metoclopramide 100 nM a relatively small increase in MEPP half width, area and decay time was seen in the AChR deficiency mice that reached statistical significance (Figure 6.1). However, at a higher concentration of 100 μM a reduction in MEPP half width and decay time of much greater magnitude was seen. This reduction in MEPP half width and decay time was also seen at 100 μM in the wild

type mice. Whether all findings were a true effect of the drug or related to experimental factors is not clear. Possible experimental factors to explain the increased MEPP half width and area at 100 nM metoclopramide could include some cumulative effect of washing off of conotoxin when each solution of different concentration was rinsed into the bath. The significance of the opposite effect seen in some of these MEPP parameters at the highest concentration is unclear, through seems less likely to be explained by experimental factors.

Although not statistically significant, EPP amplitude and quantal content were highest and appeared to increase when metoclopramide 100 nM was applied in both AChR deficiency and wild type preparations. A rise in these parameters would be most likely to translate into increased safety factor of neurotransmission. For this reason this concentration was chosen for further study in the next set of experiments in which endplate potentials were recorded from tissue exposed to a fixed concentration of drug over a longer time period.

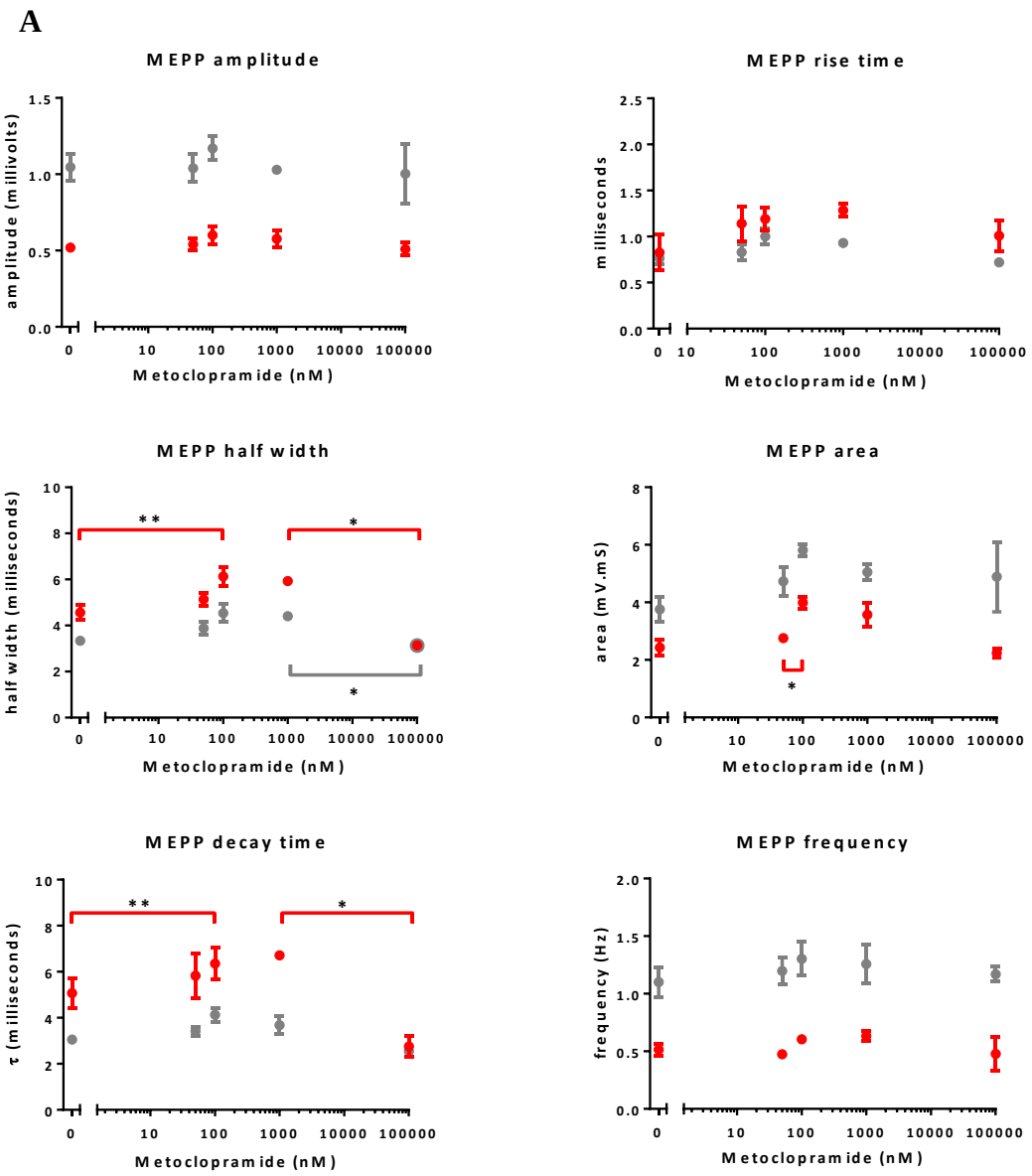

Figure 6.1: *Ex vivo* diaphragm electrophysiology at varying metoclopramide concentration: **A:** MEPP data (this page), **B:** EPP data (overleaf). Data is shown from experiments with AChR deficiency model mice (red) and from wild type mice (grey). Data was collected at different metoclopramide concentrations (no drug (0 nM), 50 nM, 100 nM, 1 µM and 100 µM; shown here on a logarithmic scale). Typically five endplates were sampled at each time point. The mean (dot) and SEM (bars) of three experiments are shown. Repeated measures one-way ANOVA with post-test Tukey's Multiple Comparison was performed. Significant variation was demonstrated in MEPP half width (ANOVA p=0.0125), area (ANOVA p=0.01625) and decay rate (ANOVA p=0.0327) in the AChR deficiency mice, and in MEPP half width of wild type mice (ANOVA p=0.0285). Statistical results from AChR deficiency mice are indicated by red bars and for wild type mice by grey bars. Stars indicate statistically significant p values from Tukey's Multiple Comparison test between the indicated concentrations (*: p = 0.01-0.05; **: p = 0.001-0.01). No significant variation in other MEPP or any EPP parameters was shown by the same analysis.

Figure 6.1: (continued)

B

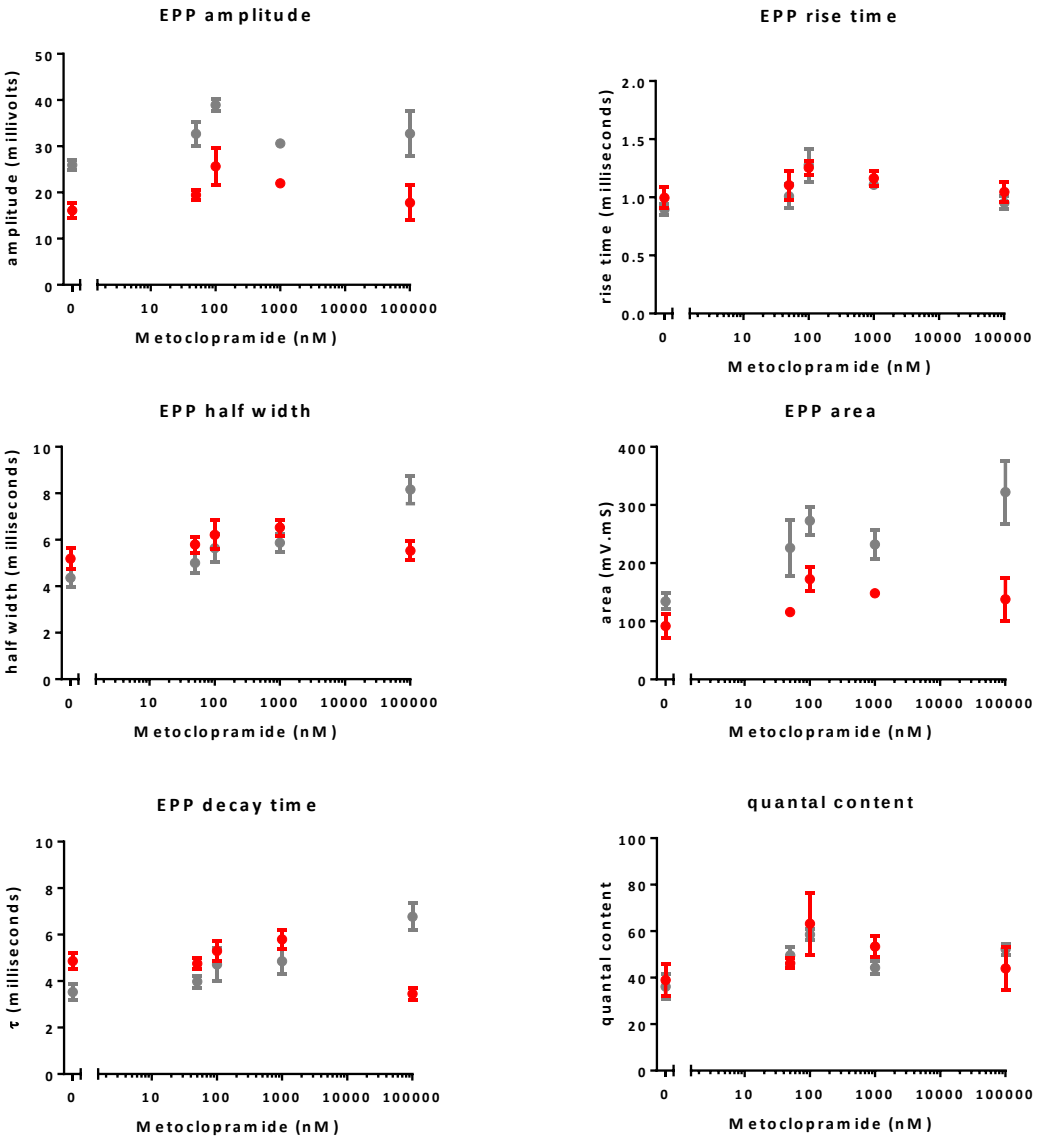

6.3.1.2 Studies with fixed metoclopramide concentration

Overall no effect likely to be clinically relevant was seen on endplate potential parameters of tissue exposed to metoclopramide 100 nM (Figure 6.2). In particular, there was no apparent effect on EPP amplitude or quantal content as had been suggested by the initial hemidiaphragm experiments in which varying metoclopramide concentrations had been applied. Variation in MEPP frequency that reached statistical significance was observed in the experiments with metoclopramide. The data show an increase in MEPP frequency with time, a trend that is mirrored in the control experiments (though here it does not reach statistical significance). It is likely that this reflects the response of the tissue to degradation over time, as it is a well observed phenomenon in previous practice experiments, and these experiments were of long duration.

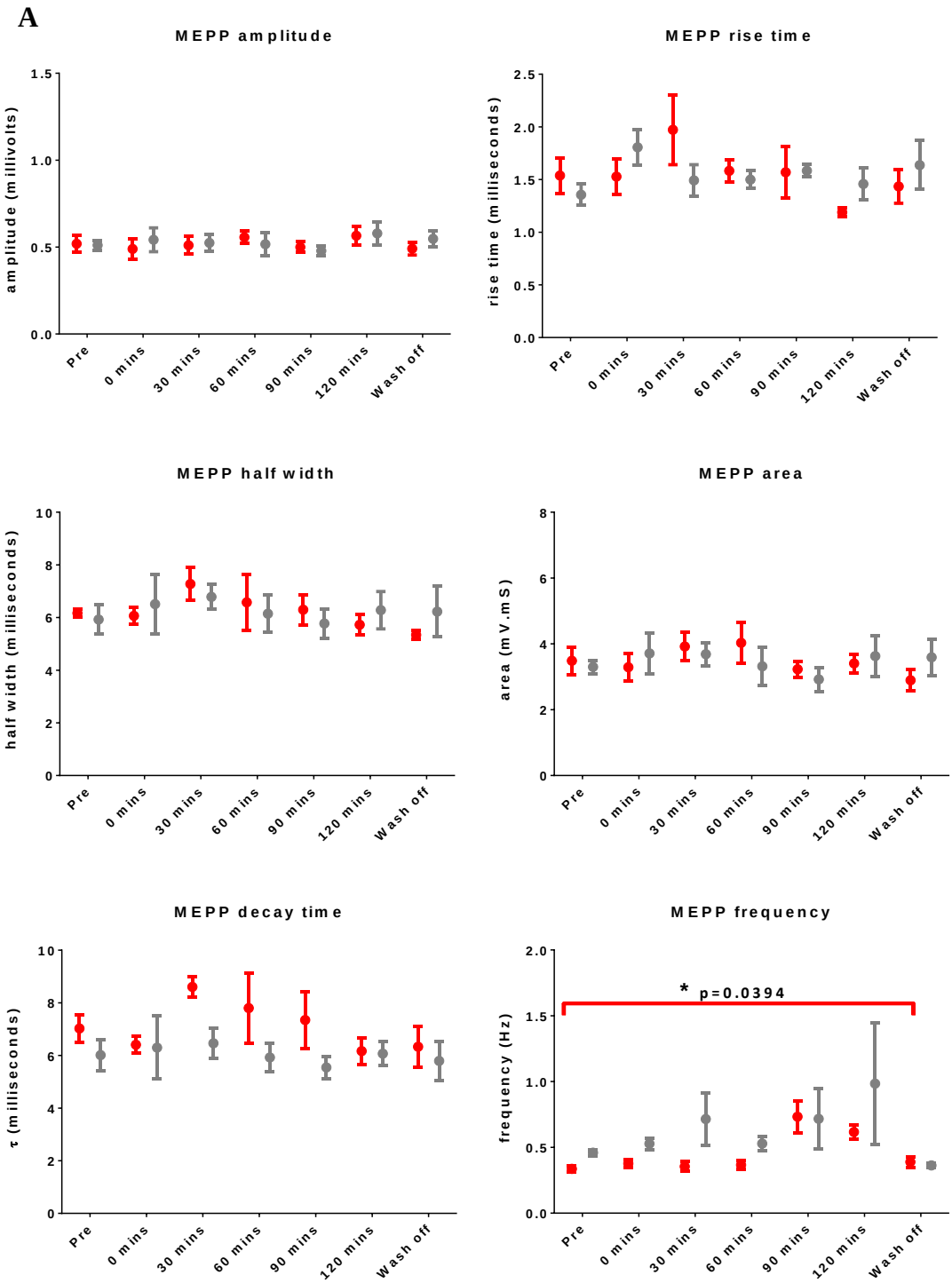

Figure 6.2: *Ex vivo* diaphragm electrophysiology at metoclopramide 100 nM: A: MEPP data (this page), **B:** EPP data (overleaf). Data is shown from experiments with metoclopramide (red) and buffer control (grey). Data was collected before the drug/buffer was added (Pre), at fixed time points (mins = minutes), and again when the drug/buffer was washed out of the bath solution. Typically five endplates were sampled at each time point. The mean (dot) and SEM (bars) of four experiments are shown. Variation in MEPP frequency reaching statistical significance was observed in experiments with metoclopramide (repeated measures ANOVA, p = 0.0394). No significant change in other parameters was shown by repeated measures ANOVA.

Figure 6.2: (continued)

B

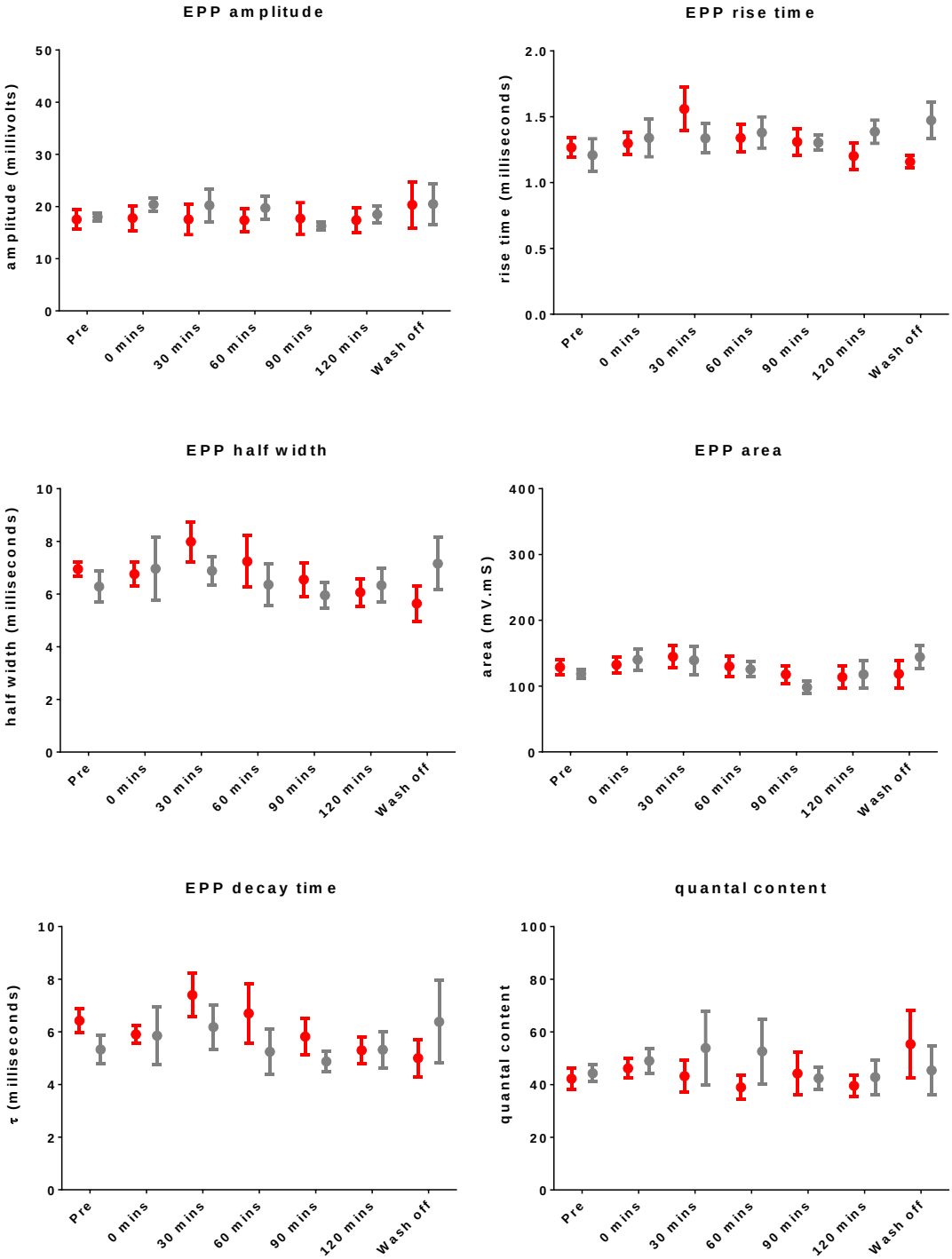

6.3.2 Treatment trials

6.3.2.1 Serum metoclopramide concentration

Metoclopramide was detected in the serum of both groups of treated mice (Figure 6.3). Results were in the nanomolar range, similar to results of pharmacological studies in humans. The serum concentration allows the treatment trial results to be placed in context with the results of microelectrode studies.

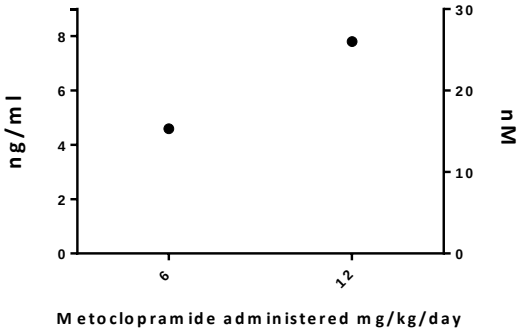

Figure 6.3: Serum metoclopramide concentration: Serum metoclopramide concentrations from mice treated with two different doses of the drug. Concentration in ng/ml on left Y-axis, equivalent in nM shown on right Y-axis. Each data point is from the pooled serum of 5–7 mice.

6.3.2.2 The inverted screen test

Figure 6.4 shows inverted screen performance in untreated and treated AChR deficiency model mice at baseline and at set intervals during the 4 week treatment period. All mice exhibited weakness and were unable to hold onto the screen for the set maximum of 600 s. No significant change in performance was detected in any group over the course of the experiment.

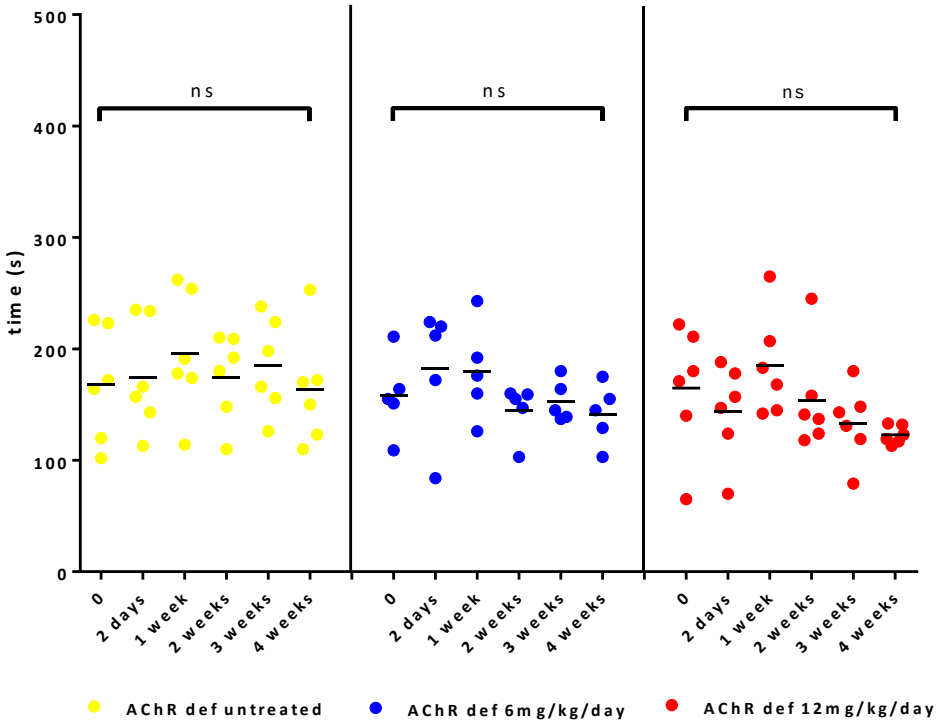

Group	Mean time (+/- SEM) (s)					
	Baseline	**2 days**	**1 week**	**2 weeks**	**3 weeks**	**4 weeks**
Untreated	167.8 (20.9)	174.7 (20.3)	195.5 (22.6)	174.8 (16.0)	184.7 (17.5)	163.0 (20.7)
6 mg/kg/day	158.0 (16.3)	182.4 (26.3)	179.4 (19.3)	144.8 (10.7)	153.0 (8.3)	141.4 (12.2)
12 mg/kg/day	164.8 (23.3)	144.0 (17.5)	185.0 (18.8)	153.8 (19.1)	133.3 (13.7)	122.8 (3.3)

Figure 6.4 and Table 6.1: Metoclopramide: Inverted screen test results: Inverted screen test results showing time held on to an inverted screen in seconds at 0 (baseline), then following indicated periods of continuous treatment. Data from individual mice (dots) and the mean value (black bar) are shown at each time point. Numerical values are given in the table. Numbers of mice in each group were: untreated = 6; 6 mg/kg/day = 5; 12 mg/kg/day = 6; No significant change in performance over the treatment period was seen in any group (repeated measures one way ANOVA).

6.3.2.3 Repetitive nerve stimulation

Figure 6.5 shows the percentage CMAP decrement in treated and untreated groups at 5 Hz stimulation. At this frequency CMAP decrement was not detected in all mice, and tended to be modest where present, with just 3/17 of all model mice having ≥10% CMAP decrement (8/17 with ≥5% CMAP decrement) pre-treatment. No significant

change in CMAP decrement was seen after 4 weeks in the treated or untreated groups. Greater CMAP decrement was seen at higher stimulation frequencies (Figure 6.6). At 10 Hz, comparing the 1st to 8th stimulus, 10/17 mice had ≥10% CMAP decrement (13/17 had ≥5% CMAP decrement). This rate related increase in decrement is similar to that observed in the slow channel mouse model and is probably related to the prolonged channel opening characteristic of fetal type receptors. No significant change in CMAP decrement following treatment was seen at any stimulation frequency.

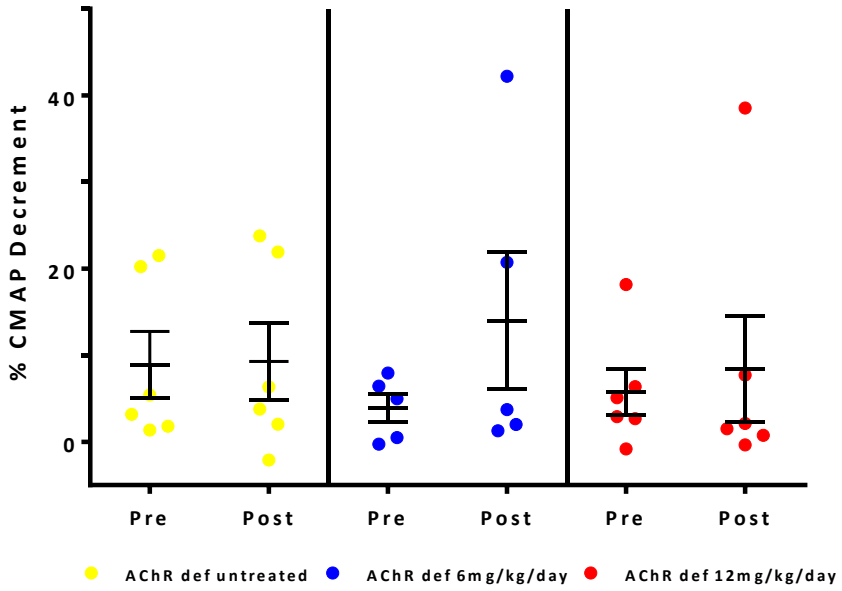

Group	% Mean decrement (+/- SEM)	
	Pre	**Post**
Untreated	8.9 (3.8)	9.3 (4.4)
6 mg/kg/day	3.9 (1.6)	14.0 (7.9)
12 mg/kg/day	5.7 (2.7)	8.4 (6.1)

Figure 6.5 & Table 6.2: Metoclopramide: Repetitive nerve stimulation results:
CMAP amplitude decrement comparing 1st to the 5th response at a stimulation frequency of 5 Hz pre- and post-treatment is shown for three groups mice; untreated = 6, treated with 6 mg/kg/day = 5, treated with 12 mg/kg/day = 6. Data points show the mean decrement of right and left sided gastrocnemius muscles of individual mice (dots) and group mean values and SEM are shown (black bars). No significant change in CMAP decrement measurement was seen in any group following the treatment period (paired t-test). Looking independently at either the right or left side gives similar results. Numerical values are given in the table.

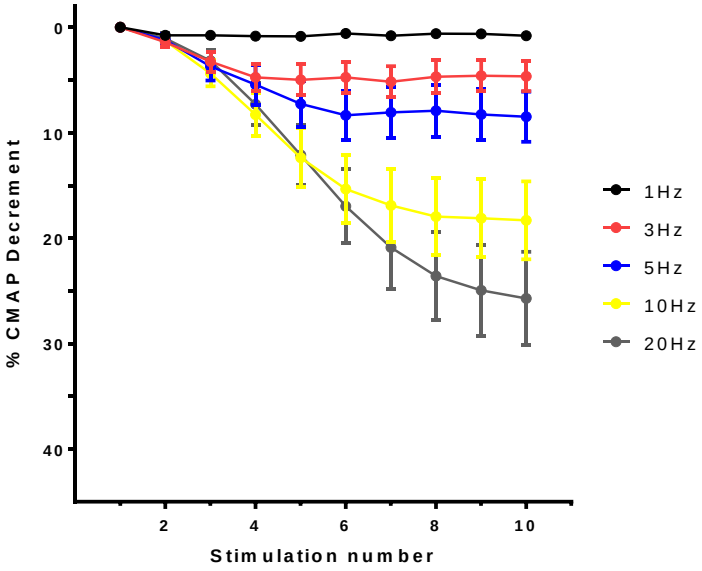

Figure 6.6: CMAP decrement at different stimulation frequencies in the mouse model of acetylcholine receptor deficiency syndrome: Mean (dots) and SEM (bars) CMAP decrement for all AChR deficiency model mice is shown for ten consecutive stimuli at each stimulation frequency tested.

6.4 Discussion

Overall, both *ex vivo* electrophysiological studies and *in vivo* treatment trials failed to demonstrate any reproducible augmentation of neurotransmission by metoclopramide. This may mean that metoclopramide has no significant net effect on neurotransmission, and is therefore not a viable treatment option in myasthenia. It follows that, in the case of the patient who was stronger after taking the drug, the pro-kinetic or anti-emetic effect of metoclopramide likely encouraged absorption of previously ingested pyridostigmine and 3,4-diaminopyridine.

Other alternatives to consider include the possibility that metoclopramide concentrations used in these experiments were insufficient to produce a detectable effect. The serum metoclopramide concentrations from treated mice were in a nanomolar range. While pharmacological studies in humans have demonstrated

nanomolar serum concentrations (Teng, Bruce, and Dunning 1977; Bateman, Kahn, and Davies 1979) there is evidence to suggest some variation in metabolism of metoclopramide between humans and the lower animals, including rats (Teng, Bruce, and Dunning 1977). However, a much wider range of concentrations (from 50 nM – 100 μM) was tested in the *ex vivo* microelectrode recordings, which are expected to detect small physiological changes that may not be evident with techniques also influenced by behaviour such as the inverted screen test. Although there was some initial suggestion of an increase in EPP amplitude and quantal content with metoclopramide 100 nM, this was not reproducible upon subsequent experiments. Other changes in MEPP parameters at 100 nM were modest and most likely explained by experimental factors. Even if the increase in MEPP frequency observed over the length of the fixed concentration experiments was a genuine result of metoclopramide triggering increased presynaptic ACh release, this alone would not necessarily be expected to translate into improved safety factor of neuromuscular transmission.

Consideration should also be given to physiological mechanisms not tested here. It could be the case that metoclopramide had some beneficial effect on the kinetic abnormality of the patient which it is not possible to test using the experimental AChR deficiency mouse model because it exhibits abnormally prolonged, rather than brief, channel opening as a result of its reliance on the fetal form of AChR. The decrease in MEPP decay time seen at the highest metoclopramide concentration could support some effect on channel kinetics, albeit the opposite of that desired in fast channel syndrome. An option for further study would be to investigate the effect of metoclopramide on fast channel mutant acetylcholine receptor opening by single-channel patch clamp.

In a similar vein, using a test of neuromuscular transmission failure with higher sensitivity than RNS may have given more information in the treatment trials. The number of mice with abnormal CMAP decrement and the degree of abnormality was modest at 5 Hz stimulation, meaning that there was little room for improvement to be demonstrated. Sensitivity of RNS in myasthenia is often quoted as between 50 and 60% (Spillane, Beeson, and Kullmann 2010; "Practice Parameter Summary Statement" 2001) typically at 3 Hz stimulation, however, this varies depending upon which muscle is tested, with weak muscles much more likely to yield an abnormal result. Variability in CMAP decrement by muscle has previously been reported in a mouse model of slow channel congenital myasthenia (Gomez et al. 1997). In that study repetitive stimulation at rates of 2-10 Hz resulted in no decrement of CMAP in gastrocnemius, but did show decrement in intrinsic muscles of the hindpaws and the forelimb flexor muscles. It is possible that testing another muscle would have given additional information, however, this was limited by the duration of anaesthesia. Perhaps a better test to perform would have been stimulated SFEMG, which can have sensitivity in patients approaching 100% ("Practice Parameter Summary Statement" 2001). However, attempts to record single-fibre potentials in gastrocnemius, even using a single-fibre recording electrode, were unsuccessful and yielded compounded motor unit potentials.

Another consideration is that neurotransmission in the patient discussed may have undergone adaptive changes or remodelling, either as a result of the underlying condition, or of regular pyridostigmine and 3,4-DAP treatment or, more likely, a combination of both. In patients with acetylcholine receptor deficiency syndrome, which is more common than fast channel syndrome and therefore has been subject to more extensive study, a range of possible compensatory mechanisms have been identified. In addition to persistent expression of fetal AChR at the muscle endplate,

these include induction of transcription of AChR subunit genes, and an increase in quantal release possibly due to an increased number of active zones or a trophic influence of muscle on nerve (Ohno et al. 1997). In the fast channel patient discussed here it is likely there will have been compensatory changes, and while these remain speculative, they may pose some challenge to constructing a representative disease model.

Should a significant beneficial effect have been seen on endplate potential parameters in the *ex vivo* microelectrode studies then this would have been good reason to consider additional experiments to try to identify further the mechanism underlying the improvement. For example, an approach of selective blockade of different receptor systems in hemidiaphragm preparations to see if any improvement in neurotransmission could be reversed or blocked could have been taken. The major caveat to this approach is that the relative uncertainty over the function of receptor systems at the synapse, their selectivity and their interaction with one another may significantly limit clear conclusions to be drawn. Overall, given such limitations and the lack of evidence of augmentation of neurotransmission by metoclopramide provided by this study, future efforts are probably better concentrated investigating alternative agents.

Chapter 7

Conclusions and future directions

Findings presented here result from a combination of clinical and laboratory research into the characterization, investigation, and treatment of congenital myasthenic syndromes. This includes the first comprehensive characterization of the recently discovered group of CMS subtypes caused by mutations in glycosylation pathway components. These subtypes, which are associated with some features not typically seen in other forms of CMS, may be misdiagnosed as purely a myopathy and hopefully clinical characterization will help to identify further patients. In addition, the muscle MRI findings presented here are the first to be systematically reported across a range of CMS subtypes. Unlike the majority of muscle MRI studies in neuromuscular disease, this study benefits from prospectively collected normal control imaging. Finally, the laboratory studies to evaluate lamotrigine and metoclopramide as potential treatments are original, albeit they do not translate into the development of clinically useful treatments. This broad and varied approach was employed in an attempt to answer questions currently relevant to this field, and the main findings contribute as follows to current understanding.

7.1 Clinical characterization

By review of history, examination and investigative findings the clinical features of four novel CMS subtypes secondary to mutations in *DPAGT1, ALG2*, *ALG14* and *GFPT1* were characterized. While the patients discussed share some features typical of CMS, including an autosomal recessive pattern of inheritance and development of muscle weakness early on in life which in most is responsive to anticholinesterase medication, a number of features were identified that could help to distinguish these conditions from other CMS subtypes. Features that may be more specific to these subtypes include a delayed onset beyond infancy, a limb-girdle pattern of weakness, relative sparing of the ocular and facial muscles and a myopathy associated with tubular aggregates. Tubular aggregates are not consistently described in any other known forms of CMS, and their presence on muscle biopsy should direct genetic testing to these genes. The lack of, or very minimal, ptosis in these patients is perhaps the most salient clinical feature to help distinguish these conditions from other CMS subtypes, where ptosis is the norm, and may contribute to under-diagnosis.

It is acknowledged that due to rarity, and probably misdiagnosis, current patient numbers are small, particularly in the ALG14 and GFPT1 subtypes. Therefore it is expected that with time, and as more patients are identified, the phenotype of these conditions will expand and the response to treatment will be better appreciated.

A particular reason to suspect that phenotypic expansion is likely to occur relates to the function of these genes in ubiquitous glycosylation pathways, and notably that two subtypes; DPAGT1 and ALG2, have already been reported in association with diseases known under the umbrella term of congenital disorders of glycosylation. Although hypotonia is described in a number of patients with CDG due to *DPAGT1*

mutations, raising the possibility of an unidentified NMJ transmission defect, this was not specifically investigated. Furthermore, some of the patients described here have evidence of disease affecting systems outwith the NMJ, including one patient with retinal disease, five with learning disability and four with ECG abnormalities. While these features could be incidental they may indicate mild multisystem involvement. It is therefore reasonable to suspect there are patients with untreated CMS who, because of additional, more severe, multisystem involvement giving rise to a complex clinical picture, remain undiagnosed. Another such obstacle to appropriate treatment is the erroneous diagnosis of a purely myopathic condition, which in a patient who may have proximal weakness without ptosis, an abnormal muscle biopsy, potentially a raised CK, and an abnormal muscle MRI appearance, is not altogether surprising. These potential obstacles to diagnosis may be partially eluded by wider availability of next generation DNA sequencing techniques expected to occur in coming years. However, they also strengthen the argument for the need of a greater understanding of investigative findings, such as serum biochemistry and muscle MRI appearance in these conditions, which, if not appreciated, may potentially mislead.

7.2 Muscle MRI in congenital myasthenia

In the MRI study lower limb muscles of 21 adult subjects with eight different forms of CMS were imaged using simple imaging protocols that would be straightforward to acquire in routine clinical practice. The main finding was that of increased hyperintensity on T1w imaging, indicative of fatty infiltration, seen in some CMS subtypes compared to control imaging. The degree of abnormality was most marked in those subjects whose CMS is caused by a glycosylation pathway gene defect. Notably

in the subjects with the most common form of CMS, AChR deficiency syndrome, who were amongst the weakest, no difference from control imaging was seen. Critically, and unlike in some forms of muscle disease where the pattern of muscle involvement can suggest a genetic diagnosis, no selective pattern of muscle involvement was observed. Therefore, T1w findings appear to range from essentially normal in some CMS subtypes to grossly abnormal in others. Though age, and hence disease duration, showed some correlation with severity of findings this did not completely explain the great variation in severity between subtypes.

Only minor differences in STIR imaging between the CMS and control cohorts were observed, and STIR findings were normal in the majority of muscles deemed abnormal on T1w imaging. This challenges previous speculation that this modality may be capable of detecting early pathological change, before fatty infiltration becomes evident on T1w imaging.

This study is the first systematic report of muscle MRI findings in a group of patients with different forms of CMS and suggests that MRI findings can help to direct genetic testing in CMS. Anecdotally, a diagnosis of CMS is often considered when muscle imaging is normal in paediatric neuromuscular practice. However, these findings in adults show that an abnormal scan is also compatible with CMS.

7.3 Studies on lamotrigine and metoclopramide

The studies on lamotrigine and metoclopramide, in transgenic mouse models of slow channel and AChR deficiency syndrome respectively, found no convincing evidence to clearly support therapeutic use of either agent. Although a reduction in endplate potential decay time that could support an open-channel blocking effect of lamotrigine

was observed in *ex vivo* diaphragm electrophysiology studies, there was no convincing benefit seen in the treatment trials. Study of metoclopramide found no convincing evidence of improved NMJ transmission in either the *ex vivo* or *in vivo* experiments. Thus, despite no new treatment becoming available as a result of laboratory evaluation of lamotrigine or metoclopramide, the results presented here may prevent inappropriate treatment of patients.

7.4 Areas for further development and research

By eliminating lamotrigine and metoclopramide as legitimate treatment options other drugs may now be considered. These studies highlight the potential benefit of the investigative techniques available to patients with rare conditions, such as congenital myasthenia. The situation of a specialist clinical service and an affiliated research laboratory within the same institution affords prime opportunity for laboratory findings to be translated into clinical practice and vice-versa.

Perhaps the area where there are most potential leads for further research is in the field of muscle MRI. The novel findings reported here provide a foundation from which to build further knowledge. Whether muscle MR imaging can be used to reliably detect clinical change over time is a key question and this would impact on its utility in clinical trials in congenital myasthenia. How small a change in fatty infiltration can be detected and the significance of this in relation to clinical findings is not fully appreciated. This issue is likely to be complex in congenital myasthenia given the heterogeneity of pathological mechanisms involved in different CMS subtypes and the variation in severity even between patients who share the same genetic subtype. A

major confound is the rarity of these disorders and consequently the relatively small numbers of patients available for study.

Clearly with further imaging of additional subjects the range of abnormality across CMS subtypes will be better appreciated. There is scope to include more patients with less common subtypes such as ChAT or COLQ CMS, as only one subject was imaged in each of these groups. No patients with fast channel syndrome were eligible for recruitment and imaging of a patient with this subtype would also be informative. Further imaging of younger and older individuals with CMS is also likely to be informative. Of particular interest would be imaging of younger patients with those CMS subtypes where marked T1w hyperintensity is known to be evident in adulthood to study the development of abnormalities over time as this may offer some insight into disease mechanisms.

It is also worth considering whether alternative and particularly more quantitative MRI modalities would be more sensitive at detecting pathological change in muscle and specifically better at detecting earlier changes than fatty infiltration. Such an approach may allow earlier drug intervention. However, imaging time would be an important consideration if alternative techniques were employed; many quantitative techniques currently require lengthy times for data acquisition or analysis, which may not be practicable in routine clinical practice.

Lastly, further characterization of the CMS subtypes described in Chapter 3 should follow with the identification of additional patients and perhaps will clarify the extent of any multisystem involvement. Treatment response to β_2-adrenergic receptor agonists should also become better appreciated with long term follow up of known patients already on treatment. The unexpected identification of a cardiac phenotype in

some patients with glycosylation gene forms of CMS also emphasises the need for cardiac surveillance and raises questions around safe treatment particularly with β_2-adrenergic agonists.

7.5 In conclusion

Though diverse in aspect and technique the research findings presented here are complementary in nature. Both drugs evaluated as potential treatments in the laboratory were previously unstudied and only considered for evaluation because of the description of clinical improvement by patients. The understanding of the range of muscle MRI appearances in different CMS subtypes, afforded by the imaging study, directly contributes to the investigative strategy of suspected CMS in patients, as well as offering some insight into underlying pathophysiology. This is particularly important in the most recently discovered glycosylation pathway subtypes where study of disease mechanism is in its infancy. Appreciation of muscle MRI findings also has the potential to contribute to development of new treatments for CMS by acting as a surrogate marker of disease progression in clinical trials. And it is here that thorough clinical characterization of different syndromes shows its value. By documenting the natural history of newly recognized CMS subtypes the range of features of the clinical syndromes can begin to be identified, providing a baseline for further study or treatment trial. The detailed characterization of the group of CMS syndromes caused by glycosylation pathway abnormalities presented here is the first of its kind and will hopefully be of such use.

REFERENCES

Ababneh, Zaid Q, Riad Ababneh, Stephan E Maier, Carl S Winalski, Koichi Oshio, Anas M Ababneh, and Robert V Mulkern. 2008. "On the Correlation between T(2) and Tissue Diffusion Coefficients in Exercised Muscle: Quantitative Measurements at 3T within the Tibialis Anterior." *Magma (New York, N.Y.)* 21 (4): 273–78. doi:10.1007/s10334-008-0120-8.

Abicht, Angela, Marina Dusl, Constanze Gallenmüller, Velina Guergueltcheva, Ulrike Schara, Adele Della Marina, Eva Wibbeler, et al. 2012. "Congenital Myasthenic Syndromes: Achievements and Limitations of Phenotype-Guided Gene-after-Gene Sequencing in Diagnostic Practice: A Study of 680 Patients." *Human Mutation* 33 (10): 1474–84. doi:10.1002/humu.22130.

Basiri, Keivan, Katsiaryna Belaya, Wei Wei Liu, Susan Maxwell, Maryam Sedghi, and David Beeson. 2013. "Clinical Features in a Large Iranian Family with a Limb-Girdle Congenital Myasthenic Syndrome due to a Mutation in DPAGT1." *Neuromuscular Disorders: NMD,* April. doi:10.1016/j.nmd.2013.03.003.

Bateman, D N, C Kahn, and D S Davies. 1979. "Concentration Effect Studies with Oral Metoclopramide." *British Journal of Clinical Pharmacology* 8 (2): 179–82.

Beeson, D. 2008. "Congenital myasthenic syndromes." Chap. 15 in *Myasthenia Gravis and Related Disorders,* 2nd edn. Edited by Henry J. Kaminski. New York: Humana Press/Springer.

Beeson, David, Daniel Hantaï, Hanns Lochmüller, and Andrew G. Engel. 2005. "126th International Workshop: Congenital Myasthenic Syndromes, 24-26 September

2004, Naarden, The Netherlands." *Neuromuscular Disorders* 15 (7): 498–512. doi:10.1016/j.nmd.2005.05.001.

Beeson, David, Osamu Higuchi, Jackie Palace, Judy Cossins, Hayley Spearman, Susan Maxwell, John Newsom-Davis, et al. 2006. "Dok-7 Mutations Underlie a Neuromuscular Junction Synaptopathy." *Science* 313 (5795): 1975 –1978. doi:10.1126/science.1130837.

Belaya, Katsiaryna, Sarah Finlayson, Judith Cossins, Wei Wei Liu, Susan Maxwell, Jacqueline Palace, and David Beeson. 2012a. "Identification of DPAGT1 as a New Gene in Which Mutations Cause a Congenital Myasthenic Syndrome." *Annals of the New York Academy of Sciences* 1275 (December): 29–35. doi:10.1111/j.1749-6632.2012.06790.x.

Belaya, Katsiaryna, Sarah Finlayson, Clarke R. Slater, Judith Cossins, Wei Wei Liu, Susan Maxwell, Simon J. McGowan, et al. 2012b. "Mutations in DPAGT1 Cause a Limb-Girdle Congenital Myasthenic Syndrome with Tubular Aggregates." *The American Journal of Human Genetics*. doi:10.1016/j.ajhg.2012.05.022. http://www.sciencedirect.com/science/article/pii/S0002929712003072.

Beltrame, Valeria, Paolo Ortolan, Alessandro Coran, Riccardo Zanato, Matteo Gazzola, Annachiara Frigo, Luca Bello, Elena Pegoraro, and Roberto Stramare. 2014. "Muscle MR Imaging in Tubular Aggregate Myopathy." Edited by Barry J. Byrne. *PLoS ONE* 9 (4): e94427. doi:10.1371/journal.pone.0094427.

Ben Ammar, Asma, Payam Soltanzadeh, Stephanie Bauche, Pascale Richard, Evelyne Goillot, Ruth Herbst, Karen Gaudon, et al. 2013. "A Mutation Causes MuSK Reduced Sensitivity to Agrin and Congenital Myasthenia." *PLoS ONE* 8 (1).

doi:10.1371/journal.pone.0053826.
http://www.ncbi.nlm.nih.gov/pmc/articles/PMC3541344/.

Bestue-Cardiel, M., A. Sáenz de Cabezón-Alvarez, J. L. Capablo-Liesa, J. López-Pisón, J. L. Peña-Segura, J. Martin-Martinez, and A. G. Engel. 2005. “Congenital Endplate Acetylcholinesterase Deficiency Responsive to Ephedrine.” *Neurology* 65 (1): 144 –146. doi:10.1212/01.wnl.0000167132.35865.31.

Böhm, Johann, Frédéric Chevessier, André Maues De Paula, Catherine Koch, Shahram Attarian, Claire Feger, Daniel Hantaï, et al. 2013. “Constitutive Activation of the Calcium Sensor STIM1 Causes Tubular-Aggregate Myopathy.” *American Journal of Human Genetics* 92 (2): 271–78. doi:10.1016/j.ajhg.2012.12.007.

Boyd, I A, and A R Martin. 1956. “The End-Plate Potential in Mammalian Muscle.” *The Journal of Physiology* 132 (1): 74–91.

Bretthauer, Roger K. 2009. “Structure, Expression, and Regulation of UDP-GlcNAc: Dolichol Phosphate GlcNAc-1-Phosphate Transferase (DPAGT1).” *Current Drug Targets* 10 (6): 477–82.

Brown, Susan C, and Cecilia Jimenez-Mallebrera. 2010. "Biochemical and molecular basis of muscle disease." Chap. 3 in *Disorders of Voluntary Muscle,* 8th edn. Edited by George Karpati, David Hilton-Jones, Kate Bushby and Robert C Griggs. Cambridge: Cambridge University Press.

Burke, G., J. Cossins, S. Maxwell, G. Owens, A. Vincent, S. Robb, M. Nicolle, et al. 2003. “Rapsyn Mutations in Hereditary Myasthenia.” *Neurology* 61 (6): 826 –828. doi:10.1212/01.WNL.0000085865.55513.AE.

Burke, G., J. Cossins, S. Maxwell, S. Robb, M. Nicolle, A. Vincent, J. Newsom-Davis, J. Palace, and D. Beeson. 2004. “Distinct Phenotypes of Congenital Acetylcholine Receptor Deficiency.” *Neuromuscular Disorders* 14 (6): 356–64. doi:16/j.nmd.2004.03.005.

Carrera, Ignacio Arroyo, Gert Matthijs, Belen Perez, and Celia Pérez Cerdá. 2012. “DPAGT1-CDG: Report of a Patient with Fetal Hypokinesia Phenotype.” *American Journal of Medical Genetics. Part A* 158A (8): 2027–30. doi:10.1002/ajmg.a.35472.

Chaouch, Amina, David Beeson, Daniel Hantaï, and Hanns Lochmüller. 2012. “186th ENMC International Workshop: Congenital Myasthenic Syndromes 24-26 June 2011, Naarden, The Netherlands.” *Neuromuscular Disorders: NMD* 22 (6): 566–76. doi:10.1016/j.nmd.2011.12.004.

Chaouch, Amina, Juliane S Müller, Velina Guergueltcheva, Marina Dusl, Ulrike Schara, Vidosava Rakocević-Stojanović, Christopher Lindberg, et al. 2012. “A Retrospective Clinical Study of the Treatment of Slow-Channel Congenital Myasthenic Syndrome.” *Journal of Neurology* 259 (3): 474–81. doi:10.1007/s00415-011-6204-9.

Cheung, H, D Kamp, and E Harris. 1992. “An in Vitro Investigation of the Action of Lamotrigine on Neuronal Voltage-Activated Sodium Channels.” *Epilepsy Research* 13 (2): 107–12.

Chevessier, Frédéric, Brice Faraut, Aymeric Ravel-Chapuis, Pascale Richard, Karen Gaudon, Stéphanie Bauché, Cassandra Prioleau, et al. 2004. “MUSK, a New Target for Mutations Causing Congenital Myasthenic Syndrome.” *Human Molecular Genetics* 13 (24): 3229–40. doi:10.1093/hmg/ddh333.

Chevessier, Frédéric, Christoph Peter, Ulrike Mersdorf, Emmanuelle Girard, Eric Krejci, Joseph J McArdle, and Veit Witzemann. 2012. “A New Mouse Model for the Slow-Channel Congenital Myasthenic Syndrome Induced by the AChR εL221F Mutation.” *Neurobiology of Disease* 45 (3): 851–61. doi:10.1016/j.nbd.2011.10.024.

Cossins, Judith, Katsiaryna Belaya, Debbie Hicks, Mustafa A. Salih, Sarah Finlayson, Nicola Carboni, Wei Wei Liu, et al. 2013. “Congenital Myasthenic Syndromes due to Mutations in ALG2 and ALG14.” *Brain* 136 (3): 944–56. doi:10.1093/brain/awt010.

Cossins, Judy, Richard Webster, Susan Maxwell, Georgina Burke, Angela Vincent, and David Beeson. 2004. “A Mouse Model of AChR Deficiency Syndrome with a Phenotype Reflecting the Human Condition.” *Human Molecular Genetics* 13 (23): 2947 –2957. doi:10.1093/hmg/ddh320.

Das, M, K P Mohanakumar, S P Chauhan, and D K Ganguly. 1989. “5-Hydroxytryptamine in the Phrenic Nerve Diaphragm: Evidence for Its Existence and Release.” *Neuroscience Letters* 97 (3): 345–49.

Dobkin, B H, and M A Verity. 1978. “Familial Neuromuscular Disease with Type 1 Fiber Hypoplasia, Tubular Aggregates, Cardiomyopathy, and Myasthenic Features.” *Neurology* 28 (11): 1135–40.

DrugBank, ed. 2013. “Metoclopramide (DB01233).” *DrugBank*. http://www.drugbank.ca/drugs/DB01233.

Egorin, Merrill J. 2003. “Horseshoes, Hand Grenades, and Body-Surface Area–Based Dosing: Aiming for a Target.” *Journal of Clinical Oncology* 21 (2): 182–83. doi:10.1200/JCO.2003.10.084.

Engel, A G, E H Lambert, D M Mulder, C F Torres, K Sahashi, T E Bertorini, and J N Whitaker. 1982. “A Newly Recognized Congenital Myasthenic Syndrome Attributed to a Prolonged Open Time of the Acetylcholine-Induced Ion Channel.” *Annals of Neurology* 11 (6): 553–69. doi:10.1002/ana.410110603.

Engel, Andrew G. 2011. “Congenital Myasthenic Syndromes in 2012.” *Current Neurology and Neuroscience Reports*, October. doi:10.1007/s11910-011-0234-7. http://www.ncbi.nlm.nih.gov/pubmed/21997714.

Engel, Andrew G, Xin-Ming Shen, Duygu Selcen, and Steven M Sine. 2010. “What Have We Learned from the Congenital Myasthenic Syndromes.” *Journal of Molecular Neuroscience: MN* 40 (1-2): 143–53. doi:10.1007/s12031-009-9229-0.

Engel, Andrew G, and Steven M Sine. 2005. “Current Understanding of Congenital Myasthenic Syndromes.” *Current Opinion in Pharmacology* 5 (3): 308–21. doi:10.1016/j.coph.2004.12.007.

Engel, W. King, Donald W. Bishop, and Guy G. Cunningham. 1970. “Tubular Aggregates in Type II Muscle Fibers: Ultrastructural and Histochemical Correlation.” *Journal of Ultrastructure Research* 31 (5–6): 507–25. doi:10.1016/S0022-5320(70)90166-8.

Eymard, B, T Stojkovic, D Sternberg, P Richard, S Nicole, E Fournier, A Béhin, et al. 2013. “[Congenital Myasthenic Syndromes: Difficulties in the Diagnosis, Course and Prognosis, and Therapy - The French National Congenital Myasthenic Syndrome Network Experience].” *Revue Neurologique* 169 Suppl 1 (February): S45–55. doi:10.1016/S0035-3787(13)70060-2.

Faridian-Aragh, Neda, Kathryn R Wagner, Doris G Leung, and John A Carrino. 2014. "MRI Phenotyping of Becker Muscular Dystrophy." *Muscle & Nerve*, March. doi:10.1002/mus.24246.

Farrugia, Maria Elena, Matthew D Robson, Linda Clover, Phil Anslow, John Newsom-Davis, Robin Kennett, David Hilton-Jones, Paul M Matthews, and Angela Vincent. 2006. "MRI and Clinical Studies of Facial and Bulbar Muscle Involvement in MuSK Antibody-Associated Myasthenia Gravis." *Brain: A Journal of Neurology* 129 (Pt 6): 1481–92. doi:10.1093/brain/awl095.

Fatt, P, and B Katz. 1951. "An Analysis of the End-Plate Potential Recorded with an Intracellular Electrode." *The Journal of Physiology* 115 (3): 320–70.

Finlayson, Sarah, David Beeson, and Jacqueline Palace. 2013. "Congenital Myasthenic Syndromes: An Update." *Practical Neurology* 13 (2): 80–91. doi:10.1136/practneurol-2012-000404.

Finlayson, Sarah, and Jacqueline Palace. 2014. "Inherited myasthenic syndromes." Chap. 19 in *The Oxford Textbook of Neuromuscular Disorders*, edited by David Hilton-Jones and Martin R. Turner. Oxford: Oxford University Press.

Finlayson, Sarah, Jacqueline Palace, Katsiaryna Belaya, Timothy J Walls, Fiona Norwood, Georgina Burke, Janice L Holton, Samuel I Pascual-Pascual, Judith Cossins, and David Beeson. 2013a. "Clinical Features of Congenital Myasthenic Syndrome due to Mutations in DPAGT1." *Journal of Neurology, Neurosurgery, and Psychiatry*, February. doi:10.1136/jnnp-2012-304716.

Finlayson, Sarah, Jennifer Spillane, Dimitri M Kullmann, Robin Howard, Richard Webster, Jacqueline Palace, and David Beeson. 2013b. "Slow Channel

Congenital Myasthenic Syndrome Responsive to a Combination of Fluoxetine and Salbutamol." *Muscle & Nerve* 47 (2): 279–82. doi:10.1002/mus.23534.

Fischer, D, R A Kley, K Strach, C Meyer, T Sommer, K Eger, A Rolfs, et al. 2008. "Distinct Muscle Imaging Patterns in Myofibrillar Myopathies." *Neurology* 71 (10): 758–65. doi:10.1212/01.wnl.0000324927.28817.9b.

Footitt, E J, A Karimova, M Burch, T Yayeh, T Dupré, S Vuillaumier-Barrot, I Chantret, S E H Moore, N Seta, and S Grunewald. 2009. "Cardiomyopathy in the Congenital Disorders of Glycosylation (CDG): A Case of Late Presentation and Literature Review." *Journal of Inherited Metabolic Disease* 32 Suppl 1 (December): 313–19. doi:10.1007/s10545-009-1262-1.

Garcia, Neus, Marta Tomàs, Manel M Santafé, Nuria Besalduch, Maria A Lanuza, and Josep Tomàs. 2010. "The Interaction Between Tropomyosin-Related Kinase B Receptors and Presynaptic Muscarinic Receptors Modulates Transmitter Release in Adult Rodent Motor Nerve Terminals." *The Journal of Neuroscience* 30 (49): 16514–22. doi:10.1523/JNEUROSCI.2676-10.2010.

Gomez, C M, B B Bhattacharyya, P Charnet, J W Day, C Labarca, R L Wollmann, and E H Lambert. 1996. "A Transgenic Mouse Model of the Slow-Channel Syndrome." *Muscle & Nerve* 19 (1): 79–87. doi:10.1002/(SICI)1097-4598(199601)19:1<79::AID-MUS11>3.0.CO;2-Z.

Gomez, C M, R Maselli, J E Gundeck, M Chao, J W Day, S Tamamizu, J A Lasalde, M McNamee, and R L Wollmann. 1997. "Slow-Channel Transgenic Mice: A Model of Postsynaptic Organellar Degeneration at the Neuromuscular Junction." *The Journal of Neuroscience: The Official Journal of the Society for Neuroscience* 17 (11): 4170–79.

Gomez, Christopher M, Ricardo A Maselli, Jason Groshong, Roberto Zayas, Robert L Wollmann, Thierry Cens, and Pierre Charnet. 2002. “Active Calcium Accumulation Underlies Severe Weakness in a Panel of Mice with Slow-Channel Syndrome.” *The Journal of Neuroscience: The Official Journal of the Society for Neuroscience* 22 (15): 6447–57. doi:20026643.

Guergueltcheva, Velina, Juliane S. Müller, Marina Dusl, Jan Senderek, Anders Oldfors, Christopher Lindbergh, Susan Maxwell, et al. 2012. “Congenital Myasthenic Syndrome with Tubular Aggregates Caused by GFPT1 Mutations.” *Journal of Neurology* 259 (5): 838–50. doi:10.1007/s00415-011-6262-z.

Harper, C M, and A G Engel. 1998. “Quinidine Sulfate Therapy for the Slow-Channel Congenital Myasthenic Syndrome.” *Annals of Neurology* 43 (4): 480–84. doi:10.1002/ana.410430411.

Harper, C Michel, Takayasu Fukodome, and Andrew G Engel. 2003. “Treatment of Slow-Channel Congenital Myasthenic Syndrome with Fluoxetine.” *Neurology* 60 (10): 1710–13.

Hirsch, L. J., D. Weintraub, Y. Du, R. Buchsbaum, H. T. Spencer, M. Hager, T. Straka, et al. 2004. “Correlating Lamotrigine Serum Concentrations with Tolerability in Patients with Epilepsy.” *Neurology* 63 (6): 1022 –1026. doi:10.1212/01.WNL.0000138424.33979.0C.

Hoffmann, Katrin, Juliane S. Müller, Sigmar Stricker, Andre Megarbane, Anna Rajab, Tom H. Lindner, Monika Cohen, et al. 2006. “Escobar Syndrome Is a Prenatal Myasthenia Caused by Disruption of the Acetylcholine Receptor Fetal Γ Subunit.” *American Journal of Human Genetics* 79 (2): 303–12.

Hutchinson, D O, T J Walls, S Nakano, S Camp, P Taylor, C M Harper, R V Groover, H A Peterson, D G Jamieson, and A G Engel. 1993. “Congenital Endplate Acetylcholinesterase Deficiency.” *Brain: A Journal of Neurology* 116 (Pt 3) (June): 633–53.

Huzé, Caroline, Stéphanie Bauché, Pascale Richard, Frédéric Chevessier, Evelyne Goillot, Karen Gaudon, Asma Ben Ammar, et al. 2009. “Identification of an Agrin Mutation That Causes Congenital Myasthenia and Affects Synapse Function.” *American Journal of Human Genetics* 85 (2): 155–67. doi:10.1016/j.ajhg.2009.06.015.

Imtiaz, Faiqa, Abeer Al-Mostafa, and Zuhair N Al-Hassnan. 2012. “Further Delineation of the Phenotype of Congenital Disorder of Glycosylation DPAGT1-CDG (CDG-Ij) Identified by Homozygosity Mapping.” *JIMD Reports* 2: 107–11. doi:10.1007/8904_2011_57.

Iqbal, Zafar, Mohsin Shahzad, Lisenka E L M Vissers, Monique van Scherpenzeel, Christian Gilissen, Attia Razzaq, Muhammad Yasir Zahoor, et al. 2012. “A Compound Heterozygous Mutation in DPAGT1 Results in a Congenital Disorder of Glycosylation with a Relatively Mild Phenotype.” *European Journal of Human Genetics: EJHG*, December. doi:10.1038/ejhg.2012.257.

Jackson, B J, M A Kukuruzinska, and P Robbins. 1993. “Biosynthesis of Asparagine-Linked Oligosaccharides in Saccharomyces Cerevisiae: The alg2 Mutation.” *Glycobiology* 3 (4): 357–64.

Jaeken, Jaak. 2011. “Congenital Disorders of Glycosylation (CDG): It’s (nearly) All in It!” *Journal of Inherited Metabolic Disease* 34 (4): 853–58. doi:10.1007/s10545-011-9299-3.

Jaretzki, A, R J Barohn, R M Ernstoff, H J Kaminski, J C Keesey, A S Penn, and D B Sanders. 2000. “Myasthenia Gravis: Recommendations for Clinical Research Standards. Task Force of the Medical Scientific Advisory Board of the Myasthenia Gravis Foundation of America.” *Neurology* 55 (1): 16–23.

Jephson, Chris G, Nikki A Mills, Matthew C Pitt, David Beeson, Annie Aloysius, Francesco Muntoni, Stephanie A Robb, and C Martin Bailey. 2010. “Congenital Stridor with Feeding Difficulty as a Presenting Symptom of Dok7 Congenital Myasthenic Syndrome.” *International Journal of Pediatric Otorhinolaryngology* 74 (9): 991–94. doi:10.1016/j.ijporl.2010.05.022.

Karachunski, P I, N S Ostlie, D K Okita, and B M Conti-Fine. 1997. “Prevention of Experimental Myasthenia Gravis by Nasal Administration of Synthetic Acetylcholine Receptor T Epitope Sequences.” *Journal of Clinical Investigation* 100 (12): 3027–35. doi:10.1172/JCI119857.

Katz, B, and S Thesleff. 1957. “On the Factors Which Determine the Amplitude of the Miniature End-Plate Potential.” *The Journal of Physiology* 137 (2): 267–78.

Kim, Hee Kyung, Tal Laor, Paul S Horn, Judy M Racadio, Brenda Wong, and Bernard J Dardzinski. 2010. “T2 Mapping in Duchenne Muscular Dystrophy: Distribution of Disease Activity and Correlation with Clinical Assessments.” *Radiology* 255 (3): 899–908. doi:10.1148/radiol.10091547.

Kinali, M, D Beeson, M C Pitt, H Jungbluth, A K Simonds, A Aloysius, H Cockerill, et al. 2008. “Congenital Myasthenic Syndromes in Childhood: Diagnostic and Management Challenges.” *Journal of Neuroimmunology* 201-202 (September): 6–12. doi:10.1016/j.jneuroim.2008.06.026.

Klein, Andrea, Matthew C Pitt, John C McHugh, Erik H Niks, Caroline A Sewry, Rahul Phadke, Lucy Feng, et al. 2013. “DOK7 Congenital Myasthenic Syndrome in Childhood: Early Diagnostic Clues in 23 Children.” *Neuromuscular Disorders: NMD*, July. doi:10.1016/j.nmd.2013.06.002.

Kokubun, Norito, Masahiro Sonoo, Tomihiro Imai, Yumiko Arimura, Satoshi Kuwabara, Tetsuo Komori, Masahito Kobayashi, et al. 2011. “Reference Values for Voluntary and Stimulated Single-Fibre EMG Using Concentric Needle Electrodes: A Multicentre Prospective Study.” *Clinical Neurophysiology*. doi:10.1016/j.clinph.2011.07.044. http://www.sciencedirect.com/science/article/pii/S1388245711005529.

Kraner, Simone, Iris Laufenberg, Hans M Strassburg, Joern P Sieb, and Ortrud K Steinlein. 2003. “Congenital Myasthenic Syndrome with Episodic Apnea in Patients Homozygous for a CHAT Missense Mutation.” *Archives of Neurology* 60 (5): 761–63. doi:10.1001/archneur.60.5.761.

Kuffler, S W, and D Yoshikami. 1975. “The Number of Transmitter Molecules in a Quantum: An Estimate from Iontophoretic Application of Acetylcholine at the Neuromuscular Synapse.” *The Journal of Physiology* 251 (2): 465–82.

“Lamotrigine Official FDA Information, Side Effects and Uses.” 2013. Accessed September 5. http://www.drugs.com/pro/lamotrigine.html.

Lashley, D, J Palace, S Jayawant, S Robb, and D Beeson. 2010. “Ephedrine Treatment in Congenital Myasthenic Syndrome due to Mutations in DOK7.” *Neurology* 74 (19): 1517–23. doi:10.1212/WNL.0b013e3181dd43bf.

Lefeber, Dirk J, Arjan P M de Brouwer, Eva Morava, Moniek Riemersma, Janneke H M Schuurs-Hoeijmakers, Birgit Absmanner, Kiek Verrijp, et al. 2011.

"Autosomal Recessive Dilated Cardiomyopathy due to DOLK Mutations Results from Abnormal Dystroglycan O-Mannosylation." *PLoS Genetics* 7 (12): e1002427. doi:10.1371/journal.pgen.1002427.

Leite, Maria Isabel, Saiju Jacob, Stuart Viegas, Judy Cossins, Linda Clover, B Paul Morgan, David Beeson, Nick Willcox, and Angela Vincent. 2008. "IgG1 Antibodies to Acetylcholine Receptors in 'Seronegative' Myasthenia Gravis." *Brain: A Journal of Neurology* 131 (Pt 7): 1940–52. doi:10.1093/brain/awn092.

Lewis, Andrew, Sarah Finlayson, Masliza Mahmod, Theodoros D. Karamitsos, Sairia Dass, Houman Ashrafian, Jane M. Francis, et al. 2014. "Characterisation of a Novel Cardiac Phenotype in Patients with GFPT1 or DPAGT1 Mutations." *Journal of Cardiovascular Magnetic Resonance* 16 (Suppl 1): P332. doi:10.1186/1532-429X-16-S1-P332.

Lieu, Michelle T, Bobby G Ng, Jeffrey S Rush, Tim Wood, Monica J Basehore, Madhuri Hegde, Richard C Chang, Jose E Abdenur, Hudson H Freeze, and Raymond Y Wang. 2013. "Severe, Fatal Multisystem Manifestations in a Patient with Dolichol Kinase-Congenital Disorder of Glycosylation." *Molecular Genetics and Metabolism* 110 (4): 484–89. doi:10.1016/j.ymgme.2013.09.016.

Liewluck, Teerin, Duygu Selcen, and Andrew G Engel. 2011. "Beneficial Effects of Albuterol in Congenital Endplate Acetylcholinesterase Deficiency and Dok-7 Myasthenia." *Muscle & Nerve* 44 (5): 789–94. doi:10.1002/mus.22176.

Lorenzoni, Paulo J, Rosana H Scola, Cláudia S K Kay, Luciane Filla, Anna P P Miranda, João M R Pinheiro, Amina Chaouch, Hanns Lochmüller, and Lineu C Werneck. 2013. "Salbutamol Therapy in Congenital Myasthenic Syndrome due

to DOK7 Mutation." *Journal of the Neurological Sciences*, June. doi:10.1016/j.jns.2013.05.017.

Lorenzoni, Paulo José, Rosana Herminia Scola, Cláudia Suemi Kamoi Kay, and Lineu Cesar Werneck. 2012. "Congenital Myasthenic Syndrome: A Brief Review." *Pediatric Neurology* 46 (3): 141–48. doi:10.1016/j.pediatrneurol.2011.12.001.

Lovitt, Steven, Sandra L. Moore, and Franklin A. Marden. 2006. "The Use of MRI in the Evaluation of Myopathy." *Clinical Neurophysiology* 117 (3): 486–95. doi:10.1016/j.clinph.2005.10.010.

Lu, Jishun, Tetsuo Takahashi, Atsuko Ohoka, Kei-ichi Nakajima, Ryo Hashimoto, Nobuaki Miura, Hiroyuki Tachikawa, and Xiao-Dong Gao. 2012. "Alg14 Organizes the Formation of a Multiglycosyltransferase Complex Involved in Initiation of Lipid-Linked Oligosaccharide Biosynthesis." *Glycobiology* 22 (4): 504–16. doi:10.1093/glycob/cwr162.

Marklová, Eliška, and Ziad Albahri. 2007. "Screening and Diagnosis of Congenital Disorders of Glycosylation." *Clinica Chimica Acta* 385 (1–2): 6–20. doi:10.1016/j.cca.2007.07.002.

Martin, A R. 1976. "The Effect of Membrane Capacitance on Non-Linear Summation of Synaptic Potentials." *Journal of Theoretical Biology* 59 (1): 179–87.

Maselli, R A, J J Ng, J A Anderson, O Cagney, J Arredondo, C Williams, H B Wessel, H Abdel-Hamid, and R L Wollmann. 2009. "Mutations in LAMB2 Causing a Severe Form of Synaptic Congenital Myasthenic Syndrome." *Journal of Medical Genetics* 46 (3): 203 –208. doi:10.1136/jmg.2008.063693.

Mercuri, Eugenio, Claudio Cini, Serena Counsell, Joanna Allsop, Zuella Zolkipli, Heinz Jungbluth, Caroline Sewry, Susan C Brown, Guglielmina Pepe, and Francesco Muntoni. 2002c. “Muscle MRI Findings in a Three-Generation Family Affected by Bethlem Myopathy.” *European Journal of Paediatric Neurology: EJPN: Official Journal of the European Paediatric Neurology Society* 6 (6): 309–14.

Mercuri, Eugenio, Anne Lampe, Joanna Allsop, Ravi Knight, Marika Pane, Maria Kinali, Carsten Bonnemann, et al. 2005. “Muscle MRI in Ullrich Congenital Muscular Dystrophy and Bethlem Myopathy.” *Neuromuscular Disorders* 15 (4): 303–10. doi:10.1016/j.nmd.2005.01.004.

Mercuri, Eugenio, Anna Pichiecchio, Joanna Allsop, Sonia Messina, Marika Pane, and Francesco Muntoni. 2007. “Muscle MRI in Inherited Neuromuscular Disorders: Past, Present, and Future.” *Journal of Magnetic Resonance Imaging: JMRI* 25 (2): 433–40. doi:10.1002/jmri.20804.

Mercuri, Eugenio, Anna Pichiecchio, Serena Counsell, Joanna Allsop, Claudio Cini, Heinz Jungbluth, Carla Uggetti, and Graeme Bydder. 2002a. “A Short Protocol for Muscle MRI in Children with Muscular Dystrophies.” *European Journal of Paediatric Neurology: EJPN: Official Journal of the European Paediatric Neurology Society* 6 (6): 305–7.

Mercuri, Eugenio, Beril Talim, Behzad Moghadaszadeh, Nathalie Petit, Martin Brockington, Serena Counsell, Pascale Guicheney, Francesco Muntoni, and Luciano Merlini. 2002b. “Clinical and Imaging Findings in Six Cases of Congenital Muscular Dystrophy with Rigid Spine Syndrome Linked to Chromosome 1p (RSMD1).” *Neuromuscular Disorders: NMD* 12 (7-8): 631–38.

Mihaylova, Violeta, Juliane S. Müller, Juan J. Vilchez, Mustafa A. Salih, Mohammad M. Kabiraj, Adele D'Amico, Enrico Bertini, et al. 2008. "Clinical and Molecular Genetic Findings in COLQ-Mutant Congenital Myasthenic Syndromes." *Brain* 131 (3): 747 –759. doi:10.1093/brain/awm325.

Miledi, R, P Molinoff, and L T Potter. 1971. "Isolation of the Cholinergic Receptor Protein of Torpedo Electric Tissue." *Nature* 229 (5286): 554–57.

Milton, R L, and M A Behforouz. 1995. "Na Channel Density in Extrajunctional Sarcolemma of Fast and Slow Twitch Mouse Skeletal Muscle Fibres: Functional Implications and Plasticity after Fast Motoneuron Transplantation on to a Slow Muscle." *Journal of Muscle Research and Cell Motility* 16 (4): 430–39.

Minic, Jasmina, Jordi Molgó, Evert Karlsson, and Eric Krejci. 2002. "Regulation of Acetylcholine Release by Muscarinic Receptors at the Mouse Neuromuscular Junction Depends on the Activity of Acetylcholinesterase." *The European Journal of Neuroscience* 15 (3): 439–48.

Miyazawa, Atsuo, Yoshinori Fujiyoshi, and Nigel Unwin. 2003. "Structure and Gating Mechanism of the Acetylcholine Receptor Pore." *Nature* 423 (6943): 949–55. doi:10.1038/nature01748.

Monies, Dorota M, Hindi N Al-Hindi, Mohamed A Al-Muhaizea, Dyala J Jaroudi, Banan Al-Younes, Ewa A Naim, Salma M Wakil, Brian F Meyer, and Saeed Bohlega. 2014. "Clinical and Pathological Heterogeneity of a Congenital Disorder of Glycosylation Manifesting as a Myasthenic/myopathic Syndrome." *Neuromuscular Disorders: NMD* 24 (4): 353–59. doi:10.1016/j.nmd.2013.12.010.

Morar, Bharti, David Gresham, Dora Angelicheva, Ivailo Tournev, Rebecca Gooding, Velina Guergueltcheva, Carolin Schmidt, et al. 2004. “Mutation History of the Roma/Gypsies.” *The American Journal of Human Genetics* 75 (4): 596–609. doi:10.1086/424759.

Morgan, Neil V, Louise A Brueton, Phillip Cox, Marie T Greally, John Tolmie, Shanaz Pasha, Irene A Aligianis, et al. 2006. “Mutations in the Embryonal Subunit of the Acetylcholine Receptor (CHRNG) Cause Lethal and Escobar Variants of Multiple Pterygium Syndrome.” *American Journal of Human Genetics* 79 (2): 390–95. doi:10.1086/506256.

Morrow, Jasper M, Emma Matthews, Dipa L Raja Rayan, Arne Fischmann, Christopher D J Sinclair, Mary M Reilly, John S Thornton, Michael G Hanna, and Tarek A Yousry. 2013b. “Muscle MRI Reveals Distinct Abnormalities in Genetically Proven Non-Dystrophic Myotonias.” *Neuromuscular Disorders: NMD*, June. doi:10.1016/j.nmd.2013.05.001.

Morrow, Jasper M, Robert D S Pitceathly, Ros M Quinlivan, and Tarek A Yousry. 2013a. “Muscle MRI in Bethlem Myopathy.” *BMJ Case Reports* 2013. doi:10.1136/bcr-2013-008596.

Morrow, Jasper M, Christopher D J Sinclair, Arne Fischmann, Mary M Reilly, Michael G Hanna, Tarek A Yousry, and John S Thornton. 2014. “Reproducibility, and Age, Body-Weight and Gender Dependency of Candidate Skeletal Muscle MRI Outcome Measures in Healthy Volunteers.” *European Radiology*, April. doi:10.1007/s00330-014-3145-6.

Müller, J S, G Mildner, W Müller-Felber, U Schara, K Krampfl, B Petersen, S Petrova, et al. 2003. “Rapsyn N88K Is a Frequent Cause of Congenital Myasthenic Syndromes in European Patients.” *Neurology* 60 (11): 1805–10.

Nakatani, Yoshihiko, Haruka Masuko, and Taku Amano. 2013. “The Effect of Lamotrigine on Na(v)1.4 Voltage-Gated Sodium Channels.” *Journal of Pharmacological Sciences* 123 (2): 203–6.

Niakan, E., Y. Harati, and M.J. Danon. 1985. “Tubular Aggregates: Their Association with Myalgia.” *Journal of Neurology Neurosurgery and Psychiatry* 48 (9): 882–86.

Ohkawara, Bisei, Macarena Cabrera-Serrano, Tomohiko Nakata, Margherita Milone, Nobuyuki Asai, Kenyu Ito, Mikako Ito, et al. 2013. “LRP4 Third B-Propeller Domain Mutations Cause Novel Congenital Myasthenia by Compromising Agrin-Mediated Musk Signaling in a Position-Specific Manner.” *Human Molecular Genetics*, November. doi:10.1093/hmg/ddt578.

Ohno, K, P A Quiram, M Milone, H L Wang, M C Harper, J N Pruitt 2nd, J M Brengman, et al. 1997. “Congenital Myasthenic Syndromes due to Heteroallelic Nonsense/missense Mutations in the Acetylcholine Receptor Epsilon Subunit Gene: Identification and Functional Characterization of Six New Mutations.” *Human Molecular Genetics* 6 (5): 753–66.

Ohno, K, H L Wang, M Milone, N Bren, J M Brengman, S Nakano, P Quiram, J N Pruitt, S M Sine, and A G Engel. 1996. “Congenital Myasthenic Syndrome Caused by Decreased Agonist Binding Affinity due to a Mutation in the Acetylcholine Receptor Epsilon Subunit.” *Neuron* 17 (1): 157–70.

Ohno, Kinji, Andrew G Engel, Xin-Ming Shen, Duygu Selcen, Joan Brengman, C Michel Harper, Akira Tsujino, and Margherita Milone. 2002. “Rapsyn Mutations in Humans Cause Endplate Acetylcholine-Receptor Deficiency and Myasthenic Syndrome.” *American Journal of Human Genetics* 70 (4): 875–85. doi:10.1086/339465.

Okada, Kumiko, Akane Inoue, Momoko Okada, Yoji Murata, Shigeru Kakuta, Takafumi Jigami, Sachiko Kubo, et al. 2006. “The Muscle Protein Dok-7 Is Essential for Neuromuscular Synaptogenesis.” *Science* 312 (5781): 1802 –1805. doi:10.1126/science.1127142.

Oosterhuis, H J, J Newsom-Davis, J H Wokke, P C Molenaar, T V Weerden, B S Oen, F G Jennekens, H Veldman, A Vincent, and D W Wray. 1987. “The Slow Channel Syndrome. Two New Cases.” *Brain: A Journal of Neurology* 110 (Pt 4) (August): 1061–79.

Palace, Jackie, and David Beeson. 2008. “The Congenital Myasthenic Syndromes.” *Journal of Neuroimmunology* 201-202 (September): 2–5. doi:10.1016/j.jneuroim.2008.05.030.

Palace, Jacqueline, Daniel Lashley, Stephen Bailey, Sandeep Jayawant, Aisling Carr, John McConville, Stephanie Robb, and David Beeson. 2012. “Clinical Features in a Series of Fast Channel Congenital Myasthenia Syndrome.” *Neuromuscular Disorders: NMD* 22 (2): 112–17. doi:10.1016/j.nmd.2011.08.002.

Palace, Jacqueline, Daniel Lashley, John Newsom-Davis, Judy Cossins, Susan Maxwell, Robin Kennett, Sandeep Jayawant, Yuji Yamanashi, and David Beeson. 2007. “Clinical Features of the DOK7 Neuromuscular Junction

Synaptopathy." *Brain: A Journal of Neurology* 130 (Pt 6): 1507–15. doi:10.1093/brain/awm072.

Parr, J R, and S Jayawant. 2007. "Childhood Myasthenia: Clinical Subtypes and Practical Management." *Developmental Medicine and Child Neurology* 49 (8): 629–35. doi:10.1111/j.1469-8749.2007.00629.x.

Parr, Jeremy Ross, Morag Jane Andrew, Maria Finnis, David Beeson, Angela Vincent, and Sandeep Jayawant. 2014. "How Common Is Childhood Myasthenia? The UK Incidence and Prevalence of Autoimmune and Congenital Myasthenia." *Archives of Disease in Childhood*, February. doi:10.1136/archdischild-2013-304788.

Pavlovicová, M, M Novotová, and I Zahradník. 2003. "Structure and Composition of Tubular Aggregates of Skeletal Muscle Fibres." *General Physiology and Biophysics* 22 (4): 425–40.

Petroianu, G, F Kühn, C Thyes, V Ewald, and A Missler. 2003. "In Vitro Protection of Plasma Cholinesterases by Metoclopramide from Inhibition by Paraoxon." *Journal of Applied Toxicology: JAT* 23 (1): 75–79. doi:10.1002/jat.891.

Peyer, Anne-Kathrin, Angela Abicht, Karl Heinimann, Michael Sinnreich, and Dirk Fischer. 2013. "Quinine Sulfate as a Therapeutic Option in a Patient with Slow Channel Congenital Myasthenic Syndrome." *Neuromuscular Disorders: NMD*, May. doi:10.1016/j.nmd.2013.04.001.

"Practice Parameter for Repetitive Nerve Stimulation and Single Fiber EMG Evaluation of Adults with Suspected Myasthenia Gravis or Lambert-Eaton Myasthenic Syndrome: Summary Statement." 2001. *Muscle & Nerve* 24 (9): 1236–38.

Rosenberg, N.L., H.E. Neville, and S.P. Ringel. 1985. “Tubular Aggregates. Their Association with Neuromuscular Diseases, Including the Syndrome of Myalgias/cramps.” *Archives of Neurology* 42 (10): 973–76.

Santafé, Manel M, Isabel Salon, Neus Garcia, M Angel Lanuza, Osvaldo D Uchitel, and Josep Tomàs. 2003. “Modulation of ACh Release by Presynaptic Muscarinic Autoreceptors in the Neuromuscular Junction of the Newborn and Adult Rat.” *The European Journal of Neuroscience* 17 (1): 119–27.

Schiaffino, Stefano. 2012. “Tubular Aggregates in Skeletal Muscle: Just a Special Type of Protein Aggregates?” *Neuromuscular Disorders: NMD* 22 (3): 199–207. doi:10.1016/j.nmd.2011.10.005.

Schleicher, Erwin D., and Cora Weigert. 2000. “Role of the Hexosamine Biosynthetic Pathway in Diabetic Nephropathy.” *Kidney International* 58 (S77): S13–S18. doi:10.1046/j.1523-1755.2000.07703.x.

Schmidt-Nielsen, Knut. 1984. *Scaling, Why Is Animal Size so Important?* Cambridge; New York: Cambridge University Press. http://dx.doi.org/10.1017/CBO9781139167826.

Selcen, Duygu, Margherita Milone, Xin-Ming Shen, C. Michel Harper, Anthony A. Stans, Eric D. Wieben, and Andrew G. Engel. 2008. “Dok-7 Myasthenia: Phenotypic and Molecular Genetic Studies in 16 Patients.” *Annals of Neurology* 64 (1): 71–87. doi:10.1002/ana.21408.

Selcen, Duygu, Xin-Ming Shen, Joan Brengman, Ying Li, Anthony A Stans, Eric Wieben, and Andrew G Engel. 2014. “DPAGT1 Myasthenia and Myopathy: Genetic, Phenotypic, and Expression Studies.” *Neurology*, April. doi:10.1212/WNL.0000000000000435.

Senderek, Jan, Juliane S. Müller, Marina Dusl, Tim M. Strom, Velina Guergueltcheva, Irmgard Diepolder, Steven H. Laval, et al. 2011. “Hexosamine Biosynthetic Pathway Mutations Cause Neuromuscular Transmission Defect.” *The American Journal of Human Genetics* 88 (2): 162–72. doi:10.1016/j.ajhg.2011.01.008.

Shoji, Hiroki, Noriko Takahashi, Hiroshi Nomoto, Masami Ishikawa, Ichio Shimada, Yoji Arata, and Kyozo Hayashi. 1992. “Detailed Structural Analysis of Asparagine-Linked Oligosaccharides of the Nicotinic Acetylcholine Receptor from Torpedo Californica.” *European Journal of Biochemistry* 207 (2): 631–41. doi:10.1111/j.1432-1033.1992.tb17090.x.

Slater, C. R., P. R. W. Fawcett, T. J. Walls, P. R. Lyons, S. J. Bailey, D. Beeson, C. Young, and D. Gardner-Medwin. 2006. “Pre- and Post-Synaptic Abnormalities Associated with Impaired Neuromuscular Transmission in a Group of Patients with ‘limb-Girdle Myasthenia.’” *Brain* 129 (8): 2061 –2076. doi:10.1093/brain/awl200.

Spillane, Jennifer, David J. Beeson, and Dimitri M. Kullmann. 2010. “Myasthenia and Related Disorders of the Neuromuscular Junction.” *Journal of Neurology, Neurosurgery & Psychiatry* 81 (8): 850–57. doi:10.1136/jnnp.2008.169367.

Straub, Volker, Pierre G Carlier, and Eugenio Mercuri. 2012. “TREAT-NMD Workshop: Pattern Recognition in Genetic Muscle Diseases Using Muscle MRI: 25-26 February 2011, Rome, Italy.” *Neuromuscular Disorders: NMD* 22 Suppl 2 (October): S42–53. doi:10.1016/j.nmd.2012.08.002.

Teerapong, P, and A L Harvey. 1979. “The Actions of 5-Hydroxytryptamine on Isolated Skeletal Muscle Preparations.” *European Journal of Pharmacology* 57 (4): 329–34.

Teng, Lina, Robert B Bruce, and L. Kay Dunning. 1977. “Metoclopramide Metabolism and Determination by High-pressure Liquid Chromatography.” *Journal of Pharmaceutical Sciences* 66 (11): 1615–18. doi:10.1002/jps.2600661128.

Thiel, Christian, Markus Schwarz, Jianhe Peng, Michal Grzmil, Martin Hasilik, Thomas Braulke, Alfried Kohlschütter, Kurt von Figura, Ludwig Lehle, and Christian Körner. 2003. “A New Type of Congenital Disorders of Glycosylation (CDG-Ii) Provides New Insights into the Early Steps of Dolichol-Linked Oligosaccharide Biosynthesis.” *The Journal of Biological Chemistry* 278 (25): 22498–505. doi:10.1074/jbc.M302850200.

Timal, Sharita, Alexander Hoischen, Ludwig Lehle, Maciej Adamowicz, Karin Huijben, Jolanta Sykut-Cegielska, Justyna Paprocka, et al. 2012. “Gene Identification in the Congenital Disorders of Glycosylation Type I by Whole-Exome Sequencing.” *Human Molecular Genetics* 21 (19): 4151–61. doi:10.1093/hmg/dds123.

Torriani, Martin, Elise Townsend, Bijoy J. Thomas, Miriam A. Bredella, Reza H. Ghomi, and Brian S. Tseng. 2012. “Lower Leg Muscle Involvement in Duchenne Muscular Dystrophy: An MR Imaging and Spectroscopy Study.” *Skeletal Radiology* 41 (4): 437–45. doi:10.1007/s00256-011-1240-1.

Tsujino, Akira, Chantal Maertens, Kinji Ohno, Xin-Ming Shen, Taku Fukuda, C. Michael Harper, Stephen C. Cannon, and Andrew G. Engel. 2003. “Myasthenic Syndrome Caused by Mutation of the SCN4A Sodium Channel.” *Proceedings of the National Academy of Sciences* 100 (12): 7377 –7382. doi:10.1073/pnas.1230273100.

Uemura, Yuhei, Tsugumi Fujita, Sena Ohtsubo, Naomi Hirakawa, Yoshiro Sakaguchi, and Eiichi Kumamoto. 2014. “Effects of Various Antiepileptics Used to Alleviate Neuropathic Pain on Compound Action Potential in Frog Sciatic Nerves: Comparison with Those of Local Anesthetics.” *BioMed Research International* 2014: 540238. doi:10.1155/2014/540238.

Unwin, Nigel. 2013. “Nicotinic Acetylcholine Receptor and the Structural Basis of Neuromuscular Transmission: Insights from Torpedo Postsynaptic Membranes.” *Quarterly Reviews of Biophysics*, September, 1–40. doi:10.1017/S0033583513000061.

Vallés, Ana S, Ingrid Garbus, and Francisco J Barrantes. 2007. “Lamotrigine Is an Open-Channel Blocker of the Nicotinic Acetylcholine Receptor.” *Neuroreport* 18 (1): 45–50. doi:10.1097/01.wnr.0000246323.66438.94.

Vincent, Angela, Claire Newland, Rebecca Croxen, and David Beeson. 1997. “Genes at the Junction--Candidates for Congenital Myasthenic Syndromes.” *Trends in Neurosciences* 20 (1): 15–22. doi:10.1016/S0166-2236(96)10066-7.

Vuillaumier-Barrot, S. 2005. “Diagnostic Moléculaire Des Anomalies Congénitales de La Glycosylation.” *Annales de Biologie Clinique* 63 (2): 135–43.

Wang, H L, M Milone, K Ohno, X M Shen, A Tsujino, A P Batocchi, P Tonali, J Brengman, A G Engel, and S M Sine. 1999. “Acetylcholine Receptor M3 Domain: Stereochemical and Volume Contributions to Channel Gating.” *Nature Neuroscience* 2 (3): 226–33. doi:10.1038/6326.

Wargon, I, P Richard, T Kuntzer, D Sternberg, S Nafissi, K Gaudon, A Lebail, et al. 2011. “Long-Term Follow-up of Patients with Congenital Myasthenic Syndrome Caused by COLQ Mutations.” *Neuromuscular Disorders: NMD*,

November. doi:10.1016/j.nmd.2011.09.002. http://www.ncbi.nlm.nih.gov/pubmed/22088788.

Webster, R G, J Cossins, D Lashley, S Maxwell, W W Liu, J R Wickens, P Martinez-Martinez, M de Baets, and D Beeson. 2013. “A Mouse Model of the Slow Channel Myasthenic Syndrome: Neuromuscular Physiology and Effects of Ephedrine Treatment.” *Experimental Neurology*, June. doi:10.1016/j.expneurol.2013.06.012.

Wolfe, G I, L Herbelin, S P Nations, B Foster, W W Bryan, and R J Barohn. 1999. “Myasthenia Gravis Activities of Daily Living Profile.” *Neurology* 52 (7): 1487–89.

Wolfensohn, Sarah, and Maggie Lloyd. 2003. *Handbook of Laboratory Animal Management and Welfare*. 3rd Edition. Wiley-Blackwell, 233-71.

Wood, S J, and C R Slater. 2001. “Safety Factor at the Neuromuscular Junction.” *Progress in Neurobiology* 64 (4): 393–429.

Wu, Haitao, Wen C Xiong, and Lin Mei. 2010. “To Build a Synapse: Signaling Pathways in Neuromuscular Junction Assembly.” *Development (Cambridge, England)* 137 (7): 1017–33. doi:10.1242/dev.038711.

Wu, Xiaohua, Jeffrey S Rush, Denise Karaoglu, Donna Krasnewich, Mark S Lubinsky, Charles J Waechter, Reid Gilmore, and Hudson H Freeze. 2003. “Deficiency of UDP-GlcNAc:Dolichol Phosphate N-Acetylglucosamine-1 Phosphate Transferase (DPAGT1) Causes a Novel Congenital Disorder of Glycosylation Type Ij.” *Human Mutation* 22 (2): 144–50. doi:10.1002/humu.10239.

Würde, A E, J Reunert, S Rust, C Hertzberg, S Haverkämper, G Nürnberg, P Nürnberg, L Lehle, R Rossi, and T Marquardt. 2012. “Congenital Disorder of Glycosylation Type Ij (CDG-Ij, DPAGT1-CDG): Extending the Clinical and Molecular Spectrum of a Rare Disease.” *Molecular Genetics and Metabolism* 105 (4): 634–41. doi:10.1016/j.ymgme.2012.01.001.

Zhu, X Y, and M A Lehrman. 1990. “Cloning, Sequence, and Expression of a cDNA Encoding Hamster UDP-GlcNAc:dolichol Phosphate N-Acetylglucosamine-1-Phosphate Transferase.” *The Journal of Biological Chemistry* 265 (24): 14250–55.

Zoltowska, Katarzyna, Richard Webster, Sarah Finlayson, Susan Maxwell, Judith Cossins, Juliane Müller, Hanns Lochmüller, and David Beeson. 2013. “Mutations in GFPT1 That Underlie Limb-Girdle Congenital Myasthenic Syndrome Result in Reduced Cell-Surface Expression of Muscle AChR.” *Human Molecular Genetics*, April. doi:10.1093/hmg/ddt145.

Zouvelou, Vasiliki, Michael Rentzos, Panagiotis Toulas, and Ioannis Evdokimidis. 2011. “MRI Evidence of Early Muscle Atrophy in MuSK Positive Myasthenia Gravis.” *Journal of Neuroimaging: Official Journal of the American Society of Neuroimaging* 21 (3): 303–5. doi:10.1111/j.1552-6569.2009.00456.x.

Zouvelou, Vasiliki, Michael Rentzos, Panagiotis Toulas, and Ioannis Evdokimidis. 2012. “AchR-Positive Myasthenia Gravis with MRI Evidence of Early Muscle Atrophy.” *Journal of Clinical Neuroscience: Official Journal of the Neurosurgical Society of Australasia* 19 (6): 918–19. doi:10.1016/j.jocn.2011.09.022.

APPENDIX

A.1 Chemicals and solutions

This section provides a description of chemicals and solutions used in the phrenic nerve-hemidiaphragm microelectrode studies in Chapters 5 and 6.

A.1.1 Kreb's buffer solution

A solution of Kreb's buffer was prepared by adding 6.896 g NaCl, 0.350 g KCl, 2.1 g $NaHCO_3$, 0.296 g $MgSO_4 \cdot 7H_2O$, 0.164 g KH_2PO_4 to 1 L of distilled water. The solution was bubbled with 95% O_2, 5% CO_2 for ten minutes before adding 0.9 g glucose and 1.25 ml of 1M calcium chloride per 500 ml.

A.1.2 Lamotrigine isethionate

Lamotrigine isethionate ($C_9H_7Cl_2N_5.C_2H6O_4S$; molecular weight 382.22) was purchased from Tocris. A 10 mM stock solution was made by dissolving 10 mg in 2.616 ml of distilled water. This was serially diluted with Kreb's buffer to make bath solutions at concentrations of 20 µM, 50 µM, 100 µM, 300 µM and 400 µM. Lamotrigine itself is poorly water soluble and initial experiments using lamotrigine dissolved in dimethyl sulfoxide (DMSO) caused degradation of diaphragm tissue and poor quality recordings.

A.1.3 Isethionic acid sodium salt

Isethionic acid sodium salt ($HOCH_2CH_2SO_3Na$; molecular weight 148.11) was purchased from Sigma-Aldrich. A 10 mM stock solution was made by dissolving 100 mg in 67.517 ml of distilled water. This was serially diluted with Kreb's buffer to make bath solutions at concentrations of 20 µM, 50 µM, 100 µM, 300 µM and 400 µM.

A.1.4 Metoclopramide

Metoclopramide ($C_{14}H_{22}ClN_3O_2$; molecular weight 299.80) was purchased from Sigma-Aldrich. 1 mM stock solution was prepared by adding 10 mg to 33.356 ml of distilled water. Bath solutions for experiments at concentrations of 50 nM, 100 nM, 1 µM and 100 µM were made by serial dilution with Kreb's buffer.